Recent advances in understanding secondary organic aerosol : Implications for global climate forcing

Shrivastava, Manish

2017-06

Shrivastava , M , Cappa , C D , Fan , J , Goldstein , A H , Guenther , A B , Jimenez , J L , Kuang , C , Laskin , A , Martin , S T , Ng , N L , Petäjä , T , Pierce , J R , Rasch , P J , Roldin , P , Seinfeld , J H , Shilling , J , Smith , J N , Thornton , J A , Volkamer , R , Wang , J , Worsnop , D R , Zaveri , R A , Zelenyuk , A & Zhang , Q 2017 , ' Recent advances in understanding secondary organic aerosol : Implications for global climate forcing ' , Reviews of Geophysics , vol. 55 , no. 2 , pp. 509-559 . https://doi.org/10.1002/2016RG000540

http://hdl.handle.net/10138/308168
https://doi.org/10.1002/2016RG000540

AGU PUBLICATIONS

Reviews of Geophysics

REVIEW ARTICLE
10.1002/2016RG000540

Key Points:
- We review some important developments in secondary organic aerosol (SOA) that could impact aerosol radiative forcing and response of climate to greenhouse gases
- We highlight some of the important processes that involve interactions between natural biogenic emissions and anthropogenic emissions
- We discuss fundamental SOA properties volatility and viscosity and their relation to evolution of aerosol mass and number concentrations in the atmosphere

Correspondence to:
M. Shrivastava,
manishkumar.shrivastava@pnnl.gov

Citation:
Shrivastava, M., et al. (2017), Recent advances in understanding secondary organic aerosol: Implications for global climate forcing, *Rev. Geophys.*, *55*, 509–559, doi:10.1002/2016RG000540.

Received 4 OCT 2016
Accepted 12 MAY 2017
Accepted article online 18 MAY 2017
Published online 15 JUN 2017

Recent advances in understanding secondary organic aerosol: Implications for global climate forcing

Manish Shrivastava[1], Christopher D. Cappa[2], Jiwen Fan[1], Allen H. Goldstein[3], Alex B. Guenther[4], Jose L. Jimenez[5], Chongai Kuang[6], Alexander Laskin[1], Scot T. Martin[7], Nga Lee Ng[8], Tuukka Petaja[9], Jeffrey R. Pierce[10], Philip J. Rasch[1], Pontus Roldin[11], John H. Seinfeld[12], John Shilling[1], James N. Smith[4], Joel A. Thornton[13], Rainer Volkamer[5], Jian Wang[6], Douglas R. Worsnop[14], Rahul A. Zaveri[1], Alla Zelenyuk[1], and Qi Zhang[15]

[1]Pacific Northwest National Laboratory, Richland, Washington, USA, [2]Department of Civil and Environmental Engineering, University of California, Davis, California, USA, [3]Department of Environmental Science, Policy and Management and Department of Civil and Environmental Engineering, University of California, Berkeley, California, USA, [4]Department of Earth System Science, University of California, Irvine, California, USA, [5]Cooperative Institute for Research in Environmental Sciences and Department of Chemistry and Biochemistry, University of Colorado Boulder, Boulder, Colorado, USA, [6]Brookhaven National Laboratory, Upton, New York, USA, [7]School of Engineering and Applied Sciences and Department of Earth and Planetary Sciences, Harvard University, Cambridge, Massachusetts, USA, [8]School of Chemical and Biomolecular Engineering and School of Earth and Atmospheric Sciences, Georgia Institute of Technology, Atlanta, Georgia, USA, [9]Department of Physics, University of Helsinki, Helsinki, Finland, [10]Department of Atmospheric Science, Colorado State University, Fort Collins, Colorado, USA, [11]Department of Physics, Lund University, Lund, Sweden, [12]Division of Chemistry and Chemical Engineering, California Institute of Technology, Pasadena, California, USA, [13]Department of Atmospheric Sciences, University of Washington, Seattle, Washington, USA, [14]Aerodyne Research, Inc., Billerica, Massachusetts, USA, [15]Department of Environmental Toxicology, University of California, Davis, California, USA

Abstract Anthropogenic emissions and land use changes have modified atmospheric aerosol concentrations and size distributions over time. Understanding preindustrial conditions and changes in organic aerosol due to anthropogenic activities is important because these features (1) influence estimates of aerosol radiative forcing and (2) can confound estimates of the historical response of climate to increases in greenhouse gases. Secondary organic aerosol (SOA), formed in the atmosphere by oxidation of organic gases, represents a major fraction of global submicron-sized atmospheric organic aerosol. Over the past decade, significant advances in understanding SOA properties and formation mechanisms have occurred through measurements, yet current climate models typically do not comprehensively include all important processes. This review summarizes some of the important developments during the past decade in understanding SOA formation. We highlight the importance of some processes that influence the growth of SOA particles to sizes relevant for clouds and radiative forcing, including formation of extremely low volatility organics in the gas phase, acid-catalyzed multiphase chemistry of isoprene epoxydiols, particle-phase oligomerization, and physical properties such as volatility and viscosity. Several SOA processes highlighted in this review are complex and interdependent and have nonlinear effects on the properties, formation, and evolution of SOA. Current global models neglect this complexity and nonlinearity and thus are less likely to accurately predict the climate forcing of SOA and project future climate sensitivity to greenhouse gases. Efforts are also needed to rank the most influential processes and nonlinear process-related interactions, so that these processes can be accurately represented in atmospheric chemistry-climate models.

Plain Language Summary Secondary organic aerosol (SOA), formed in the atmosphere by oxidation of organic gases, often represents a major fraction of global submicron-sized atmospheric organic aerosol. Myriad processes affect SOA formation, several of which relate to interactions between natural biogenic emissions and predominantly anthropogenic species such as SO_2, NO_x, sulfate, nitrate, and ammonium. Many of these key processes are nonlinear and can be synergistic or act to compensate each other in terms of climate forcing. Current atmospheric chemistry-climate models mostly do not treat these processes. We highlight a number of process-level mechanisms related to the interactions between anthropogenic and biogenic SOA precursors, for which the corresponding impacts on the radiative effects of

SOA need to be investigated in atmospheric chemistry-climate models. Ultimately, climate models need to capture enough important features of the chemical and dynamic evolution of SOA, in terms of both aerosol number and aerosol mass, as a function of atmospheric variables and anthropogenic perturbations to reasonably predict the spatial and temporal distributions of SOA. A better understanding of SOA formation mechanisms and physical properties is needed to improve estimates of the extent to which anthropogenic emissions and land use changes have modified global aerosol concentrations and size distributions since preindustrial times.

1. Introduction

Small particles suspended in the atmosphere, ranging from a few nanometers to a few micrometers in size, are an important component of the climate system. Known as aerosols, they absorb and scatter radiant energy in the atmosphere and also affect cloud properties by providing surface for condensation of water vapor to form liquid droplets and ice particles. When particles serve in this function, they are often called cloud condensation nuclei (CCN) or ice nuclei [*Seinfeld and Pandis*, 1998; *Seinfeld et al*., 2016]. Changes in aerosol amount can thus affect the planetary energy budget directly and indirectly through changes in clouds and cloud processes [*Quaas et al*., 2009; *Stevens and Feingold*, 2009; *DeMott et al*., 2010; *Yun and Penner*, 2012; *Bond et al*., 2013; *Carslaw et al*., 2013; *Fan et al*., 2013; *Xie et al*., 2013]. Aerosol climate forcing is the difference between the radiative fluxes of the present-day and preindustrial times due to anthropogenic changes. The uncertainty in climate forcing is due to a combination of uncertainties in effective radiative forcing due to aerosol-radiation (ERFari) and aerosol-cloud (ERFaci) interactions [*Boucher et al*., 2013], which depend on the differences between present-day and preindustrial aerosol abundances, life cycle, and properties. Since preindustrial global aerosol concentrations and composition are mostly unknown due to lack of measurements, it is necessary to rely on global models to estimate the change in aerosol concentration and composition and the associated effect on cloud radiative properties [*Carslaw et al*., 2013]. Aerosol impacts on clouds and precipitation constitute some of the largest uncertainties in net climate forcing, affecting our ability to understand how human activities affect our climate systems and also to project future climate change [*Stevens and Feingold*, 2009; *Stocker et al*., 2013; *Seinfeld et al*., 2016].

Particulate organic material, often called organic aerosol (OA), is a ubiquitous and major component of submicron-sized atmospheric aerosol throughout the globe [*Murphy et al*., 2006; *Zhang et al*., 2007]. There are two main types of OA sources. One is the direct emission of OA, known as primary OA (POA), and the other is formed by oxidation of gas-phase organics in the atmosphere, known as secondary organic aerosol (SOA). POA can be emitted from human activities, such as fossil fuel combustion, biofuel burning, or cooking. The atmosphere is a large oxidative chemical reactor, where thousands of volatile organic compounds (VOCs), semivolatile and intermediate-volatility organic compounds (SIVOCs), react either during the daytime (mainly with OH radicals and ozone (O_3)) or during the nighttime with O_3 and other oxidants, such as nitrate radicals (NO_3) [*Robinson et al*., 2007; *Jimenez et al*., 2009; *Poschl et al*., 2010; *Kurtén et al*., 2016; *Ng et al*., 2016; *Trostl et al*., 2016]. These reactions lead, in part, to the formation of more functionalized organic products that have lower volatility and higher solubility. Many of these oxidized product species have a high propensity to partition to preexisting particles to form SOA or to nucleate new particles. Biogenic VOCs (BVOCs) are emitted naturally from vegetation, and anthropogenic VOC (AVOC) and SIVOC are either emitted into the atmosphere (typically along with POA) or formed through oxidation chemistry of BVOC and AVOC [*Donahue et al*., 2006; *Robinson et al*., 2007; *Donahue et al*., 2012b]. Emissions of BVOC such as isoprene and terpenes from terrestrial vegetation dominate the global reactive VOC source [*Guenther et al*., 2012]. Biomass burning can be either anthropogenic or natural and also produces POA, VOC, and SIVOC. Reactions between particle-phase organics, or even between predominantly gas-phase organics and particle components, known as heterogeneous chemistry, can also contribute to SOA by forming lower volatility accretion products or salts [*Claeys et al*., 2004; *Kalberer et al*., 2004; *Kroll and Seinfeld*, 2008; *Hallquist et al*., 2009; *Ziemann and Atkinson*, 2012; *Glasius and Goldstein*, 2016].

The importance of OA is reflected by measurements that suggest that OA concentrations are comparable to sulfate aerosol throughout the Northern Hemisphere [*Jimenez et al*., 2009]. In addition, the contribution of oxidized organics to submicron aerosol dominates in remote forested locations such as the Amazon [*Martin et al*., 2010, 2016]. A critical connection between SOA and climate is due to the ability of SOA to

scatter and absorb radiation and also to influence the number of CCN-sized particles, through either the formation of new particles or the growth of preexisting particles. The ability of particles to serve as CCN depends on both their size and composition [*McFiggans et al*., 2006; *Wang et al*., 2008; *Kammermann et al*., 2010; *Ward et al*., 2010; *Mei et al*., 2013a]. A recent modeling study suggested that low-volatility SOA may be responsible for more than half the CCN in many continental locations [*D'Andrea et al*., 2013].

Recent laboratory and field studies have shown that highly functionalized oxidation products of terpenes participate in the formation of nanometer-sized molecular clusters with each other and with inorganic compounds such as H_2SO_4 and ammonia [*Zhang et al*., 2012; *Keskinen et al*., 2013; *Ehn et al*., 2014; *Riccobono et al*., 2014; *Kirkby et al*., 2016; *Trostl et al*., 2016]. In addition, the growth of such nanometer-sized clusters to CCN sizes (typically greater than ~80 nm diameter) is strongly driven by the condensation of very low volatility organic compounds, i.e., by SOA formation, in many rural and remote continental settings [*Riipinen et al*., 2011, 2012]. The relatively rapid growth provided by the ubiquitous condensing organic vapors can enable the particles to survive scavenging by the larger aerosol and therefore reach the CCN sizes contributing to the CCN budget [*Kulmala et al*., 1998]. This contribution of natural and anthropogenic VOC to SOA formation that affects CCN and particle size has potentially important impacts on our understanding of ERFari and ERFaci over time.

In most climate models, the sources of SOA are generally treated in a very simplified way, if at all [*X. Liu et al*., 2012; *Tsigaridis et al*., 2014], which results in large uncertainties in model assessments of SOA-climate interactions. Early modeling efforts at simulating SOA concentrations underpredicted measured SOA mass concentrations by 1–2 orders of magnitude, with the discrepancies generally increasing with photochemical age or proxies of photochemical age such as distance from emission source [*de Gouw et al*., 2005; *Heald et al*., 2005; *Volkamer et al*., 2006]. These studies motivated research that attempted to understand why models were predicting SOA concentrations so poorly. A second set of studies found unexpectedly large fractions of modern carbon (indicating a nonfossil fuel source) in aerosol with increasingly larger modern carbon fractions found downwind of urban areas [*Weber et al*., 2007; *Schichtel et al*., 2008], indicating chemical pathways wherein anthropogenic pollution likely enhances biogenic SOA formation [*Weber et al*., 2007; *Goldstein et al*., 2009; *Carlton et al*., 2010; *Shilling et al*., 2013], or other urban nonfossil sources of carbon such as emissions from meat cooking and woodstoves [*Hildemann et al*., 1991; *Schauer et al*., 2001; *Zotter et al*., 2014; *Hayes et al*., 2015]. For example, a few studies indicate that present-day anthropogenic pollution, e.g., from combustion-related emissions of sulfur dioxide (SO_2) and reactive oxides of nitrogen (NO_x), has most likely caused an increase in the amount of biogenic SOA [e.g., *Spracklen et al*., 2011; *Shilling et al*., 2013]. Aerosol sulfate and nitrate have increased significantly (about a factor of 2–4) since preindustrial times [*Fischer et al*., 1998], and these anthropogenic combustion byproducts are shown to affect formation of SOA from a range of VOC precursors [*Liggio and Li*, 2006; *Surratt et al*., 2007b, 2010; *Kampf et al*., 2013; *Ehn et al*., 2014; *Jokinen et al*., 2015; *Kurtén et al*., 2015; *Waxman et al*., 2015; *J. Liu et al*., 2016; *Marais et al*., 2016]. However, we note that these effects of anthropogenic emissions on SOA are more complex than their current representation in models. For example, while NO_x can increase SOA due to several processes such as organonitrate formation, salt-interactions (salting-in) or by increase in oxidative capacity of the atmosphere, increasing NO can also suppress SOA through fragmentation reactions that form more volatile products (sections 2.2 and 2.3). The ultimate effects of NO_x on SOA budgets are not clear.

Similarly, biomass burning is another large global source of nonfossil carbon in OA that has likely changed since preindustrial times [*Andreae and Merlet*, 2001; *van der Werf et al*., 2010; *Bond et al*., 2013]. However, the biomass burning source of SOA is not well constrained in global climate models [*Spracklen et al*., 2011; *Tsigaridis et al*., 2014; *Shrivastava et al*., 2015]. The majority of carbonaceous aerosol on regional to global scales is thought to be of nonfossil fuel origin [*Spracklen et al*., 2011].

In addition to directly affecting the yield of low-volatility products during the gas-phase radical chemistry, anthropogenic species like sulfate and nitrate can also alter condensed-phase processes such as oligomerization/accretion or the formation of organosulfates [*Gao et al*., 2004; *Dommen et al*., 2006; *Surratt et al*., 2007a, 2008, 2010; *Hall and Johnston*, 2012; *Tan et al*., 2012; *Xu et al*., 2014; *Lopez-Hilfiker et al*., 2016]. Oligomerization/accretion refers to reactions that link two or more organic molecules through chemical bonds, potentially reversibly, to form larger molecules that are less likely to evaporate back to the gas phase or reactions that involve interactions between organics and inorganics such as organosulfate formation

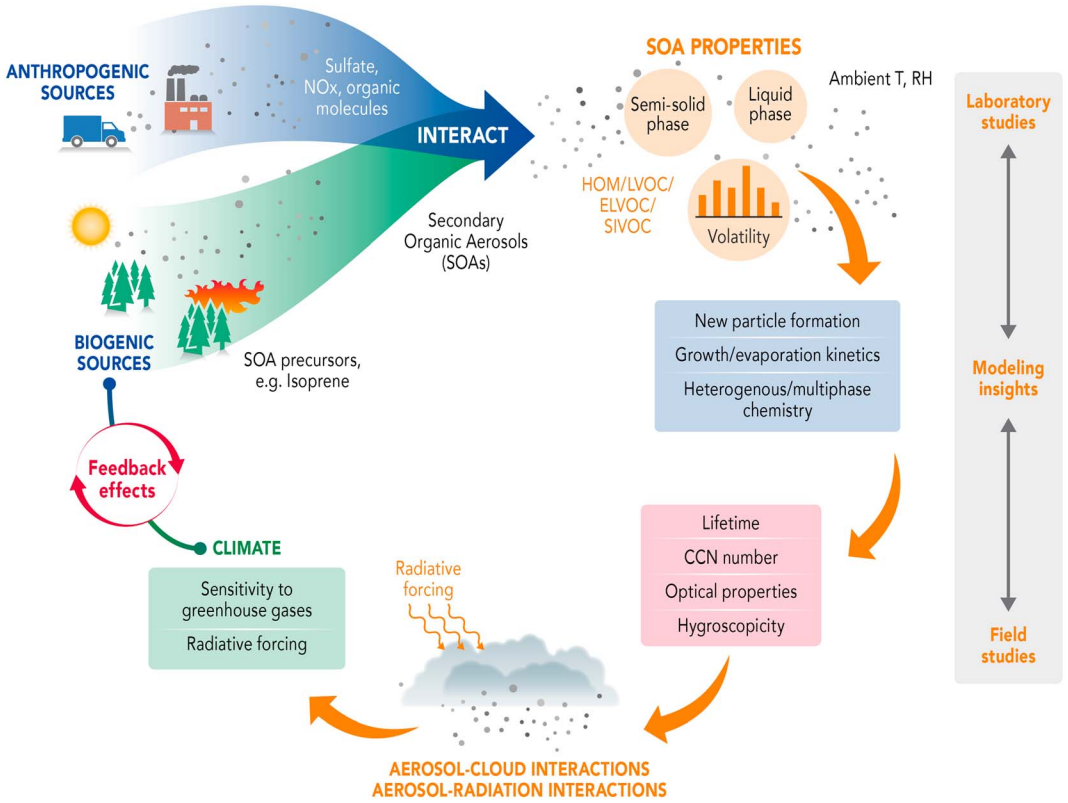

Figure 1. Processes governing the climatic importance of SOA. Anthropogenic and biogenic emissions could interact through a variety of pathways that affect SOA. Fundamental SOA properties including phase and volatility affect new particle formation, growth/evaporation, and multiphase reactive kinetics of these particles. These processes affect the lifetime, CCN number, and optical and hygroscopic properties of SOA, relevant to aerosol-radiation and cloud radiation interactions. These interactions affect the sensitivity of climate systems to greenhouse gases.

[*Jang et al.*, 2002; *Barsanti and Pankow*, 2004; *Gao et al.*, 2004; *Kalberer et al.*, 2004; *Tolocka et al.*, 2004; *Liggio et al.*, 2005; *Ziemann*, 2011]. This oligomerization process alters the composition of SOA, causing large reductions of SOA particle volatility [*Barsanti and Pankow*, 2004, 2005, 2006; *Cappa and Wilson*, 2011; *Kolesar et al.*, 2015a; *Kurtén et al.*, 2016]. Moreover, weakly bound sulfate complexes with biogenic oxygenated VOC can strongly increase the effective Henry's law coefficient of biogenic precursors, decrease volatility [*Zhang et al.*, 2004; *Kurtén et al.*, 2015], and modify the rates of oligomerization and nanoparticle growth [*Wang et al.*, 2010]. Such nonlinear interactions between human and natural systems could lead to even larger variations in the regional forcing of SOA as compared to the global average. On the whole, global climate models, and even regional chemical transport models, mostly do not treat such interactions [e.g., *Carslaw et al.*, 2013]. These interactions could largely impact the difference between the present-day radiative effects of SOA as compared to preindustrial times when emissions of SO_2, NO_x, and other predominantly anthropogenic pollutants were lower [*Martin et al.*, 2010].

A key goal of recent research related to SOA has therefore been to determine the mechanisms of, and the extent to which, interactions between natural biogenic emissions and predominantly anthropogenic species such as SO_2, NO_x, sulfate, nitrate, and ammonium quantitatively affect predictions of direct and indirect aerosol radiative forcing. Ultimately, the aim is to arrive at more accurate model treatments of how SOA particles influence the climate using measurement-based fundamental insights. Over the past decade, many studies have produced fundamental new insights into the formation and atmospheric evolution of SOA and the interactions between anthropogenic and natural biogenic emissions.

Figure 1 schematically illustrates how biogenic emissions, anthropogenic-biogenic interactions, and fundamental properties of SOA, such as phase and volatility, affect CCN number concentrations, lifetimes of SOA, and their climate-relevant optical and hygroscopic properties. These processes and properties affect

aerosol-radiation and aerosol-cloud interactions that also affect understanding of the sensitivity of climate systems to greenhouse gases.

This review covers the following main themes, based on the some of the latest advances in scientific understanding of the processes governing the SOA life cycle: (1) biogenic emissions and SOA formation, (2) role of low-volatility and extremely low volatility organics in SOA, (3) role of particle-phase state on size evolution of SOA and CCN, (4) biomass burning SOA, (5) laboratory systems for SOA formation, (6) SOA interactions with clouds, (7) optical properties of SOA and radiative forcing, and (8) implications for global climate forcing.

A recently published report from the National Academies of Sciences provided broad atmospheric chemistry research priorities for the future [*National Academies of Sciences, Engineering, and Medicine*, 2016]. Several of the topics listed above were also included among a range of aerosol-related topics mentioned in that report. The present effort is much more selective and focuses on biogenic SOA and mechanisms related to anthropogenic interactions with biogenic SOA. We note that although anthropogenic SOA formation is also important, especially if low-volatility anthropogenic SOA precursors are considered [*Hallquist et al*., 2009; *Jathar et al*., 2014; *Gentner et al*., 2017], discussions on anthropogenic SOA are beyond the scope of this work. However, we have included a short discussion of key issues related to biomass burning SOA, since very few global models include this source, and it is potentially of great importance to global OA budgets. We also largely focus on chemistry related to SOA formation. Topics related to particle-phase photolysis and heterogeneous oxidation are not included. However, we discuss particle-phase aging chemistry in the context of oligomerization, which is generally accepted to be a condensed-phase process after aerosol formation. We also discuss how aerosol processes affect fundamental physical properties of SOA, i.e., volatility and viscosity. Both volatility and viscosity are key properties that affect SOA loadings, number concentrations, and lifetime. The ultimate goal is to identify mechanisms that could be most influential in affecting the abundance and size evolution of SOA and its properties and to incorporate these processes in climate models in order to assess their regional and global impacts.

2. Biogenic Emissions and SOA Formation

Direct BVOC emissions from vegetation and from combustion of vegetation (biomass burning) are two of the major sources of nonfossil carbon in atmospheric OA [*Andreae and Merlet*, 2001; *Guenther et al*., 2006; *van der Werf et al*., 2010; *Guenther et al*., 2012; *Yokelson et al*., 2013]. The emissions from both these sources undergo complex chemical transformation pathways in the atmosphere, which result in formation of SOA. In this section, we review some of the latest advances on biogenic VOC emissions and their oxidation pathways leading to SOA formation and also identify critical gaps that need to be addressed in future studies.

2.1. Biogenic VOC

2.1.1. Emissions

Isoprene and other reactive BVOC are the dominant VOC emitted on a global basis [*Guenther et al*., 2006, 2012]. Uncertainties in BVOC emission estimates contribute to the overall uncertainties associated with model predictions of SOA production rates [*Warneke et al*., 2010; *Kaser et al*., 2015]. The short lifetimes (~1.5 h or less) and the large temporal and spatial variability in emission strength can result in BVOC concentrations varying by an order of magnitude over a distance of few kilometers. Therefore, it is necessary to accurately characterize the regional variability in BVOC emissions to determine the amount of BVOC available for SOA production at a given location and time.

In addition to challenges in estimating emissions, there are uncertainties in the fraction of emitted BVOC that is transformed to SOA. *Kaser et al*. [2015] have recently shown that in addition to uncertainties in atmospheric chemistry schemes, the limited spatial resolution of models masks the true spatial covariability and spatial segregation of BVOC and atmospheric oxidants, which can result in up to 30% overestimation of isoprene oxidation rates. Figure 2 depicts this process where two different air parcels over heterogeneous landscapes (cropland versus mixed oak forests) that are separated by a distance of just a few kilometers have very different concentrations of OH radicals and isoprene: one with high OH and low isoprene and the other with low OH and high isoprene. Net isoprene oxidation in the region is consequently slowed as a result of limiting the mixing of high-OH air parcels with high isoprene air parcels. In comparison, most climate models with much coarser grid spacing assume that OH and isoprene are well mixed. Thus, subgrid-scale heterogeneities in

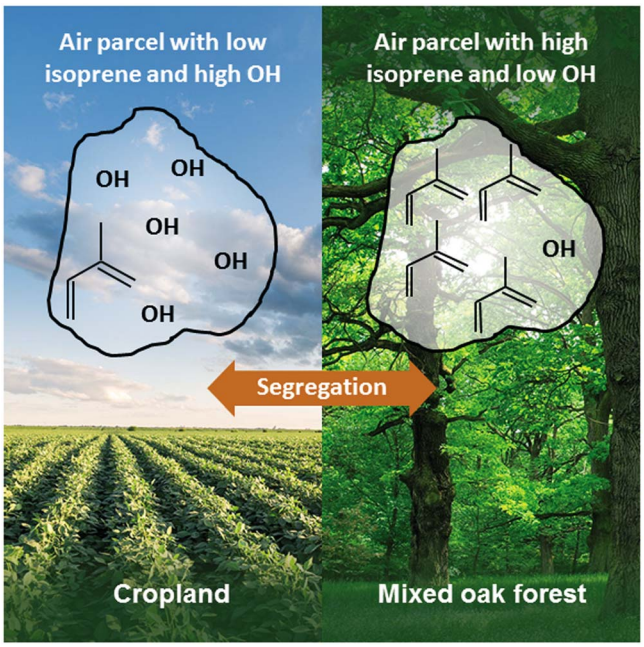

Figure 2. Segregation of isoprene and OH in the boundary layer above a heterogeneous landscape (e.g., cropland and mixed oak forest) can effectively lower OH reaction rates by limiting the ability of OH to come in contact with isoprene. In contrast, climate models assume that OH and isoprene are well mixed within a grid cell.

landscapes and associated mixing and chemistry processes may be very different than what is currently represented in climate model simulations.

BVOC emissions are also highly sensitive to environmental conditions, especially temperature, solar radiation, and land cover, including vegetation type and amount. The development of an airborne technique for high spatial resolution (~2 km) measurements of isoprene fluxes using eddy covariance techniques has extended capabilities for quantifying regional variations of isoprene fluxes and enabled evaluation of emission variations in regional models [*Karl et al.*, 2013; *Misztal et al.*, 2016]. In addition to uncertainties in emissions, the deposition sinks of biogenic VOC and their oxidation products also have to be carefully evaluated [*Hodzic et al.*, 2013; *Knote et al.*, 2014a]. New modeling approaches, which include better integration with the ecophysiological representations in land-atmosphere models, have the potential to reduce emission and deposition uncertainties of isoprene and other BVOC. This must be accompanied by long-term, canopy-scale measurements of emission response to environmental drivers and large-scale measurements of speciated BVOC (e.g., aircraft flux measurements) to afford parameterization of these emissions as a function of vegetation type and land use.

Among the several BVOC emissions, isoprene is the most abundant and is emitted to the atmosphere by terrestrial vegetation at globally integrated rates that are factors of 5 larger by carbon mass than any other reactive hydrocarbon [*Guenther et al.*, 2006, 2012]. Owing to the abundance of isoprene in many forested regions and its rapid reaction with OH (its lifetime is ~1.5 h for [OH] ~1×10^6 cm^{-3} [*Atkinson*, 1997]), it occupies a prominent position in tropospheric chemistry and its oxidation mechanism is of critical importance to understanding the VOC budget of the troposphere and SOA formation. Here we review how an understanding of the role of isoprene in SOA formation has evolved over the past decade.

2.1.2. Isoprene SOA Chemistry

Like many hydrocarbons, the primary fate of isoprene in the atmosphere is reaction with the OH radical, with less important pathways including reaction with ozone and NO_3 radicals. Reactions of isoprene proceed through multiple generations of chemistry similar to other VOC. In order to provide perspectives on how our understanding of isoprene oxidation products has evolved, this review first describes previous historical work in terms of the role of isoprene in SOA formation, followed by descriptions of first-generation and second- and higher-generation oxidation products of isoprene. Also, it has long been understood that NO_x plays a critical role in governing SOA yields and these yields may either increase or decrease as NO_x increases depending on the concentration and structure of SOA precursor VOC [*Pandis et al.*, 1991; *Kroll et al.*, 2005a; *Presto et al.*, 2005a; *Song et al.*, 2005; *Ng et al.*, 2007b; *Nguyen et al.*, 2011a; *Loza et al.*, 2014; *Xu et al.*, 2014]. In most polluted regions of the world, NO_x is mainly anthropogenic in origin. In forested regions of central Amazonia and Southeast Asia, for example, the contribution of soil-emitted NO_x could be significant [*Bakwin et al.*, 1990; *Garcia-Montiel et al.*, 2001; *Hewitt et al.*, 2009]. Similarly, sulfate also affects formation of SOA from isoprene [*Surratt et al.*, 2006, 2007b, 2010]. This study also discusses the role of anthropogenic species like sulfate and NO_x in isoprene chemistry based on recent measurements.

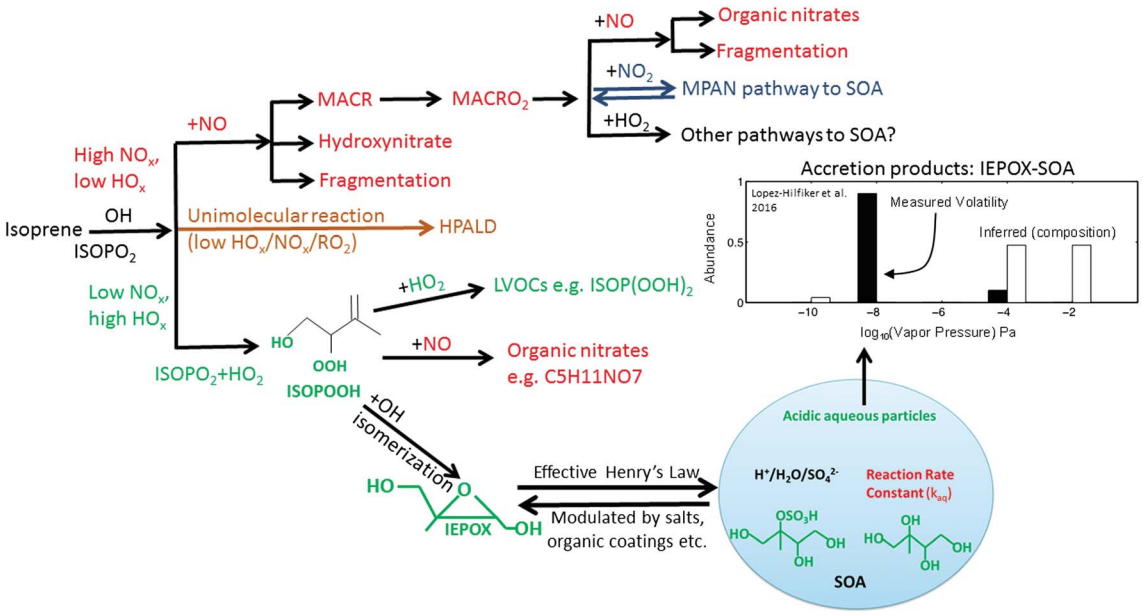

Figure 3. Fate of isoprene RO_2 radicals ($ISOPO_2$) depicting different chemical pathways that depend on the NO_x, HO_x, and RO_2 regimes. Several pathways lead to SOA formation, but the particle loading/composition differs greatly between different regimes and also depends on acidic/nonacidic seeds. Other pathways to SOA formation at low NO_x/high HO_x from isoprene that are not shown arise from multiphase chemistry of glyoxal [*Knote et al*., 2014b], ISOPOOH, and formation of other species such as organic hydroperoxides [*Krechmer et al*., 2015; *J. Liu et al*., 2016].

2.1.2.1. Overview

Atmospheric isoprene oxidation was studied in an outdoor chamber as early as 1982 [*Kamens et al*., 1982]. In outdoor chamber studies, *Pandis et al*. [1991] measured particle formation from isoprene oxidation at carbon yields <0.8% over a range of isoprene mixing ratios of 40 to 10,000 ppb and at NO mixing ratios ranging from 47 to 860 ppb. The experiments were carried out with either few or no seed particles at a temperature of ~304°K. The lack of significant SOA formation was attributed to the high volatility of isoprene oxidation products. In 2004, however, unique oxidation products of isoprene, methyltetrols, were detected in Amazonian aerosol [*Claeys et al*., 2004]. The identification of these aerosol-phase tracers for isoprene reignited interest in laboratory chamber studies aimed at understanding the mechanism of formation and yield of SOA from isoprene oxidation [*Kroll et al*., 2005a; *Wang et al*., 2005; *Dommen et al*., 2006; *Kroll et al*., 2006; *Ng et al*., 2006; *Surratt et al*., 2006, 2007b; *Kroll and Seinfeld*, 2008; *Surratt et al*., 2008; *Paulot et al*., 2009a, 2009b; *King et al*., 2010; *Nguyen et al*., 2010; *Chen et al*., 2011; *Nguyen et al*., 2011a, 2012a; *Bregonzio-Rozier et al*., 2015]. It became understood that the conditions of the early outdoor chamber studies were not conducive to isoprene SOA formation. This was due to several potential reasons in those early measurements: high NO levels, the relatively high temperature, lower OH concentrations resulting in slower oxidation chemistry, and the low concentrations of seed aerosol. In addition, the latter two reasons both contribute to larger gas-phase wall loss. Over the decade since the *Claeys et al*. [2004] paper, much has been learned about the mechanism of SOA formation from isoprene under both high- and low-NO conditions, although much remains to be done. Chamber studies suggest that isoprene SOA yields are significant and that they vary depending on the fate of intermediate radical species, particularly peroxy radicals [*Kroll et al*., 2005a, 2006; *A. Chan et al*., 2010; *Chen et al*., 2011; *Xu et al*., 2014, 2015b]. Reaction products of isoprene are created through several successive generations of isoprene oxidation pathways, as described below.

Figure 3 presents a simplified reaction schematic showing some of the important isoprene oxidation pathways initiated by OH radicals. After addition of the OH radical to one of the two double bonds, the hydroxyalkyl radical of isoprene reacts with molecular oxygen to form an organic peroxy radical ($ISOPO_2$). The fate of the $ISOPO_2$ radical depends largely on the NO_x concentration, though, in general, these first-generation reaction products are themselves too volatile to partition to the condensed phase in the absence of further reaction. In high NO_x environments, reaction with NO forms an alkoxy radical, which likely fragments to form

higher volatility products, including methacrolein (MACR) and methylvinyl ketone (MVK), and/or isomerizes to form hydroxycarbonyl isomers [*Atkinson et al*., 1989; *Tuazon and Atkinson*, 1990; *Paulson and Seinfeld*, 1992; *Miyoshi et al*., 1994; *Kwok et al*., 1995; *Kroll and Seinfeld*, 2008; *Carlton et al*., 2009; *Bates et al*., 2016]. A minor (about 7% yield) fraction of $ISOPO_2$/NO reactions produce hydroxy nitrate isomer species, but these reactions are potentially important to SOA formation [*Tuazon and Atkinson*, 1990; *Patchen et al*., 2007; *Lockwood et al*., 2010]. When NO_x concentrations are sufficiently low, isoprene oxidation proceeds primarily by a pathway in which the $ISOPO_2$ radical may react with a hydroperoxyl radical (HO_2), other organic peroxy (RO_2) radicals, or undergo isomerization reactions. Reaction of the $ISOPO_2$ radical with HO_2 leads to the formation of a family of isoprene hydroxyl hydroperoxides (denoted ISOPOOH) in molar yields exceeding 70% [*Paulot et al*., 2009b; *Y. J. Liu et al*., 2013; *Bates et al*., 2014]. Reactions of $ISOPO_2$ with other RO_2 radicals are less well understood but likely produce carbonyl and functionalized carbonyl products and hydroxylated products [*Ruppert and Becker*, 2000]. In pristine regions where lifetimes of $ISOPO_2$ radicals are long, unimolecular isomerization reactions produce hydroperoxyaldehydes (HPALDs) [*Crounse et al*., 2011; *Peeters and Nguyen*, 2012; *Crounse et al*., 2013; *Bates et al*., 2014; *Peeters et al*., 2014]. In general, different RO_2 radicals can also undergo unimolecular reactions to compete with the RO_2+NO channel, though the kinetics of this channel are highly uncertain [*Peeters et al*., 2009; *Da Silva et al*., 2010; *Stavrakou et al*., 2010; *Crounse et al*., 2011; *Berndt*, 2012; *Orlando and Tyndall*, 2012; *Wolfe et al*., 2012; *Ziemann and Atkinson*, 2012; *Fuchs et al*., 2013]. Also, the second- and higher-generation oxidation products of isoprene are more likely to partition to the condensed phase than first-generation products [*Carlton et al*., 2009]. The following sections discuss some of the important advances in isoprene multiphase chemistry relevant to SOA formation (as illustrated in Figure 3).

2.1.2.2. Advances in Multiphase Chemistry of Isoprene Epoxydiols

ISOPOOH reacts further by OH addition and isomerization to form isoprene epoxydiols (IEPOX) in molar yields exceeding 75% [*Paulot et al*., 2009b] under low-NO_x conditions. Subsequent multiphase chemistry of IEPOX in the presence of aqueous acidic particle seeds results in SOA formation. The high water solubility and reactivity of IEPOX are conducive to partitioning into the aerosol phase and subsequent transformation into lower volatility and/or higher solubility products such as organosulfates, 2-methyltetrols, and oligomers thereof, which can contribute significantly to ambient SOA [*Surratt et al*., 2007b, 2008; *Paulot et al*., 2009a; *Surratt et al*., 2010]. The finding of significant IEPOX production from ISOPOOH [*Paulot et al*., 2009b] therefore validated the existence of IEPOX (first proposed by Claeys and coworkers) as a reactive intermediate that could explain the formation of 2-methyltetrols, C_5-alkene triols, and dimers observed in the Amazon in ambient aerosol influenced by isoprene [*Wang et al*., 2005; *Surratt et al*., 2006]. The importance of the IEPOX-SOA pathway has been demonstrated repeatedly in field measurements using both a suite of molecular tracers [*Wang et al*., 2005; *Surratt et al*., 2008; *Froyd et al*., 2010; *Surratt et al*., 2010; *Y. H. Lin et al*., 2012, 2013a, 2014; *Budisulistiorini et al*., 2015; *Liao et al*., 2015; *Rattanavaraha et al*., 2016] and aerosol mass spectral analyses [*Robinson et al*., 2011; *Budisulistiorini et al*., 2013; *Allan et al*., 2014; *Y. H. Lin et al*., 2014; *Nguyen et al*., 2014a]. Field measurements also demonstrate that IEPOX-SOA components indicated by 2-methyl tetrols and C_5 alkene triols comprise a substantial fraction of total OA mass (8–15% with maximum contributions of up to 35%) in two distinct regions: the southeastern United States and the Amazon [*Isaacman-VanWertz et al*., 2016]. Based on positive matrix factorization (PMF) analysis of aerosol mass spectrometry (AMS) data, an "IEPOX-SOA factor," which is considered to be a surrogate for isoprene SOA through IEPOX uptake, has been identified at multiple sampling sites, including the Amazon Basin, southeastern United States, and boreal forests, as indicated in Figure 4 [*Robinson et al*., 2011; *Slowik et al*., 2011; *Budisulistiorini et al*., 2013, 2015; *Chen et al*., 2015; *Hu et al*., 2015; *Xu et al*., 2015b, 2015a; *Budisulistiorini et al*., 2016; *Lopez-Hilfiker et al*., 2016].

Recent laboratory studies have provided important mechanistic constraints of IEPOX reactive uptake to particles and SOA formation while also raising some new questions. The kinetics of IEPOX reactive uptake influences the IEPOX lifetime and thus its spatial distribution, as well as the rate of SOA formation, depending mainly on the solubility of IEPOX (determined by an effective Henry's law coefficient H^*) and its condensed-phase reactivity [*Eddingsaas et al*., 2010; *Gaston et al*., 2014; *Xu et al*., 2016]. The concentration of aqueous-phase species (i.e., H^+, SO_4^{2-}, HSO_4^-) and aerosol water can also govern the solubility of organic compounds by the so-called Setschenow salting effects on the Henry's law coefficient and thus modulate the multiphase mass transfer rate of IEPOX [*Waxman et al*., 2015].

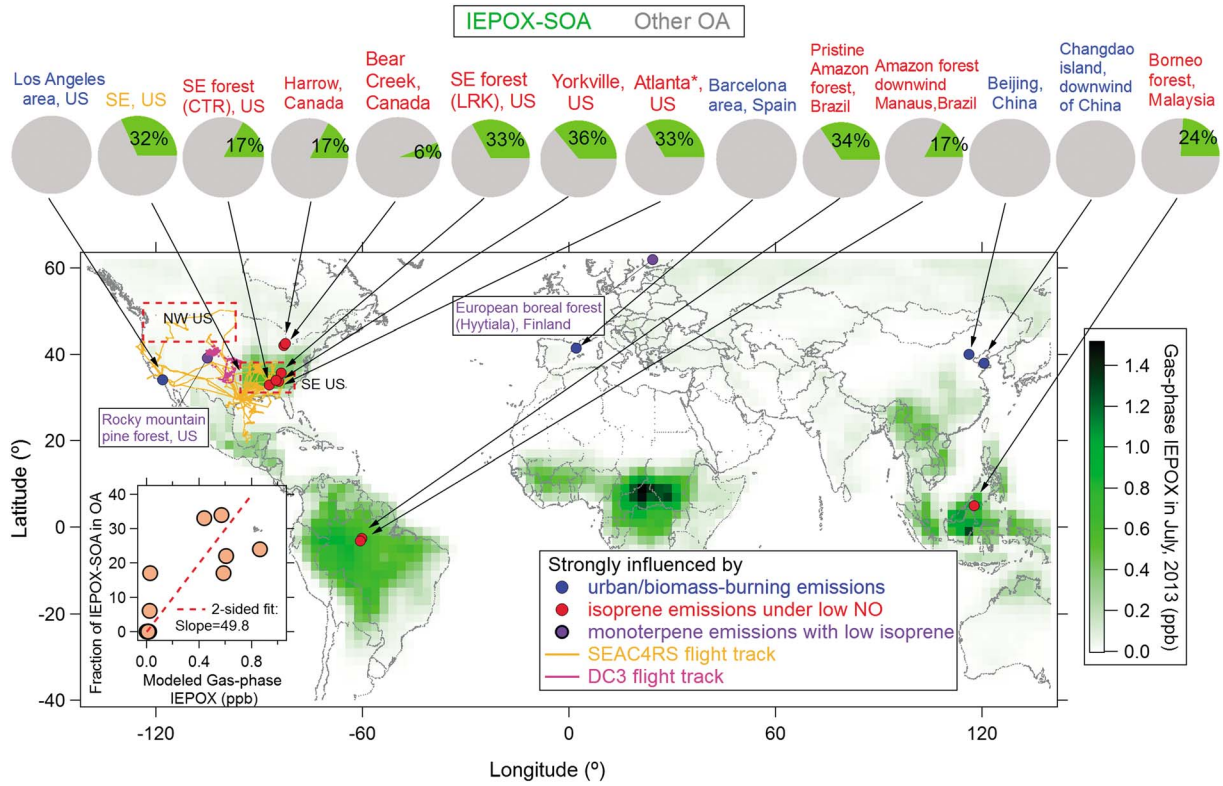

Figure 4. IEPOX-SOA fractions of OA in various studies around the world from Figure 1 in *Hu et al.* [2015].

These salting effects depend on the organic compound, the inorganic ions in solution, and other factors and modulate the multiphase mass transfer and reaction rates of IEPOX and other water soluble species [*Waxman et al.*, 2015]. We briefly review the Setschenow salting effects in the following paragraph.

Salting effects have been known since the late nineteenth century [*Setschenow*, 1889], but they remain poorly understood mechanistically and are not well characterized at high salt concentrations characteristic of atmospheric aerosol. Inorganic ionic species, in particular sulfate (SO_4^{2-}), and also nitrate (NO_3^-) and chloride (Cl^-) in aqueous solutions, are most widely known as causes for "salting-out" [*C. Wang et al.*, 2014; *Wania et al.*, 2014]. However, a "salting-in" effect, i.e., the exponential increase in the partitioning behavior at increasing salt concentration, can be observed for very polar compounds [*Almeida et al.*, 1983; *Kroll et al.*, 2005b; *Kampf et al.*, 2013]. At the molecular level salting-in has been assigned to the formation of sulfate complexes that can displace water molecules from the hydration shell of sulfate ions [*Kurten et al.*, 2015]. Salting effects add a multiplicative factor (activity coefficient) that modify H (dilute conditions) to an effective Henry's law coefficient, H_{eff}, i.e., activity factor ~1/700 in the case of glyoxal (with ammonium sulfate at 50% relative humidity (RH)) and ~150 for methylglyoxal [*Waxman et al.*, 2015]. Kinetic limitations in mass transfer into the aerosol bulk have been observed at RH of up to ~63% (corresponding to the solubility limit of ammonium sulfate [*Kampf et al.*, 2013]), in mixed SOA systems [*Nakao et al.*, 2012] and in the presence of coatings [*Galloway et al.*, 2011]. On the other hand, no kinetic limitation was observed for mixed inorganic/organic seed particles at 50% RH [*Kampf et al.*, 2013]. Moreover, salting effects due to interfacial water can trigger rapid growth [*Trainic et al.*, 2012] even of nanoparticles [*Wang et al.*, 2010]. Thus, the activity of salts is complex, modifies the Henry's law coefficients, and influences multiphase reaction rates. These salting effects are currently not included in most atmospheric models.

Among other factors (such as salting effects), aqueous particle-phase components are also subject to variations in ammonia [*Kuwata et al.*, 2015], RH, and temperature. The aqueous-phase reactivity is driven by acidity, [H^+], which catalyzes the epoxide ring opening that promotes nucleophilic attack by H_2O, SO_4^{2-}, HSO_4^-, NO_3^-, etc., to form lower volatility products [*Eddingsaas et al.*, 2010; *Gaston et al.*, 2014]. *Gaston et al.* [2014] showed that the net uptake rate was controlled by acidity of aqueous ammonium bisulfate particles by

varying the RH from 30 to 75%. Increasing liquid water and/or decreasing sulfate anion concentrations (at high RH) only led to a decrease in the net uptake rate.

If reactive uptake kinetics are relatively fast, the particle size evolution will be surface area controlled, whereas with slower reactive uptake the size evolution is limited by the compound solubility, as measured, for example, by its effective Henry's law constant H^*, and is volume controlled. If the uptake process is surface area controlled, the size distribution will narrow to a greater extent during growth than if the uptake is volume controlled [*Shiraiwa et al*., 2013b; *Zaveri et al*., 2014]. Based on the epoxide ring-opening kinetics measured or inferred by *Eddingsaas et al*. [2010] and *Gaston et al*. [2014], IEPOX reactive uptake should be volume controlled. A recent study by *Riva et al*. [2016b] utilized single-particle mass spectrometry and directly demonstrated that IEPOX uptake by *pure* ammonium bisulfate and ammonium sulfate particles is a volume-controlled process. Volume-controlled IEPOX uptake by pure sulfate particles results in particles with uniform concentration of IEPOX-derived SOA across a wide range of sizes, as shown by *Riva et al*. [2016b]. One challenge to incorporating IEPOX reactive uptake into models is that the presence of organic coatings may also affect the kinetics. *Gaston et al*. [2014] reported that ammonium bisulfate particles mixed with polyethylene glycol, a surrogate for highly oxygenated SOA, exhibit lower IEPOX uptake coefficients compared to that for pure ammonium bisulfate particles. Similarly, *Riva et al*. [2016b] showed that uptake of IEPOX on ammonium bisulfate particles coated with α-pinene SOA is significantly lower than IEPOX uptake by pure ammonium bisulfate particles and is correlated with α-pinene SOA mass fraction. Moreover, *Riva et al*. [2016b] demonstrated that the fraction of IEPOX-SOA strongly depends on particle size: larger particles, which have higher ammonium bisulfate content, were shown to acquire higher fraction of IEPOX-SOA. These results are in a good agreement with recent reports of a strong size dependence of the IEPOX-SOA fraction in ambient particles in both the SE U.S. and the Amazon [*Hu et al*., 2016], with larger fractions of IEPOX-SOA for larger particles that have a higher inorganic content. These observations also point to a possible self-limiting pathway in the formation of IEPOX-SOA, wherein as more IEPOX-SOA forms, further uptake of IEPOX is hindered by the growth of an organic coating.

While SOA formation is a complex multiphase process involving gas-phase oxidation chemistry, gas-to-particle conversion, and particle-phase chemistry, the traditional measure of overall SOA formation from a parent VOC is the SOA yield. Recent laboratory work has determined that the IEPOX-SOA mass yield from the reactive uptake of IEPOX may be $<$15% [*Riedel et al*., 2015]. This work combined constraints on the reactive uptake rate of IEPOX with the observed mass growth of particles. Moreover, this finding can potentially reconcile the large IEPOX reaction probabilities measured on particles relative to those needed in models to reproduce the abundance of IEPOX-SOA tracers measured in the atmosphere. The production rate of IEPOX-SOA will be the multiplicative product of a reaction probability for IEPOX and yield describing the fraction of that uptake that results in SOA mass. Consistent with this notion, *Y. J. Liu et al*. [2016] recently showed that even as isoprene oxidation products are taken up into particles, a fraction of the condensed-phase reaction products can be released back to the gas phase. Indeed, C_5-tetrol, a dominant reaction product of isoprene SOA, has a volatility and likely solubility that would drive significant repartitioning to the gas phase under typical ambient aerosol mass concentrations.

Measurements using the semivolatile thermal desorption aerosol gas chromatograph (SV-TAG) [*Isaacman et al*., 2014] during the Green Ocean Amazon, GoAmazon 2014/5 field campaign [*Martin et al*., 2016], showed that a major fraction of methyltetrols and alkene-triols (the most commonly detected molecular tracers of IEPOX-SOA) reside in the particle phase, somewhat unexpectedly based on their estimated volatility [*Isaacman-VanWertz et al*., 2016]. Both laboratory and field measurements using the Filter Inlet for Gases and Aerosols (FIGAERO) coupled to a high-resolution, time-of-flight chemical ionization mass spectrometer (HR-ToF-CIMS) instrument have shown that tetrols and triols/furan diols thermally desorb from particles as if they have orders-of-magnitude-lower volatilities than their pure-component saturation vapor concentrations [*Lopez-Hilfiker et al*., 2016], as illustrated in Figure 3. Similar results examining the AMS PMF factor have been obtained in the southeastern United States and the Amazon using a thermal denuder-aerosol mass spectrometer (TD-AMS) coupling [*Hu et al*., 2016]. Thus, IEPOX-SOA appears to be mostly low-volatility material, even though the measured molecular species comprising 85% of IEPOX-SOA [*Hu et al*., 2015] (such as triols and tetrols) are semivolatile. *Lopez-Hilfiker et al*. [2016] suggest that the reason for this behavior is that IEPOX-SOA components exist in the form of low-volatility accretion products or inorganic-organic adducts, such as organosulfates, that undergo decomposition into the various tracers in thermal desorption-based

methods or in any offline analyses that require heating of the sample [*Tobias and Ziemann*, 2000], e.g., to promote derivatization. *Isaacman-VanWertz et al*. [2016] came to similar conclusions but demonstrated that thermal decomposition of organosulfates specifically provided negligible contributions to measured mass (<5% conversion to analogous species). Oligomers from IEPOX-SOA have also been observed in ambient aerosol in the southeastern United States [*Y. H. Lin et al*., 2014]. Such oligomers or adducts affect the volatility and evaporation characteristics of IEPOX-SOA. A model relying on gas-particle partitioning and assuming that IEPOX-SOA was mostly composed of tetrols and triols/furan diols would thus be unlikely to accurately simulate IEPOX-SOA abundance and distributions.

Based on the above developments, the IEPOX source of SOA is likely well suited for incorporation into regional/global chemistry-climate models. The gas-phase chemistry to adequately represent IEPOX formation can be reasonably simplified, and gas-particle reactive uptake can be efficiently calculated as it is in many global chemistry-transport models. Moreover, as indicated in Figure 4, there is now a wealth of field observations of IEPOX-derived SOA from a range of environments that can be used as constraints.

2.1.2.3. Future Work in Multiphase Chemistry of IEPOX-SOA

While the correlation of IEPOX-SOA and sulfate and the role of other particle properties might vary with location and season [*Surratt et al*., 2010; *Pye et al*., 2013], it can be used to connect trends in anthropogenic sulfate and IEPOX-SOA over time in a quantitative way. For example, a 1 $\mu g/m^3$ decrease in sulfate can lead to a 0.2–0.42 $\mu g/m^3$ decrease in isoprene SOA [*Xu et al*., 2015b; *Blanchard et al*., 2016; *Xu et al*., 2016]. Comparison of multiyear chemistry-climate models to such data taken from around the Northern Hemisphere and the tropics would enable us to gain insights into the variability of the anthropogenic-biogenic interactions and parameterize such effects based on the characteristics of different regions (e.g., pH, water content, and sulfate concentrations), so as to quantify an anthropogenic aerosol climate forcing *via* IEPOX.

In addition to advancing implementation into models, additional mechanistic and product studies of IEPOX multiphase chemistry are needed. We note that literature H^* values for IEPOX uptake span 2 orders of magnitude [*M. N. Chan et al*., 2010; *Eddingsaas et al*., 2010; *Pye et al*., 2013; *Gaston et al*., 2014; *Nguyen et al*., 2014a; *Budisulistiorini et al*., 2015]. Also, measurements of Setschenow salting constants (K_S) are particularly scarce. There is a critical lack of experimental data for H^* and K_S of IEPOX, and ISOPOOH in atmospherically relevant inorganic aerosol components, which are needed to establish efficient parameterizations of IEPOX-SOA in atmospheric models [*Waxman et al*., 2015]. Laboratory chamber experiments are also needed to better constrain and evaluate the opposing effects of particle water on IEPOX-SOA formation [*Xu et al*., 2015b, 2016]. As noted above, *Gaston et al*. [2014] found that variations in RH between 30 and 70% changed the IEPOX reactive uptake coefficient by a factor of 2, likely due to associated changes in acidity. Not investigated, though, was the associated competition between sulfate and water as nucleophiles, which would affect the consequent distribution of products, as in *Riva et al*. [2016b], and the SOA volatility.

Sulfate, particle water, and particle acidity could have convoluted interactions in the atmosphere, affecting IEPOX-SOA formation [*Xu et al*., 2015b, 2016]. For example, it was shown that the AMS IEPOX-SOA PMF factor is strongly correlated with sulfate but not with particle water and acidity [*Xu et al*., 2015b]. The lack of correlation between IEPOX-SOA and acidity could arise from persistence of low particle pH (hence, acidity is not limiting) and/or change of particle pH during atmospheric transport [*Budisulistiorini et al*., 2013, 2015; *Guo et al*., 2015; *Xu et al*., 2016]. The lack of correlation between IEPOX-SOA and water may be due to compensating effects between increase of particle surface area with particle water and decrease in aqueous-phase reactions due to dilution by particle water. Recently, rapid formation of isoprene SOA via IEPOX uptake has also been observed downwind of power plant plumes, where sulfate enhances IEPOX-SOA formation due to both enhanced particle surface area and particle acidity [*Xu et al*., 2016].

There may well be other effects of changing RH, as in other systems [*Volkamer et al*., 2009; *Kampf et al*., 2013] such as glyoxal related to changes in particle composition, phase, morphology, or viscosity. Whether changes in the uptake rate and associated IEPOX-SOA properties would have spatial gradients similar to model predictions of glyoxal-SOA between the western and southeastern U.S. [*Knote et al*., 2014b] will ultimately need to be assessed.

While a robust mechanistic understanding of the competing effects of sulfate, water, and acidity on IEPOX-SOA formation is developing, an expanded set of laboratory measurements at RH exceeding 70% could

help improve model parameterizations. *Eddingsaas et al*. [2010], owing to the lack of data, assumed that sulfate has the same nucleophilic strength as nitrate, an assumption that affects the calculated reaction constants between IEPOX, acid, and nucleophiles. Accurate measurements of the reaction rates coefficients between IEPOX, acids, and possible nucleophiles (H_2O, HSO_4^-, NO_3^-, organics, etc.) in aqueous, acidic aerosol relevant to the atmosphere are imperative. The uncertainties in these parameters including H^* highly limit the ability to predict the reactive uptake rate of IEPOX in the atmosphere, as demonstrated in *Xu et al*. [2016]. Further, there remains a limited understanding of IEPOX-SOA formation in mixed organic-inorganic particles, such as inorganics coated with SOA as discussed above [*Gaston et al*., 2014; *Riva et al*., 2016b]. Future models will ultimately need to account for this complex dependence of IEPOX uptake kinetics on mixed organic-inorganic particles.

2.1.2.4. Other Low-NO_x SOA Pathways From Isoprene

The previous section discussed reactions of IEPOX, which in terms of molar yield is the major product formed from oxidation of ISOPOOH. However, recent studies have shown that ISOPOOH reaction products with smaller molar yield may also be important sources of SOA mass if their oxidation products efficiently partition to the particle phase [*St. Clair et al*., 2016]. Oxidation of ISOPOOH can also produce a peroxy radical, which can subsequently react with HO_2 or NO_x to produce semivolatility and low-volatility products that partition to the condensed phase. Several studies have shown that SOA could form from low-NO_x (RO_2+HO_2 dominant) isoprene photooxidation under dry conditions where IEPOX reactions were suppressed and that organic peroxides were a significant fraction of the OA [*Kroll et al*., 2006; *Surratt et al*., 2006; *Xu et al*., 2014]. Later studies explored the chemistry in more detail. *Krechmer et al*. [2015] measured the molecular composition and concentrations of gas-phase oxidation products of an ISOPOOH standard using the Nitrate Ion CIMS instrument and formation of SOA with an AMS instrument. They estimated the SOA mass yield from the reaction of ISOPOOH with OH in the absence of seed particles as 4%, mainly due to formation of LVOC. *J. Liu et al*. [2016] measured SOA mass yields from isoprene photochemical oxidation of up to 15% under conditions where the RO_2 reacted primarily with HO_2. They also observed a dependence of the SOA yield on the relative amounts of isoprene and H_2O_2 (a proxy for HO_2 level), suggesting the potential for chamber radical conditions to strongly impact isoprene SOA yields even at low NO and low RO_2. Moreover, the higher SOA yields found by *J. Liu et al*. [2016] compared to *Krechmer et al*. [2015] suggests that semivolatile products from isoprene oxidation not passing through the ISOPOOH pathway may also contribute significantly to SOA mass formation through unresolved mechanisms. Using the FIGAERO CIMS instrument, they measured the molecular composition of both the gas and particle phases and identified a highly oxygenated compound, $C_5H_{12}O_6$, as the largest contributor to the condensed-phase mass. Both studies proposed that LVOC compounds produced from oxidation of ISOPOOH in the presence of HO_2 are potentially important higher-generation isoprene SOA components. In addition, *Riva et al*. [2016b] measured similar LVOC compounds in isoprene-derived SOA and showed that they may well undergo condensed-phase chemistry that further alters the ultimate yield and volatility of the SOA formed initially. Similarly, low-NO_x non-IEPOX pathways were also suggested to contribute to SOA mass in southeastern United States [*Riva et al*., 2016c].

Further experiments on the product distribution as a function of oxidation conditions and of aging time scales are warranted. Later generation steps leading to formation of small molecular products such as HCHO, HCOOH, and glyoxal are not fully understood, nor are the fates of the highly oxygenated ISOPOOH-derived products. A similar situation may exist with regard to small-yield, but potentially important, products for SOA formation. While much of the focus to date has been on SOA formation from OH-driven oxidation of isoprene, ozonolysis and reaction with the nitrate radical may require further study. For example, reactions of Criegee radicals produced from isoprene ozonolysis with other oxygenated VOC have been implicated as a potential source of condensable vapors or vapors subject to acidic multiphase chemistry [*Inomata et al*., 2014; *Riva et al*., 2016a, 2017]. While the overall yields of SOA appear to be small (~0.5%) for some ozonolysis conditions [*Inomata et al*., 2014], it is likely that aging through aqueous acidic chemistry enhances the SOA pathway. Given the large mass emission rates of isoprene on a global basis, identification of major atmospheric oxidation products of isoprene relevant to SOA formation is an essential step in constraining SOA yields in regional and global models.

2.2. Role of NO_x in BVOC-Derived SOA

The oxidation chemistry of compounds like isoprene or monoterpenes exhibits particularly complex dependencies on NO_x concentration. For example, isoprene SOA yields in some studies increase and then decrease

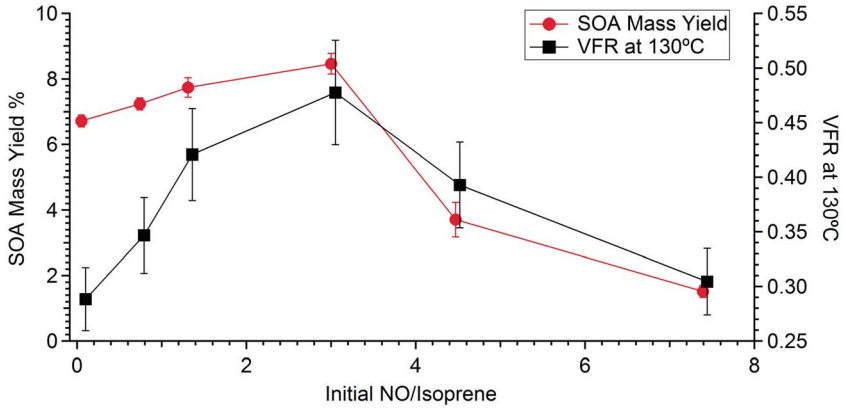

Figure 5. Dependence of SOA mass yield and volume fraction remaining on initial NO/isoprene ratio, adapted from *Xu et al.* [2014].

as the NO_x concentrations increase [*Kroll et al.*, 2006; *Ng et al.*, 2007b; *Xu et al.*, 2014]. In another study, addition of NO_x has a small effect on the SOA yield up to a threshold level, above which SOA yields decrease [*J. Liu et al.*, 2016]. In that study, *J. Liu et al.* [2016] found that with increasing NO, the abundance of $ISOP(OOH)_2$ decreased, while a series of organic nitrates, some of which have been observed in the ambient atmosphere [*Lee et al.*, 2016], increased in both the gas and particle phases. Such differences in the SOA yield as a function of NO_x from the same precursor likely reflect different modes of chamber operation, different absolute concentrations of NO, and the consequent nonlinear response and time evolution of radical families with NO_x and aging time. Studies have shown that the RO_2+NO_2 reaction in isoprene photooxidation under the "high NO_x" condition can potentially lead to substantial SOA formation through further oxidation of peroxy methacryloyl nitrate (MPAN), resulting in SOA yields that can be as high as in "low-NO_x" experiments [*A. Chan et al.*, 2010; *Y. H. Lin et al.*, 2012; *Lin et al.*, 2013b; *Nguyen et al.*, 2015]. Recently, *Xu et al.* [2014] and *D'Ambro et al.* [2016] found that both the volatility and mass yield of chamber-generated isoprene SOA exhibit a nonlinear dependence on NO_x level (Figure 5). The nonlinear behavior in volume fraction remaining (VFR) upon heating was interpreted as being possibly the result of an optimum NO_x concentration for facilitating oligomerization [*Nguyen et al.*, 2011a]. Organic peroxy radical-NO_x chemistry could be the explanation for this nonlinearity in SOA yields since the relative roles of functionalization reactions (decreasing volatility) and fragmentation reactions (increasing volatility) change with NO_x levels [*Xu et al.*, 2014], although the composition of oligomers and their volatility likely also depend on NO_x conditions [*Hallquist et al.*, 2009; *Xu et al.*, 2014].

Organic nitrate functional groups formed as a secondary but nonnegligible branch of RO_2+NO have been observed to contribute significantly to atmospheric aerosol in field studies [*Brown et al.*, 2009; *Day et al.*, 2010; *Zaveri et al.*, 2010; *Beaver et al.*, 2012; *Rollins et al.*, 2012; *Brown et al.*, 2013; *Fry et al.*, 2013; *Lin et al.*, 2015; *Xu et al.*, 2015b, 2015a; *Lee et al.*, 2016] and chamber experiments [e.g., *Boyd et al.*, 2015; *D'Ambro et al.*, 2016; *J. Liu et al.*, 2016]. The importance of BVOC+NO_3 chemistry as a nighttime SOA formation mechanism has gained recent attention [*Griffin et al.*, 1999; *Ng et al.*, 2008; *Rollins et al.*, 2012; *Fry et al.*, 2014; *Boyd et al.*, 2015; *Rindelaub et al.*, 2015; *Xu et al.*, 2015b; *Nah et al.*, 2016a], as described in a recent review [*Ng et al.*, 2017]. Once formed, particulate organic nitrates can hydrolyze, photolyze, deposit, and/or potentially undergo further oxidation. The photochemical fate and lifetime of particulate organic nitrates depend highly on their molecular structure [*Hinks et al.*, 2016; *Nah et al.*, 2016a]. Taken together, these measurements clearly indicate that nitrate radical chemistry can play an important role in SOA formation, but its effects on SOA yields and organic nitrate formation will likely vary with the structure of the BVOC. Moreover, the importance of NO_3 chemistry is expected to vary vertically in the atmosphere, even within the first 1 km, given that the largest impact is at night when vertical mixing is suppressed and isoprene emissions have ceased [*Brown et al.*, 2009].

The potential for NO_x to affect SOA extends beyond changing the fate of RO_2 radicals and thus the volatility distribution of BVOC oxidation products. These include enhancing acid-catalyzed accretion reactions in the particle phase through nitric acid partitioning and the condensed-phase reactivity of organic nitrates or

other products formed under high NO_x conditions. For example, methylglyceric acid (MGA) and oligoesters composed of MGA units are routinely detected in the SOA formed during high NO_x oxidation of isoprene [*Surratt et al*., 2006; *Szmigielski et al*., 2007; *Lin et al*., 2013b; *D'Ambro et al*., 2016]. MGA and its oligomers are tracers of isoprene SOA in ambient particles under high NO_x conditions [*Rattanavaraha et al*., 2016]. These SOA tracers suggest that multiphase chemistry of small oxygenated VOC may play an important role in SOA formation under high NO_x conditions, where overall yields might be lower but driven by a significant contribution from accretion chemistry. For example, it was recently shown that 2-methyglyceric acid (2MGA), a tracer for isoprene SOA under high NO_x conditions, is semivolatile and its accommodation in aerosol water decreases with increasing acidity [*Nguyen et al*., 2015]. In addition, the production of SOA precursors such as methacrylic acid epoxide and methacrolein was found to be negligible. In addition to acidity, RH reportedly affected the particle-phase concentrations of 2MGA [*H. Zhang et al*., 2011]. Thus, the formation of 2MGA and its oligoesters was enhanced in particle-phase under lower RH compared to higher RH conditions. As noted above, future work requires more systematic assessment of the SOA response to atmospheric concentrations of NO and NO_2, and the NO/NO_2 ratio, and the role of particle-phase acidity and water content in order to better quantify the SOA formation potential of BVOC oxidation in the presence of NO_x.

2.3. Future Research Needs on Role of NO_x in SOA

Laboratory experiments are often performed under limiting NO_x conditions to restrict the peroxy radical to react with either NO (often called "high-NO" condition) or HO_2 (often called "low-NO" condition) in order to simplify the mechanistic interpretation of the data. However, these conditions are not necessarily representative of radical concentrations found in the ambient atmosphere. In the absence of direct measurements of peroxy radicals in laboratory experiments, studies sometimes rely on the hydrocarbon/NO_x ratio as a metric to define NO_x condition in experiments [*Presto et al*., 2005b; *Song et al*., 2005; *L. J. Li et al*., 2015; *X. Liu et al*., 2016; *Deng et al*., 2017]. However, this definition is overly general and does not necessary correspond to specific peroxy radical fates that affect SOA formation in the atmosphere [*Wennberg*, 2013]. Further, it has been shown that the fate of peroxy radicals could be drastically different even for experiments conducted under the same hydrocarbon/NO_x ratio [*Ng et al*., 2007a]. As such, significant effort in future laboratory experiments should aim to more realistically, and in an internally consistent way, span the concentrations of NO, NO_2, HO_2, and RO_2 found in the atmosphere. In addition, a focus on measuring HO_2 and individual RO_2 with mass spectrometry [e.g., *Ehn et al*., 2014; *Berndt et al*., 2015] so as to directly observe RO_2 responses to $NO/HO_2/RO_2$ perturbations would aid in mechanism development. For example, a new technique using bromide chemical ionization mass spectrometry (Br-CIMS) has been recently developed for the direct measurement of HO_2 [*Sanchez et al*., 2016]. As measurement techniques advance in terms of quantifying $NO/HO_2/RO_2$, gas-phase chemistry mechanisms need to be evaluated and improved to reproduce measured radical concentrations.

Current atmospheric SOA models treat the effects of NO_x level at best as a linear combination of SOA formation under two extremes ("low NO_x" and high NO_x conditions, where "RO_2+HO_2" and "RO_2+NO" reaction pathways dominated) [*Henze et al*., 2008; *Lane et al*., 2008; *Pye et al*., 2010]. However, NO_x has complex nonlinear effects on SOA formation since several factors such as RO_2 isomerization reactions and aerosol volatility change with NO_x levels. Note that a "linear two extremes" approach used in current models is insufficient to represent "nonlinear NO_x effects," as described above. In addition, chamber yield measurements do not reflect how properties of SOA, e.g., volatility and particle-phase chemistry, e.g., oligomerization, change with NO_x. Understanding the functional relationship between SOA formation/properties and NO_x is important for parameterizing and extrapolating laboratory findings to atmospheric conditions. In addition, as NO_x increases, the competing roles of decreased RO_2-HO_2 reaction products and the increase of organic nitrates contribute to SOA formation. While current chamber yields implicitly include mass yields of organic nitrates, these yields could vary in the atmosphere due to varying radical and oxidant regimes. Further laboratory experiments and field measurements are needed to constrain the formation, and yields of organic nitrates. Given the potentially labile nature of the nitrate moiety in condensed phases, further work on the fate of organic nitrates in SOA is also needed [*Darer et al*., 2011; *Hu et al*., 2011; *Boyd et al*., 2015; *Rindelaub et al*., 2015; *Hinks et al*., 2016; *Lee et al*., 2016; *Nah et al*., 2016a]. Field measurements that provide vertically resolved observations of nocturnal NO_3-BVOC chemistry are necessary for constraining the ambient importance of this

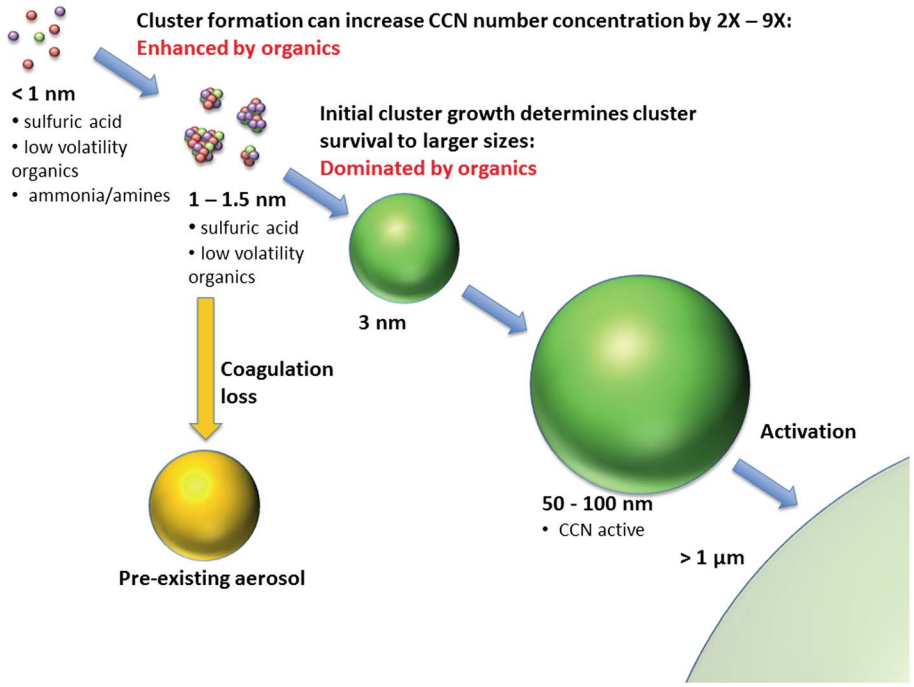

Figure 6. A schematic illustrating the participation of organic oxidation products as newly formed clusters either grow and survive to CCN-active sizes or are lost by coagulation with the preexisting aerosol.

pathway. It is likely that enough observations now exist for models to constrain the abundance and fates of particulate organic nitrates and therefore simulate the dual roles of NO_x emissions on SOA formation.

Incorporating such mechanistic effects of NO_x (and other anthropogenic pollutants such as SO_2) into models is required to assess the net outcome on SOA budgets. For example, in recent studies using a chemical transport model over the southeastern United States, *Marais et al.* [2016] predicted that isoprene SOA concentrations increase with decreasing NO_x but decrease more strongly when SO_2 emissions decrease due to the effects of sulfate on aerosol acidity and volume. However, most previous model predictions of the competing roles of NO_x and SO_2 (including the modeling study listed above) need to be revised in the light of recent measurements, as discussed above. In addition, mechanistic insights from laboratory studies incorporated into models should be tested against measurements from different regions of the world that have been the foci of recent intensive measurements, such as the southeastern United States, the Amazon, and boreal forests, to assess factors controlling isoprene SOA such as sulfate level, aerosol phase water, particle acidity, and NO_x.

Volatility, phase state (solid, liquid, and semisolid), and viscosity are important fundamental properties that affect mass and number concentrations of all SOA types (including biogenic SOA). In sections 3 and 4 below, we discuss some of the important advances in understanding how these properties influence SOA.

3. Low-Volatility and Extremely Low Volatility Organics

Although particles larger than about 100 nm in diameter generally act as efficient CCN under common atmospheric conditions [*Petters and Kreidenweis*, 2007], these particles often originate from smaller particles that were nucleated or were directly emitted from combustion or other processes [*Merikanto et al.*, 2009; *Pierce and Adams*, 2009; *Spracklen et al.*, 2010]. The competition between the decrease of number concentrations of these smaller particles due to coagulation and their growth rate to larger sizes, which affects their survival against coagulation, determines their contribution to the budget of CCN number concentrations. Figure 6 schematically illustrates how the initial molecular cluster formation and growth can be enhanced by low-volatility organics. Since newly formed smaller particles could especially coagulate with larger preexisting aerosol [*Seinfeld and Pandis*, 1998; *Kuang et al.*, 2010], they could increase the CCN number concentration

budget by factors of 2 to 9 [*Kuang et al*., 2009] at high enough growth rates. Organic vapors responsible for the early stages of particle growth are often highly oxygenated molecules (HOMs), which span a wide range of volatility ranging from ELVOC compounds (saturation vapor concentration, $C^* < 10^{-4.5}$ μg m^{-3}) to low-volatility (LVOC, $10^{-4.5} \leq C^* \leq 10^{-0.5}$ μg m^{-3}) and semivolatile (SVOC, $10^{-0.5} \leq C^* \leq 10^{2.5}$ μg m^{-3}) [*Ehn et al*., 2012; *Trostl et al*., 2016]. Thus, initial cluster formation (nucleation) is likely driven by multicomponent condensation of various inorganics as well as ELVOC [*Kulmala et al*., 2007; *Sipila et al*., 2010; *Petaja et al*., 2011; *Kulmala et al*., 2013; *Ehn et al*., 2014; *Trostl et al*., 2016] or of organic compounds that form dimers/trimers through particle-phase accretion chemistry or acid-base chemistry [*Keskinen et al*., 2013; *Riccobono et al*., 2014]. Subsequent growth of these clusters to form SOA is mainly through gas-particle partitioning of organic compounds in the ELVOC/LVOC/SVOC range. Measurements have shown that oxidized organics, e.g., from α-pinene ozonolysis, play a significant role in particle growth even at 10 nm sizes [*Claeys et al*., 2009; *Bzdek and Johnston*, 2010; *Winkler et al*., 2012; *Zhang et al*., 2012; *Trostl et al*., 2016]. Other studies have also found that the growth of new particles can best be explained if a large fraction of the SOA condenses as if it is nonvolatile [*Barsanti et al*., 2011; *Pierce et al*., 2011; *Riipinen et al*., 2011].

In addition to their role in new particle formation and growth, low-volatility organic compounds have also been reported to contribute substantially to larger SOA particle sizes (>10 nm). Thus, recent studies suggest that a major fraction of atmospheric SOA has an effective volatility considerably lower than what was previously assumed, such that much of SOA can be treated as effectively nonvolatile—i.e., of such low volatility that it does not evaporate under atmospheric conditions [*Wehner et al*., 2005; *Ehn et al*., 2007; *Cappa and Jimenez*, 2010; *Pierce et al*., 2011; *Vaden et al*., 2011; *Hakkinen et al*., 2012; *Shrivastava et al*., 2013a; *Ehn et al*., 2014; *Kolesar et al*., 2015a; *Lopez-Hilfiker et al*., 2015, 2016].

3.1. Advances in Gas-Phase Chemistry of Low-Volatility Organics

The production of SVOC, LVOC, and ELVOC can result from either multigenerational aging wherein a few functional groups are added from each reaction [*Jimenez et al*., 2009; *Kroll et al*., 2011; *Donahue et al*., 2012b, 2012a] or from rapid addition of many functional groups after a single reaction between a VOC and oxidant [*Crounse et al*., 2013; *Ehn et al*., 2014; *Trostl et al*., 2016]. This rapid production is thought to result from autoxidation of the organic radical intermediates by O_2, especially from endocyclic monoterpene ozonolysis [*Crounse et al*., 2013; *Ehn et al*., 2014; *Rissanen et al*., 2014; *Jokinen et al*., 2015; *Rissanen et al*., 2015]. In autoxidation, peroxy radicals (RO_2) produced after initial reaction with an oxidant (e.g., OH or O_3) undergo a unimolecular isomerization reaction to produce an alkyl radical and a hydroperoxide functional group. This alkyl radical can react with O_2 to again become an RO_2. This process can continue until the RO_2 reacts with NO, HO_2, another RO_2, or through OOH radicals formed by RO_2 isomerization [*Crounse et al*., 2012; *Ehn et al*., 2014] and thus is a pathway by which functional groups (specifically hydroperoxides) can be rapidly added to the molecule. In the absence of autoxidation, subsequent reaction of the oxidation products can lead to further functional group addition and is a multigeneration pathway to lower volatility multifunctional products. The key difference is that autoxidation produces lower volatility products on a much more rapid time scale than multigeneration oxidation.

Due to their exceptionally low volatility, ELVOC condense essentially irreversibly onto growing particles at a rate controlled by the Fuchs-adjusted particle surface area. The specific importance depends on their concentrations, but ELVOC have the capability to overcome Kelvin effects and grow the smallest particles during a new particle formation event [*Trostl et al*., 2016]. This can be contrasted with the phase partitioning of semivolatile organics into sufficiently low viscosity particles, as the higher volatility of LVOC and especially SVOC allows them to both condense and evaporate. The process of equilibrium growth ultimately favors the growth of particles with diameters exceeding ~100 nm as opposed to growth of smaller particles below the CCN-relevant range. This is because equilibrium growth is essentially volume controlled, whereas growth by nonvolatile condensation is surface area controlled [*Seinfeld and Pandis*, 1998]. However, the relative importance of ELVOC, LVOC, and SVOC in this framework is influenced by particle-phase properties such as viscosity as this can influence the time scale for reaching equilibrium, discussed further below. In addition to their contribution to condensation-driven growth, recent work has also shown that ELVOC can nucleate homogeneously [*Kirkby et al*., 2016] or with inorganics to form new particles [*Ehn et al*., 2014; *Riccobono et al*., 2014]. A global modeling study showed that inclusion of

prompt gas-phase ELVOC formation from monoterpene oxidation increased the number concentration of CCN (at 1% supersaturation) in pristine areas such as the Amazon compared to the control simulation. However, this increase was minor (~2.25%), likely due to competing effects from other sinks such as condensational sinks for the remaining ELVOC, which increase with increasing particle number concentrations [*Jokinen et al*., 2015].

In addition to these new insights into monoterpene organic peroxy radical chemistry, there is good evidence that larger molecular weight low-volatility products that contribute to SOA can be formed from ozonolysis reactions of monoterpene in the gas phase [*Docherty and Ziemann*, 2003; *Kristensen et al*., 2014, 2016]. Commonly identified products in the SOA are multifunctional C_{16}–C_{19} esters with 6–10 oxygens. The current mechanistic explanations for these products, which have been measured in ambient SOA [*Kristensen et al*., 2016], remain inconclusive. Hypotheses include reactions of stabilized Criegee with oxygenated VOC or acyl peroxy radical self-reactions followed by condensed-phase conversion of the peroxide to an ester [*Docherty and Ziemann*, 2003; *Kristensen et al*., 2014, 2016]. Given that both suggested processes are likely to have a nonlinear dependence on monoterpene oxidation rates, further experiments should aim to constrain the production yields of such dimers under atmospherically relevant oxidation rates.

3.2. Role of Heterogeneous/Multiphase Accretion Processes

Although measurements have shown formation of low-volatility organics in the gas phase as discussed in the previous section, the condensing organic molecules do not necessarily have to be ELVOC to ultimately be treated as effectively nonvolatile. Similar kinetically limited particle growth may also occur if LVOC or SVOC undergo rapid heterogeneous/multiphase reactions within the particles to form lower or even extremely low volatility products, such as organic accretion products, dimers/oligomers, organosulfate formation, or salts [*Grosjean et al*., 1978; *Jang and Kamens*, 2001; *Barsanti and Pankow*, 2004; *Claeys et al*., 2004; *Gao et al*., 2004; *Kalberer et al*., 2004; *Tolocka et al*., 2004; *Barsanti and Pankow*, 2005, 2006; *Liggio and Li*, 2006; *Smith et al*., 2008; *Barsanti et al*., 2009; *Smith et al*., 2010; *Wang et al*., 2010; *Ziemann and Atkinson*, 2012; *Shiraiwa et al*., 2013b; *Yli-Juuti et al*., 2013; *Roldin et al*., 2014]. If these reactions are rapid enough (e.g., the molecular lifetime due to heterogeneous reactions is substantially shorter than the lifetime due to evaporation), the condensing molecules can be treated as effectively nonvolatile although their initial saturation vapor pressure may be much larger than ELVOC [*Kurtén et al*., 2016]. A number of heterogeneous/multiphase oligomer-forming reactions can occur on time scale relevant to the atmosphere, which can significantly alter SOA composition and yields [*Ziemann and Atkinson*, 2012]. For example, under clean conditions, the most likely oligomers are peroxyhemiacetals formed from reactions of hydroperoxides and carbonyls, and esters formed from reactions of alcohols and carboxylic acids. Under polluted conditions, hemiacetals formed from reactions of carbonyls and alcohols, and esters from reactions of isoprene, might be important for oligomer formation [*Ziemann and Atkinson*, 2012]. In addition, the presence of hydrophobic organic molecules of anthropogenic origin, such as polycyclic aromatic hydrocarbons (PAHs), during SOA formation has been shown to significantly increase fraction of nonvolatile components including oligomers, increase SOA viscosity, and reduce the evaporation rates and effective volatility of SOA [*Vaden et al*., 2011; *Zelenyuk et al*., 2012, 2017]. PAHs are in turn shielded by viscous SOA coatings, especially at low temperature and relative humidity in the atmosphere, which increases the oxidation lifetime, global long-range transport and health risks from PAHs [*Shrivastava et al*., 2017]. The presence of PAHs was also shown to significantly increase SOA mass loadings and particle number concentrations [*Zelenyuk et al*., 2017].

Further, *Kolesar et al*., 2015a measured heating-induced evaporation kinetics of several anthropogenic and biogenic SOA precursor classes and also suggested that decomposition of effectively nonvolatile oligomers (or dimers) likely plays a major role in controlling SOA evaporation and that oligomer-forming reactions must be rapid on time scales less than a minute. *Trump and Donahue* [2014] similarly show that oligomer decomposition can play an important role in limiting evaporation rates of SOA. Both studies conclude that reversible oligomerization (or dimerization) can, at least in part, explain the hysteresis between observations of SOA formation and evaporation. Also, as discussed in the section on IEPOX-SOA, a substantial fraction of some of the semivolatile IEPOX-SOA components have been found in the particle phase, mostly likely due to formation of accretion products [*Isaacman-VanWertz et al*., 2016; *Lopez-Hilfiker et al*., 2016].

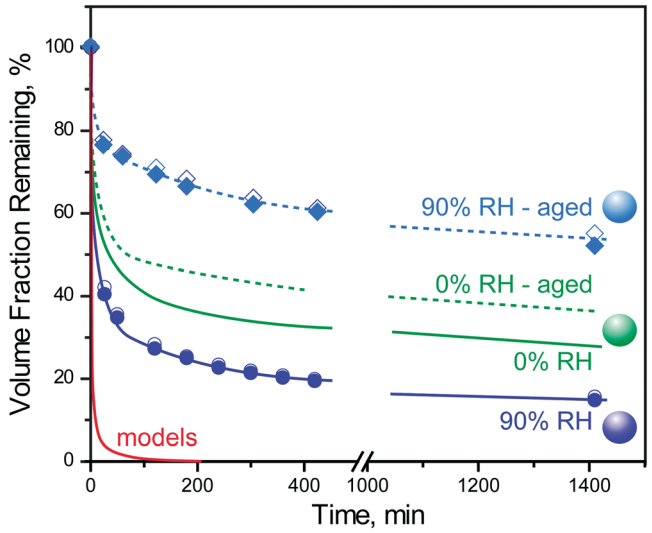

Figure 7. Effects of relative humidity on the room temperature evaporation kinetics of SOA particles, generated based on *Wilson et al.* [2015]. Each curve shows the time-dependent evaporation behavior of particles that are held in evaporation chamber filled with activated carbon to scavenge organic gases. The observations are compared with a model prediction (red line) of the evaporation behavior based on the volatility distribution of SOA as determined from analysis of SOA growth experiments in *Pathak et al.* [2007].

3.3. Role of Aerosol Water in Accretion Products

Aerosol water is thought to play an important role in particle-phase oligomerization and organic salt formation [*Hastings et al.*, 2005; *Loeffler et al.*, 2006; *Altieri et al.*, 2008; *Axson et al.*, 2010; *Nguyen et al.*, 2011b; *H. Zhang et al.*, 2011; *Tan et al.*, 2012], in terms of both the initial formation step and the long-term stability, thereby affecting SOA volatility. For example, Figure 7 adapted from a recent study [*Wilson et al.*, 2015] showed that SOA particles formed at high RH (~90%) and "aged" for ~24 h (by leaving the particles in the Teflon chamber where they were initially produced) exhibit lower effective volatility compared to particles formed and aged under dry conditions (labeled as 0% RH in Figure 7). However, when the same particles formed at high RH were characterized prior to their aging, they were found to be more volatile (higher effective volatility) compared to the equivalent dry case. This behavior illustrates the complexity associated with organic particle-RH interactions, which must be better understood mechanistically. The RH effect on the SOA volatility is governed by both kinetic and thermodynamic processes. The aerosol water content influences the thermodynamics of various accretion reactions [e.g., *Barsanti and Pankow*, 2005, 2006], and the SOA viscosity, and thus indirectly the molecular diffusion (mixing) within the particle phase (section 4.1). Limited mixing, imposed by low particulate water content, can influence both the uptake of SVOC and the evaporation of SVOC, which can decrease the effective SOA volatility (section 4.2), at least for fresh SOA. Figure 7 also illustrates that in comparison to measurements, predictions of evaporation behavior of SOA (red line) based on effective volatility of SOA determined from an analysis of SOA growth experiments (using seven-species VBS in *Pathak et al.* [2007]) show much faster evaporation. As stated earlier, oligomerization in the particle phase is one explanation of slow evaporation [*Shrivastava et al.*, 2013a; *Trump and Donahue*, 2014; *Kolesar et al.*, 2015a]. In other words, the distribution of product volatilities inferred from analysis of particle growth experiments is inconsistent with the product volatility distribution inferred from particle evaporation experiments [*Shrivastava et al.*, 2013a; *Wilson et al.*, 2015]. Investigation into the extent to which particle-phase reactions control net uptake of organics and contribute to SOA formation under atmospherically relevant conditions needs to be a continued focus.

3.4. Comparison of Various Pathways Affecting SOA Volatility

Figure 8 illustrates the different pathways affecting SOA volatility, as discussed above. In the traditional pathway, SOA is formed by condensation of semivolatile organic vapors on preexisting nuclei, and this SOA remains semivolatile SOA (referred to as SVSOA) throughout its life cycle in the atmosphere. The time scale of SVSOA formation depends on multigenerational chemistry that creates semivolatile organic vapors and their condensation. In the second pathway, subsequent to its formation, a vast majority of the SVSOA compounds undergo rapid particle-phase oligomerization/accretion [*Kroll et al.*, 2007; *Cappa and Wilson*, 2011; *Hall and Johnston*, 2011; *Shrivastava et al.*, 2013a; *Kolesar et al.*, 2015a; *Lopez-Hilfiker et al.*, 2016] and is converted to low-volatility SOA that is "effectively nonvolatile" at atmospheric conditions [*Cappa and Jimenez*, 2010] and is referred to as NVSOA [*Shrivastava et al.*, 2015]. NVSOA formation could be fairly rapid due to oligomerization reactions that occur on the order of minutes as indicated in a few recent studies [*Cappa and*

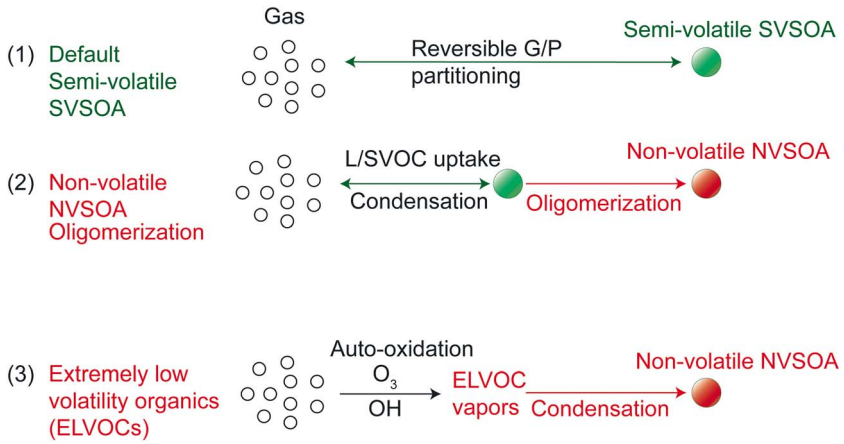

Figure 8. Pathways to formation of low-volatility and extremely low volatility organics as compared to the default semivolatile SOA pathway used in most aerosol models.

Wilson, 2011; *Kolesar et al*., 2015a]. It is important to note that NVSOA formation through the oligomerization pathway is different from direct condensation of nonvolatile gas-phase oxidation products, as assumed in several global models [*Tsigaridis et al*., 2014]. First, the size-dependent oligomerization rates in pathway 2 might not match the size-dependent condensation rates in pathway 1, which may lead to differences in size distribution evolution. In addition, the gas-particle distribution of semivolatile SOA precursors and aerosol condensational and coagulation sinks are likely very different between the two pathways, which could greatly affect SOA evolution in the atmosphere. In the third pathway, rapid autoxidation leads to formation of ELVOC. Autoxidation occurs on a much faster time scale as compared to several generations of chemistry needed for SVSOA formation. Also, sulfate complexes of volatile molecules can form LVOC or ELVOC on the time scale of seconds (or faster) and add to the pool of species that form LVSOA via pathways 2 and 3 [*Zhang et al*., 2004; *Wang et al*., 2010; *Kurtén et al*., 2015]. However, oligomer formation may be reduced by dilution of monomers, and oligomers can potentially decompose [*Roldin et al*., 2014; *Trump and Donahue*, 2014; *Kolesar et al*., 2015b; *Lopez-Hilfiker et al*., 2015]. Such behavior might, in fact, be used to distinguish between salt formation and organic molecule cross reactions, which likely have different thermal stabilities, as routes to extremely low volatility SOA. Each of these processes still fit within OA partitioning framework, but each acts to lower OA volatility or slow evaporation of OA.

Oligomerization/accretion processes affect SOA particle concentrations and their lifetimes. For example, a global modeling study [*Shrivastava et al*., 2015] compared SOA loadings calculated by the default semivolatile, purely reversible partitioning approach to one in which particle-phase processes rapidly and irreversibly lead to the formation of effectively nonvolatile SOA (NVSOA), as illustrated in Figure 9. This approach was also

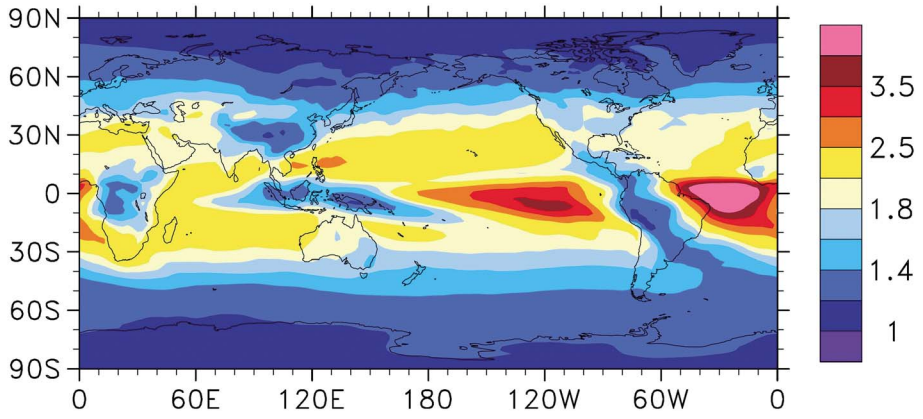

Figure 9. Simulated ratio of global annual mean SOA burdens from the nonvolatile to semivolatile SOA treatment, adapted from *Shrivastava et al*. [2015].

applied in a previous global modeling study [*Tsigaridis and Kanakidou*, 2003] to investigate the sensitivity of SOA to particle-phase chemical reactions that form nonvolatile compounds and/or inhibition of evaporation by other nonvolatile components in particles. The NVSOA approach led to a substantial increase in the average lifetime of SOA (by a factor of 3), and the SOA burden (by up to a factor of 5), most notably in continental outflow over clean marine environments (Figure 9). Since cloud albedo is especially sensitive to variations in aerosol levels over pristine locations where particle number concentrations are small, such as the oceans [*Carslaw et al*., 2013], the predicted increase in SOA burdens could have large implications on cloud albedo and radiative forcing. Another modeling study investigated the sensitivity of SOA to several parameters, using a variance-based approach within a regional model, and found that the rapid decrease of effective volatility of SOA due to oligomer formation was the most influential factor controlling SOA concentrations [*Shrivastava et al*., 2016].

3.5. Further Research Needs in Low-Volatility SOA

Recent laboratory studies have indicated that the detection of newly formed particles (1–2 nm in diameter) depends strongly upon their chemical composition. Sub-3 nm particles composed of oxidized organics are detected by condensation particle counters with orders-of-magnitude-less sensitivity than sub-3 nm particles composed of ammonium sulfate [*Kangasluoma et al*., 2014]. As a result, the ambient concentration of newly formed particles, the composition of which is often dominated by oxidized organic molecules, may be significantly underestimated. Uncertainties in cluster composition therefore have substantial impacts on accurately determining ambient organic cluster concentrations and their impact on the >2 nm in diameter particle number concentration budget. Precise measurements of the oxidized organic content of newly formed clusters are needed in order not only to assess the contribution of oxidized organics to cluster formation, activation, and growth, but also to determine basic quantities such as the cluster number concentration budget. Understanding the mechanisms by which particles grow to CCN size through the condensation and/or reaction of oxidized organic vapors across the spectrum of compound volatilities is key to CCN production.

As with SOA, in general, one challenge in assessing the importance of the formation of low-volatility SOA stems from the so far limited understanding of the linkage of these pathways to VOC precursor identity and concentrations, oxidant identity and concentrations, NO_x levels, concentrations of atmospheric bases (e.g., ammonia and amines), and atmospheric variables such as temperature, relative humidity, and light availability. For example, the effect of temperature and NO_x on gas-phase autoxidation and subsequent HOM formation has not been fully quantified. It has also been demonstrated that gas-phase production of ELVOC is strongly linked to precursor VOC [*Ehn et al*., 2014; *Jokinen et al*., 2015], and most work to date has primarily been focused on BVOC.

A number of advances in speciation of compounds relevant to SOA formation have been achieved by new developments in mass spectrometry [*Kalberer et al*., 2004; *Williams et al*., 2006; *Surratt et al*., 2007b, 2010; *Laskin et al*., 2012, 2013; *Ehn et al*., 2014; *Isaacman et al*., 2014; *Lopez-Hilfiker et al*., 2014; *Romonosky et al*., 2015; *X. Zhang et al*., 2015; *Krechmer et al*., 2016b; *Sanchez et al*., 2016]. Such advances in measurement techniques should ideally be corroborated by filter-based techniques [e.g., *Nizkorodov et al*., 2011; *Kampf et al*., 2013]. This expanded ability to characterize the concentrations and molecular identities of species produced in the gas and particle phases in detail, and their distribution with respect to volatility, can facilitate development of more robust and physically realistic parametrizations of SOA formation.

That said, testing the proposed mechanisms of SOA formation and properties using such molecular-level detail often requires estimates of the vapor pressures of the highly oxidized multifunctional organics that characterize SOA. Current computational approaches to vapor pressure estimation of pure species are based on functional group contribution methods, the predictions of which can be uncertain by orders of magnitude [*Valorso et al*., 2011; *O'Meara et al*., 2014]. A related approach to assess volatilities of individual SOA constituents is based on their elemental composition measured by soft-ionization high-resolution mass spectrometry, referred to as "molecular corridors" [*Y. Li et al*., 2016]. But the utility of this approach for overall volatility of SOA, and the evolution of SOA volatility with aging is yet to be tested.

Current models vary in terms of the number of simulated SOA precursor source categories (e.g., isoprene and monoterpenes), oxidants (e.g., OH, O_3, and NO_3 radicals), and/or reaction conditions (e.g., NO_x-dependent

SOA yield parameterizations). However, there is likely much larger variation in SOA yields given that there are likely thousands of biogenic SOA precursors, many of which are not measured [*Goldstein and Galbally*, 2007]. Thus, models may not be able to capture the variability in SOA formation potential between different BVOC [*Jokinen et al*., 2015]. Also, different BVOC can have very different HOM formation potentials that further depend on the oxidant type—e.g., ozone, OH, or nitrate radical pathways for monoterpenes, and oxidation by OH radicals for isoprene [*Jokinen et al*., 2015]. Advances in measurement capabilities allow for improved real-time speciation of BVOC and their oxidation products in both gas and particle phases [*Isaacman et al*., 2014; *Lopez-Hilfiker et al*., 2014; *Isaacman-VanWertz et al*., 2016]. As a result of these advances in molecular speciation, the potential now exists for sharpening of source categories in models based on the relative roles of VOC in SOA formation. Emission inventories, to the extent possible, need to carry VOC structure information, and finally, 3-D chemical transport models need to parameterize this dependence of formation of low-volatility products on VOC structure and their reactions with radicals. Ultimately, next generation SOA models must be developed that can account for spatial and temporal variability in SOA production within a given precursor class (e.g., monoterpenes) but that do not dramatically increase the computational burden of the model.

Models simulate SOA concentrations using parameterizations that are meant to reflect the effective properties and concentrations of the condensing molecules and the SOA formed. As they are highly simplified, special attention needs to be paid to proper reflection of the actual properties of SOA and sensitivity of SOA production and loss to environmental conditions. Moreover, lumped volatility distributions derived from fitting chamber measurements depend highly on the theory used (e.g., dynamic mass transfer versus equilibrium partitioning) and processes included (e.g., wall losses and multigenerational chemistry) during the fitting [*Cappa et al*., 2016]. Consequently, reported volatility distributions can be thought of as being "theory specific" in that they are dependent both upon the processes that are included (or excluded) and the manner in which the processes are represented. Novel approaches to estimate volatilities, or to directly measure the volatilities, of the organic compounds constituting SOA in both gas and particle phases could reduce uncertainties in quantifying their role in SOA formation and thus improve mechanistic tests of SOA formation.

Also, as noted above, the effective volatility of SOA has been found to be much lower than expected based on traditional parameterizations. Improvement of the existing parameterizations can be developed through deeper understanding of the mechanistic details associated with SOA formation and transformations. This includes the gas-phase production of ELVOC, LVOC, and SVOC and their subsequent reactions in the condensed phase.

4. Effects of Bulk Diffusion Limitations on Size Evolution of SOA and CCN

The historical treatment of SOA dynamics in many regional and global climate models considers particles as well mixed, liquid-like solutions that continuously maintain equilibrium with the gas phase through evaporation/condensation. The atmospheric evolution of these particles has been described by absorptive partitioning theory [*Pankow*, 1994; *Donahue et al*., 2006; *Mai et al*., 2015]. The typical implementation of absorptive partitioning theory to the interpretation and simulation of SOA formation assumes that the particles are "well mixed" and effectively liquid like. Under this assumption, condensed-phase diffusion is sufficiently fast that equilibrium within the particles is achieved on short time scales (less than a few minutes) relative to those on which other processes are changing [*Koop et al*., 2011; *Shiraiwa and Seinfeld*, 2012]. When accommodation of condensing molecules is also assumed rapid (mass accommodation coefficients $>$0.1 or so), gas-particle equilibrium is achieved on a time scale of minutes and thus can be considered effectively instantaneous.

4.1. Advances in Measurements of SOA Viscosity

However, recent advances in measurements of SOA properties suggest that under at least some atmospherically relevant conditions, condensed-phase diffusion processes are much slower than is consistent with the assumption of instantaneous gas-particle equilibrium. For instance, there may be important differences between boreal and tropical forests because of different precursors, oxidation pathways, and prevailing relative humidity, with semisolid particles observed over boreal forests and liquid particles over tropical forests [*Virtanen et al*., 2010; *Bateman et al*., 2016]. Under situations where diffusion is slow, the evolution of SOA particle size and CCN number can be significantly affected [*Shiraiwa et al*., 2013b].

Recent experimental data indicate that under many conditions SOA particles do not behave like liquid-like solutions but instead as highly viscous semisolids [*Vaden et al*., 2010; *Virtanen et al*., 2010; *Cappa and Wilson*, 2011; *Vaden et al*., 2011; *Kuwata and Martin*, 2012; *Abramson et al*., 2013; *Renbaum-Wolff et al*., 2013; *Robinson et al*., 2013; *O'Brien et al*., 2014; *Bateman et al*., 2015; *Y. J. Li et al*., 2015; *Pajunoja et al*., 2015; *Song et al*., 2015; *Wilson et al*., 2015; *Y. Zhang et al*., 2015; *Bateman et al*., 2016; *Grayson et al*., 2016; *Bateman et al*., 2017; *Bell et al*., 2017], which significantly impacts their morphology, composition, reactivity, evaporation, and coagulation rates. For example, *Vaden et al*. [2010] demonstrated that particles composed of the hydrophobic liquid dioctyl phthalate (DOP) and α-pinene SOA are not well mixed and can form, instead, two stable opposite morphologies: SOA core coated with DOP and DOP core coated with SOA. Similarly, *Loza et al*. [2013] inferred that SOA particles formed sequentially from two VOC precursors, α-pinene and toluene, also have core-shell morphology with a core of SOA from the initial precursor and shell from the second one. Decreased condensed-phase diffusivity in viscous organic particles can increase the time scales of semivolatile organic compound partitioning, with values depending on the particle size. Based on the Stokes-Einstein relation, condensed-phase bulk diffusivity (D_b) is estimated to exceed 10^{-10} cm^2 s^{-1} for liquid phase decreasing to between 10^{-15} and 10^{-20} cm^2 s^{-1} for viscous semisolids [*Renbaum-Wolff et al*., 2013].

Models that include effects of viscosity utilize condensed-phase diffusivity as inputs, as described in section 4.2. However, the applicability of the Stokes-Einstein equation to calculate bulk diffusivity for SOA particle is questionable because a governing assumption of similar size between diffusing species and molecular matrix does not hold [*Koop et al*., 2011; *Renbaum-Wolff et al*., 2013; *Y. J. Li et al*., 2015]. For example, the diffusivity of smaller molecules, such as water, was reported to be 4–8 orders of magnitude faster than that predicted by the Stokes-Einstein equation [*Price et al*., 2015]. Rather than inferring diffusivity with application of the Stokes-Einstein equation, direct measurements of bulk diffusivity are needed. *Abramson et al*. [2013] directly measured diffusion and evaporation rates of pyrene and other polycyclic aromatic hydrocarbon molecules embedded within an SOA matrix and derived a diffusion coefficient based on Fick's law. Similarly, *Zhou et al*. [2013] retrieved bulk diffusivity of organic molecules using their measured heterogeneous reaction rates and a kinetic multilayer model, while *P. F. Liu et al*. [2016] derived bulk diffusivity using a diffusive multislab model based on measured evaporation rates of organics from films.

Renbaum-Wolff et al. [2013] and *Bateman et al*. [2015] showed the importance of relative humidity and water content on the viscosity and physical state of SOA particle. *Y. Zhang et al*. [2015] showed that nonspherical SOA particles can flow to become spherical above a critical RH because of the decrease in viscosity associated with water uptake. It was also shown that evolution of particle mass spectra during SOA evaporation due to thermal desorption [*Cappa and Wilson*, 2011] or dilution [*Vaden et al*., 2011] does not exhibit the behavior expected for low viscosity, multicomponent liquid particles. Due to the high viscosity of SOA, semivolatile molecules like organic nitrates [*Perraud et al*., 2012] and PAHs [*Zelenyuk et al*., 2012; *Abramson et al*., 2013; *Zelenyuk et al*., 2017] can be trapped inside particles and the uptake of semivolatile molecules like ammonia from the gas phase can be restricted [*Kuwata and Martin*, 2012; *Y. J. Li et al*., 2015; *Bell et al*., 2017]. *Bell et al*. [2017] showed that heterogeneous reactions between ammonia and semisolid SOA produce a few nanometer thick solid coating ("crust") that limits additional ammonia from diffusing into the SOA particle and prevents coagulating particles from coalescence on the time scale that exceeds 2 days. *Song et al*. [2016] studied SOA particles derived from an anthropogenic precursor (toluene) and based on these results suggest that anthropogenic particles over megacities may be semisolid rather than liquid and thereby alter heterogeneous chemistry for many conditions, especially in hot afternoons characterized by low RH. *Bateman et al*. [2017] found that anthropogenic influences of urban pollution and biomass burning over Amazonia tend to decrease the particle hygroscopicity and favor a semisolid phase state of the particulate matter. At low relative humidity conditions, other recent studies reported that anthropogenic SOAs appear to be more solid like compared to biogenic SOA [*T. Liu et al*., 2016; *Q. Ye et al*., 2016]. Such differences can result in source- and composition-dependent kinetic regimes of gas-particle partitioning for semivolatile organics.

Particle viscosity is found to be a function of relative humidity and SOA precursor type. In general, increasing RH decreases the viscosity of particles [*Renbaum-Wolff et al*., 2013; *Bateman et al*., 2015; *Hinks et al*., 2016]. *Renbaum-Wolff et al*. [2013] reported that at RH $\leq$30%, 20 to 50 μm particles composed of the water-soluble fraction of α-pinene SOA are at least as viscous as asphalt/bitumen. However, at higher RH they become less viscous, with viscosities comparable to that of peanut butter and honey, at 70% and 90% RH, respectively. *Kuwata and Martin* [2012] showed that the uptake of ammonia by α-pinene ozonolysis SOA particles at

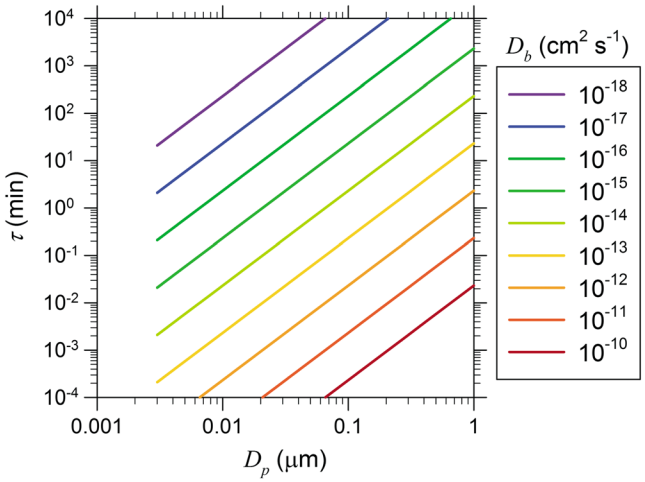

Figure 10. Dependence of diffusion time scale (τ) on particle diameter (D_p) for bulk diffusivity (D_b) values ranging from 10^{-10} to 10^{-18} cm^2 s^{-1} (adapted from *Zaveri et al.* [2014]).

low RH is consistent with adsorption by a highly viscous semisolid. However, at higher RH (>94% RH) SOA ammonium content increased significantly, indicating change in viscosity of the ammoniated SOA. These results were tested and generalized to a broader range of SOA particle types in *Y. J. Li et al.* [2015], and the point was made that the RH limit of a transition in physical state can significantly differ from the RH at which a transition in chemical reactivity occurs. In addition to the dependence on RH and precursor type, *Grayson et al.* [2016] found that viscosity of SOA particles depends inversely on the mass concentration, presumably related to variation in the chemical composition of SOA as a function of concentration. Since laboratory studies on SOA viscosity are typically carried out at much higher (up to 2–3 orders of magnitude) mass concentrations compared to ambient levels, the ambient SOA may be more viscous than suggested by such laboratory studies.

4.2. Advances in Modeling: Effects of SOA Bulk Diffusion Limitations

Traditional SOA models, which are typically based on the assumption of instantaneous equilibrium gas-particle partitioning, neglect the kinetic effects of the potentially reduced bulk diffusivity in viscous organic particles. To investigate such effects, several multilayer particle models have been developed that numerically solve Fick's second law of diffusion (unsteady state diffusion) within spherical particles [*Poschl et al.*, 2007; *Shiraiwa et al.*, 2010; *Zobrist et al.*, 2011; *Shiraiwa et al.*, 2012; *Roldin et al.*, 2014; *Zaveri et al.*, 2014; *O'Meara et al.*, 2016]. These models discretize a single particle into concentric shells to resolve the temporal evolution of concentration gradients of multiple species diffusing (and chemically reacting, in some cases) along the radius of the particle. In general, the time scale (τ) for a nonreactive species diffusing into a particle from its surface to reach a uniform radial concentration profile depends on the particle diameter (D_p) and bulk diffusivity (D_b) as illustrated in Figure 10 (adapted from *Zaveri et al.* [2014]). It is seen that for a semisolid particle with $D_b = 10^{-15}$ cm^2 s^{-1}, τ varies from 1 min to 100 min as D_p varies from 0.02 μm to 0.2 μm, respectively. In addition to D_p and D_b, the gas-particle equilibration time scale also depends on the surface mass accommodation coefficient, the volatility of the condensing species, and its initial gas-phase concentration and can range from a few microseconds to several days [*Shiraiwa and Seinfeld*, 2012; *O'Meara et al.*, 2016].

While a semisolid organic particle can inhibit the uptake of semivolatile organics, a highly viscous material formed at a particle surface (i.e., a "shell") could also increase the lifetime of particles by trapping semivolatile organics or salts such as ammonium sulfate within the particle's interior. Using the KM-GAP multilayer model, *Shiraiwa et al.* [2013a] investigated the effects of such phase separation and found that it can significantly affect the partitioning of semivolatile components and hygroscopic growth. Similarly, a modeling study by *Roldin et al.* [2014] demonstrated the effect of dimer (or oligomer) enrichment at the particle surface followed by an application of obstruction theory wherein large molecules (such as dimers) obstruct smaller molecules and lower their effective diffusion rates in the particle interior [*Stroeve*, 1975; *Pfrang et al.*, 2011]. In a more recent study *O'Meara et al.* [2016] included compositional dependence of diffusivity in their multilayer model and showed that the plasticizing effect of water, as it diffuses into a viscous organic particle, can dramatically reduce the equilibration time scale for gas-particle partitioning.

Although the multilayer particle models are useful for investigating in great detail the effects of diffusivity and particle morphology in monodisperse aerosol populations, they are impractical for modeling polydisperse aerosol in 3-D chemical transport models. To address this issue, *Zaveri et al.* [2014] extended the

dynamic gas-particle partitioning treatment in the sectional MOSAIC aerosol model [*Zaveri et al*., 2008] by accounting for the effects of volatility, bulk diffusivity, and particle-phase reaction (treated as first-order rate constant). Their model analysis of polydisperse semisolid OA suggests that the inhibited uptake of SVOC by large particles could in turn promote the growth of smaller particles that are competing for the same vapors, albeit with much shorter diffusion time scales. Moreover, slower uptake by semisolid particles suggests that the SVOC can potentially continue to react in the gas phase to form low-volatility vapors or undergo gas-phase fragmentation and depositional scavenging.

4.3. Future Research Needs in Particle Viscosity

The transition of SOA between high and low viscosity depends in a complex manner on both relative humidity and temperature. At higher altitudes close to the top of the planetary boundary layer, temperature decreases but relative humidity can increase relative to near-surface conditions. While high RH favors lower viscosity, lower temperature favors increasing viscosity. For example, using a new in situ optical method to detect the viscous states of particles, *Järvinen et al*. [2016] showed that α-pinene SOA particle may remain viscous over a wide range of atmospheric conditions in the free troposphere. In addition, a recent study indicated that the transition RH for reactivity of SOA differed considerably from the transition RH reported for phase change of SOA, i.e., from nonliquid to a liquid state [*Y. J. Li et al*., 2015]. This difference in transition RH between reactivity and phase (affecting viscosity of SOA) could vary for other SOA systems. However, the study by *Y. J. Li et al*. [2015] implies that models will also need to differentiate between phase transitions and chemical kinetics for SOA particle. Depending on whether the condensing organics are hygroscopic salts or less hygroscopic material, the chemical kinetics at the particle surface could depend significantly on the nonliquid to liquid phase transition [*Roldin et al*., 2014; *Y. J. Li et al*., 2015]. It may be useful to think of an effective viscosity for chemical uptake kinetics over SOA particle, which could be lower or higher than the actual viscosity depending on the material deposited at the surface of SOA particle, e.g., hygroscopicity of organic salts. This implies that care needs to be exercised in connecting diffusion and reaction kinetics of organic species within SOA particle to measurements of mechanical properties such as bounce and their response to poking [*Y. J. Li et al*., 2015].

Water associated with SOA can modify reactive uptake kinetics significantly. The competing effects of RH and temperature on the viscosity and reactive uptake kinetics for different SOA particle systems are not well constrained. Additionally, the variations of viscosity and reactive uptake kinetics with atmospheric aging of SOA particles require experimental investigation. For example, the relative roles of RH and temperature in particle viscosity for different precursors and at different conditions—e.g., high/low/intermediate NO_x or SOA precursor concentration—need to be systemically investigated. Explicit model treatments that account for SOA precursor volatility, including ELVOC formation, changes in particle volatility due to accretion reactions, and diffusion-controlled SOA growth/evaporation as a function of temperature and RH need to be developed to evaluate eventually impacts on the global CCN budget.

In summary, as described in sections 4.2 and 4.3, in addition to RH, there are other factors such as ambient temperature, SOA composition, atmospheric aging of SOA, and SOA mass loading, which could have complex effects on SOA viscosity. In addition, it is important to note that diffusion limitations and the transition RH determining the onset of these diffusion limitations could be very different compared to measured viscosity of particles (that could also vary depending on the measurement technique itself, e.g., bounce and poking techniques). Ultimately, these diffusion limitations are reflected in the form of limitations to uptake kinetics of organic vapors on SOA particles and particle-size evolution during growth. While direct ambient measurements of SOA viscosity are challenging, measurements of uptake kinetics of SOA precursors on the particles under atmospherically relevant conditions could provide valuable insights about SOA formation and size distribution dynamics in the atmosphere. Laboratory chamber experiments remain critical to understand the size evolution of SOA and the effects of viscosity and volatility for a range of SOA precursors, e.g., biogenic, fossil fuel, and biomass burning, over atmospherically relevant RH and temperature ranges for different precursor and oxidant regimes.

5. Biomass Burning

Biomass burning injects large amounts of OA and nonmethane organic compounds (NMOCs) into the atmosphere [*Andreae and Merlet*, 2001; *van der Werf et al*., 2010; *Bond et al*., 2013]. OA from biomass burning

sources (i.e., BBOA) are composed of primary organic aerosol (POA) directly emitted from the burning biomass and SOA formed via oxidative processing of organic gases. Biomass burning is one the largest sources of primary carbonaceous aerosol globally and also is an important source of trace gases including organic vapors, which themselves can serve as precursors for SOA [*Andreae and Merlet*, 2001; *Yokelson et al*., 2008; *De Gouw and Jimenez*, 2009; *Akagi et al*., 2011; *Bond et al*., 2013].

5.1. SVOC/IVOC Emissions From Biomass Burning

Recent studies have indicated that a significant fraction (15–37%) of NMOCs emitted from biomass burning are in the semivolatile/intermediate-volatility range (SVOC/IVOC), having saturation vapor concentrations, C^*, in the range 0.1–10^6 $\mu g\ m^{-3}$. Their emissions and role in SOA formation are not well understood [*Stockwell et al*., 2015; *Yokelson et al*., 2013]. Most current aerosol models treat only the oxidation of selected VOC as a source of SOA from biomass burning emissions and neglect the contribution of SIVOC emissions, an omission that may lead to substantial underestimation of biomass burning SOA production. Field observations continue to be a vital tool in understanding the complexities affecting BB emissions and their resulting climatic impacts, as well as helping to identify inaccuracies in current emission inventories [*Yokelson et al*., 2013]. Moreover, biomass burning OA can be transported to long distances from its source because the intense heat of large fires can inject emissions to high altitudes, where they survive longer compared to surface-level emissions sources (e.g., biogenic emissions) that are subject to removal by deposition at a higher rate.

5.2. SOA-Forming Potential of Biomass Burning Emissions

The net amount of OA mass added during aging ("net SOA") is one of the key parameters that global models need to simulate accurately in order to predict the climate impacts of biomass burning emissions. Net SOA is frequently evaluated with the parameter $\Delta OA/\Delta CO$ ratio, which can be calculated for emissions sampled downwind of a fire source by taking the ratio of the enhancement of OA mass to the enhancement of CO above their respective backgrounds. CO is a stable tracer for fire plumes, and this method accounts for the effect of dilution [*Cubison et al*., 2011].

Field studies conducted by following plumes from aircraft are useful to quantify the chemical evolution of BB emissions, as such studies can quickly follow plumes in a pseudo-Lagrangian manner. Out of the 17 published aircraft studies on aging of BB emissions, 10 reported no detectable net addition of OA mass with photochemical evolution, while 4 reported an increase and 3 reported a decrease [*Hobbs et al*., 2003; *Cubison et al*., 2011; *Akagi et al*., 2012; *Jolleys et al*., 2012; *Forrister et al*., 2015; *Jolleys et al*., 2015; *May et al*., 2015; *X. Liu et al*., 2016]. A few ground-based studies have also studied this topic, of which one reported no change and two reported an increase in net SOA [*Lee et al*., 2008; *Vakkari et al*., 2014; *Zhou et al*., 2017]. One limitation with ground-based studies is that since the plumes cannot be followed in a pseudo-Lagrangian manner, they can be more affected by variations in emissions with time of day and dispersion, which can be very large for BB fires [*Saide et al*., 2015]. However, well-designed ground-based studies can provide useful information on BB aging [*Collier et al*., 2016; *Zhou et al*., 2017].

Overall, ambient observations show that the atmospheric evolution of biomass burning emissions is different from those of urban and biogenic emissions, which show substantial increase in $\Delta OA/\Delta CO$ ratio, i.e., net SOA formation, with aging [*de Gouw et al*., 2005; *Volkamer et al*., 2006; *Shilling et al*., 2013]. However, as the biomass burning plume ages in the atmosphere, the oxygenation of OA (reflected in O/C ratio) is reported to increase significantly in almost all studies, suggesting strong chemical transformation of OA with aging and formation of more oxidized BBOA that are compositionally different than BB POA [*Capes et al*., 2008; *Cubison et al*., 2011; *Jolleys et al*., 2012; *Forrister et al*., 2015; *Zhou et al*., 2017]. These findings imply that although the mass concentration of OA (= POA + SOA) from biomass burning remains approximately constant during aging, the composition of OA changes strongly, becoming more oxidized with aging. One hypothesis for the frequent observation of little net addition of OA mass is that SOA formation is being balanced by effects of dilution and subsequent evaporation to the gas phase of semivolatile components, resulting in loss of POA mass [*Cubison et al*., 2011; *May et al*., 2015; *Zhou et al*., 2017].

In ambient studies where increases in total OA relative to CO were observed, the increases are small compared to the POA/CO ratios in BB emissions [*Cubison et al*., 2011]. In particular, the ratios of net SOA/POA for BB emissions were ~1–2 order of magnitude lower than for urban emissions [*Hayes et al*., 2013]. Several

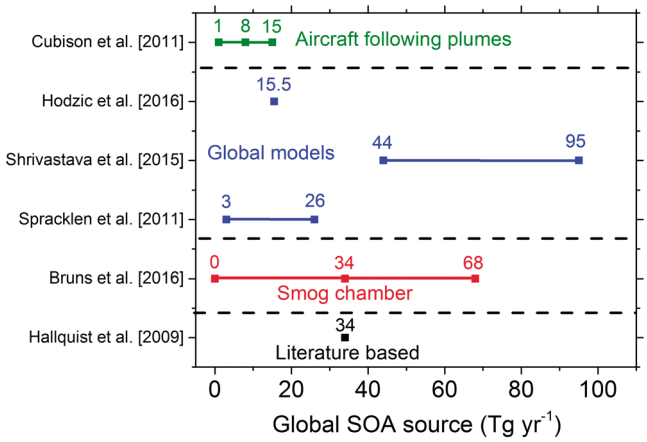

Figure 11. Global source of biomass burning SOA (Tg yr^{-1}) as estimated by different studies: aircraft following plumes of biomass burning fires (green), global models evaluated with OA measurements in regions influenced by biomass burning emissions (blue), estimate based on measurements of biomass burning SOA in smog chamber (red), and a literature estimate (black). Both measurements and modeling studies report a wide range of SOA produced from oxidation of biomass burning emissions. Aircraft-based estimates (green) report net OA (POA + SOA) corrected for dilution effects.

laboratory studies also support that the net SOA/POA ratio is significantly lower for BB than for urban or biogenic emissions [*Grieshop et al.*, 2009; *Hennigan et al.*, 2011; *Ortega et al.*, 2013; *Bruns et al.*, 2016]. However, substantial variability in net SOA production is observed in the laboratory studies across biomasses and burning conditions. In particular studies of BB in wood stoves (simulating residential combustion) versus those simulating open fires appear to lead to systematically different results, likely due to the very different combustion conditions.

Overall, the available evidence suggests that net SOA production from biomass burning is a relatively small contributor to the global OA budget, while oxidation of OA in BB emissions with aging is always observed. Change of BBOA composition with aging inevitably leads to changes to their optical and hygroscopic properties and thus has climate implications. The reasons for the variability across studies may be related to variations in fuels burned and combustion conditions, variation in key coemitted species such as NO_x, and differences in environmental conditions such as dilution rate and temperature and humidity.

5.3. Global Modeling Results on Biomass Burning SOA

Global modeling estimates of SOA from biomass burning vary substantially (shown in blue in Figure 11). While most global modeling studies estimate a low contribution of biomass burning to SOA [*Spracklen et al.*, 2011; *Tsigaridis et al.*, 2014; *Hodzic et al.*, 2016], a recent study predicted that SOA from biomass burning emissions dominated the OA budget globally, especially at high altitudes due to multigenerational oxidation of longer-lived SIVOC precursors [*Shrivastava et al.*, 2015]. While several assumptions had to be made in that modeling study due to limited understanding of variability of SIVOC emissions and chemistry from different biomass burning plumes, model-measurement agreement improved substantially compared to the standard version of the global model used in that study. However, it was noted that the split between POA and SOA was highly uncertain due to uncertainties in emissions and aging of SOA precursors and POA. A recent laboratory study estimated a global SOA source of 0–68 Tg yr^{-} (indicated by the red bar in Figure 11) based on extrapolating measurements of SOA produced by aging of residential wood combustion in a smog chamber [*Bruns et al.*, 2016]. Oxidation products of nontraditional SOA precursors like phenols and naphthalene that are not included in models were estimated to constitute most of the SOA mass. A previous literature-based estimate of the biomass burning SOA source by *Hallquist et al.* [2009] falls in the middle of this range.

5.4. Phenolic Compounds in Biomass Burning SOA

Phenolic compounds, which are produced from the combustion of lignin, are a class of gaseous compounds emitted in large amounts from biomass burning sources [*Schauer et al.*, 2001; *Bruns et al.*, 2016]. Recent laboratory studies indicate that phenol and methoxyphenols can undergo gas-phase, aqueous phase, and multiphase photochemical reactions in the atmosphere, forming SOA with a high degree of oxidation [*Sun et al.*, 2010; *Chhabra et al.*, 2011; *Yee et al.*, 2013; *Smith et al.*, 2014; *Yu et al.*, 2014, 2016]. Phenol itself has a moderate Henry's law constant (5.6×10^3 M atm^{-1} at 5°C [*Sander*, 1999]) and thus partitions only modestly to aqueous drops. However, guaiacols, syringols, and many of the substituted phenols, such as phenolic carbonyls [*Smith et al.*, 2016], have higher Henry's law constants, up to 10^5–10^6 M atm^{-1} [*Sagebiel and Seiber*, 1993; *Sander*, 1999] and will therefore be present primarily in the aqueous drops and water-containing

particles under humid conditions. In aqueous phase, phenols are rapidly oxidized by a variety of mechanisms and the mass-based yield of nonvolatile products from aqueous phenol oxidation is very large, with values over 100% in many cases [*Sun et al*., 2010; *Smith et al*., 2014; *Yu et al*., 2014; *Smith et al*., 2015]. These low-volatility products will remain in the particle phase as SOA after droplet evaporation. Photochemical aging of phenolic compounds results in multiple generations of aqueous SOA products with a wide range of volatilities and chemical composition and is a likely source of highly oxidized organic molecules [*Yu et al*., 2016]. The importance of aqueous-phase oxidation depends on how organic mass is distributed among compounds that have a range of Henry's law constants, reaction rates and SOA yields, and the abundance of condensed phase water. For some compounds, aqueous oxidation will clearly dominate, while for others gas-phase oxidation is likely more important. The different pathways for aqueous and gas-phase oxidation of phenols as source of SOA are not included in most models.

5.5. Future Research Needs in Biomass Burning SOA

Measurements need to constrain the variability of SIVOC precursor emissions from biomass burning and their potential for SOA formation. Differences in model treatments of SIVOC can lead to substantial differences in the simulated concentration of SOA and the inferred importance of SOA from biomass burning emissions. Also, the differences between laboratory and field measurements of biomass burning SOA need to be reconciled. Understanding how properties of biomass burning OA (such as phase/volatility) depend on combustion conditions, meteorology (e.g., temperature and RH), and atmospheric aging is critical. Regional and global models will need to constrain the evolution of properties of biomass burning OA and also include the variability of SIVOC emissions and their multigenerational aging in the atmosphere. Similarly, photochemical aging of nontraditional SOA precursors like phenolic compounds and their role in low-volatility aqueous SOA formation need to be better understood and represented in models. An integrated laboratory-field modeling investigation is crucial to improve our ability to predict the highly variable (in space and time) impacts of biomass burning OA on regional and global scales. Also, future modeling studies need to investigate the most plausible mechanisms that could lead to a constant net SOA and significant chemical aging of biomass burning emissions that have been observed in a large number of field studies.

6. Laboratory Systems of SOA Formation

Most of our existing knowledge of the nature of SOA formation has come from laboratory experiments. Laboratory experiments will remain the fundamental framework to unravel the detailed chemistry and physics of SOA formation, including the dependence on oxidation conditions, relative humidity, and temperature. Recent advances in mass spectrometry applied to chamber SOA have revealed, for example, the crucial role played by HOMs (some of which are most likely ELVOC) in SOA formation. New understanding of gas-phase chemistry, such as the importance of autoxidation, has allowed unraveling of new mechanisms of SOA formation that, until recently, were only speculative. In many systems RO_2 isomerization rates are key in determining competitive reaction pathways under atmospheric conditions. Overall, attention should continue to be given to understanding the role of trace radical concentrations (NO, NO_2, HO_2, and RO_2) and competitive reaction pathways. Measurements of particle-phase composition of SOA have the promise of bringing closure of the chemistry from the parent VOC to the SOA itself within reach [*X. Zhang et al*., 2015], although challenges remain in understanding the extent to which methods used to probe particle composition alter the particle composition itself [e.g., *Isaacman-VanWertz et al*., 2016; *Lopez-Hilfiker et al*., 2016]. Laboratory studies need to continue to elucidate the formation of low-volatility organics from gas-phase and particle-phase pathways and from multiphase reactions at interfaces under a range of atmospherically relevant conditions.

Three types of laboratory systems are commonly used to study SOA formation and provide data on which SOA formation models can be formulated: (1) the traditional chamber operated as a time-dependent batch reactor, (2) the chamber operated as a steady state, continuous flow, well-mixed reactor, and (3) the oxidation flow tube reactor. Limited cross characterization of these systems has been carried out, with respect to inferred detailed mechanisms and predicted levels of SOA formation [*Lambe et al*., 2015; *Peng et al*., 2015]. Focused studies involving a number of research groups at a particular laboratory with an array of instrumentation that is not possible in a single research group show enormous potential benefit [*Nguyen et al*., 2014b]. Such studies, essentially a "field experiment" carried out under well characterized laboratory conditions,

could lead to mechanistic insights beyond those achievable in a single laboratory. Such studies will not replace actual field experiments, but they provide data subject to a degree of control not possible to achieve in the ambient.

6.1. Determination of Secondary Organic Aerosol (SOA) Yields From Laboratory Chamber Data

SOA formation studies, which are typically conducted in laboratory chambers in the presence of seed particles, provide fundamental data that can be used to predict the rate of atmospheric SOA formation. An essential parameter of interest in laboratory chamber studies is the SOA mass yield (Y), which is defined as the ratio of mass concentration of SOA formed to mass concentration of parent hydrocarbon reacted (ΔHC), $Y = \Delta M_o / \Delta$HC [*Odum et al*., 1996, 1997a, 1997b]. Measured SOA mass yields can subsequently be applied in atmospheric models to predict OA levels. In order to obtain accurate SOA mass yields from the evolving aerosol size distribution in chamber experiments, deposition of both particles and vapors to the chamber walls needs to be accurately accounted for [*Crump and Seinfeld*, 1981; *McMurry and Grosjean*, 1985; *McMurry and Rader*, 1985; *Cocker et al*., 2001; *Kroll et al*., 2007; *Weitkamp et al*., 2007; *Pierce et al*., 2008; *Hildebrandt et al*., 2009; *Loza et al*., 2010; *Matsunaga and Ziemann*, 2010; *Loza et al*., 2012; *Kokkola et al*., 2014; *McVay et al*., 2014; *Yeh and Ziemann*, 2014; *Zhang et al*., 2014; *Yeh and Ziemann*, 2015; *X. Zhang et al*., 2015; *La et al*., 2016; *Nah et al*., 2016b, 2016c; *P. Ye et al*., 2016].

When accounting for particle wall loss in the computation of SOA mass yields, two limiting assumptions have traditionally been made regarding interactions between particles deposited on the chamber walls and suspended vapors [*Weitkamp et al*., 2007; *Hildebrandt et al*., 2009; *Loza et al*., 2012; *Zhang et al*., 2014]. The first case assumes that particles deposited on the walls cease to interact with suspended vapors, and therefore, the SOA mass present on these deposited particles does not change once the particle has deposited [*Loza et al*., 2012; *Zhang et al*., 2014]. Adding the SOA mass present on these particles once they have deposited to that present on the suspended particles provides a lower bound of the total SOA mass concentration. In the second case, it is assumed that particles deposited on the walls continue to interact with suspended vapors as if they had remained suspended; in this case the SOA mass present on these deposited particles increases at the same rate as those suspended, providing an upper bound of the total SOA mass concentration [*Weitkamp et al*., 2007; *Hildebrandt et al*., 2009]. The assumption of instantaneous equilibrium between the vapors and the wall-bound particles is typically made with this method.

Vapor wall deposition mechanisms in chambers are not as well understood as those for particles. Losses of low-volatility, semivolatility, and intermediate-volatility species to chamber walls during SOA formation experiments will lead to observed SOA yields to be underestimated. The degree to which SOA-forming vapors deposit onto chamber walls is governed by the rate at which these organic molecules are transported to the walls, the strength of adherence of the molecule to the wall, and the extent to which vapor-wall partitioning is reversible [*Loza et al*., 2010; *Matsunaga and Ziemann*, 2010; *X. Zhang et al*., 2015]. Recent studies show that SOA mass yields measured in chamber experiments can be significantly underestimated due to wall deposition of SOA-forming vapors that would otherwise contribute to SOA growth [*McVay et al*., 2014; *Zhang et al*., 2014; *La et al*., 2016]. *Zhang et al*. [2014] found that chamber-derived SOA mass yields from toluene photooxidation may be underestimated by as much as a factor of 4 as a result of vapor wall loss. Consequently, the use of underestimated chamber-derived SOA mass yields in atmospheric models will lead to the underprediction of ambient SOA mass concentrations [*Cappa et al*., 2016]. In *Zhang et al*. [2014], a dependence of the aerosol yield on the seed aerosol surface area was observed for experiments conducted at a particular oxidation rate of toluene. However, the variation of the oxidation rate, as, for example, with a different organic precursor, was not studied. A key aspect of vapor wall deposition is the potential interplay between the effect of increasing seed aerosol surface area and the effect of increasing the oxidation rate of the parent organic.

The extent to which wall deposition of the oxidized vapors affects SOA yields depends on the specific VOC system [*Zhang et al*., 2014; *Nah et al*., 2016b, 2016c]. *Nah et al*. [2016c] systematically examined the roles of gas-particle partitioning and VOC oxidation rate in the presence of vapor wall deposition in α-pinene ozonolysis. They showed that despite the presence of vapor wall deposition, SOA mass yields at peak SOA growth remain approximately constant regardless of the seed aerosol surface area. This observation is consistent with SOA formation in the α-pinene ozonolysis system being governed by quasi-equilibrium growth, for which there are no substantial limitations to vapor-particle mass transfer.

In the absence of seed particles, the low volatility of ELVOC makes such molecules especially prone to losses to chamber walls [*Ehn et al*., 2014; *Kokkola et al*., 2014; *Roldin et al*., 2015; *X. Zhang et al*., 2015; *Krechmer et al*., 2016a]. However, when sufficient seed particles are present, SVOC can actually be more sensitive than ELVOC to vapor wall losses because a larger fraction of SVOC than ELVOC remains in the gas phase and because the SVOC can evaporate from the suspended particles in response to wall losses [*P. Ye et al*., 2016]. For higher volatility IVOC species ($10^3\ \mu g\ m^{-3} \le C^* \le 10^6\ \mu g\ m^{-3}$ [*Robinson et al*., 2007]), species at the lower end of that C^* range will still significantly partition to walls, while the more volatile IVOCs will primarily reside in the gas phase. The limited influence of the walls on the partitioning of the higher volatility IVOC species depends upon how close the species vapor pressure is to the effective absorbing mass concentration of the walls. The full impacts of such non-SOA-forming loss pathways of ELVOC, LVOC, and SVOC must be understood and accounted for in the interpretation of laboratory chamber experiments to allow extrapolation of the chamber results to the ambient environment.

6.2. Challenges in Understanding and Modeling Paths to SOA Formation

Incorporating understanding achieved in the laboratory into computational models of SOA formation represents one of our greatest challenges. These challenges include physically realistic multigenerational aging parameterizations, representing diffusion-controlled and equilibrium growth rates of SOA, oligomer formation, and effect of loss of vapors and particles in chambers when fitting SOA yield and volatility distributions to chamber data. Since oxidation of organics results generally in both functionalization and fragmentation pathways [*Chacon-Madrid and Donahue*, 2011; *Kroll et al*., 2011; *Lambe et al*., 2012], both these types of reactions need to be included in SOA models in more explicit and self-consistent ways, especially for reactions beyond the initial generation(s) that are captured by chamber experiments. Additionally, the relative roles of functionalization versus fragmentation will vary with atmospheric conditions such as NO levels, the variability of which must be captured by models. The product yields in common fixed-yield SOA models, such as the two-product model, implicitly include the influence of fragmentation in the initial reaction period. However, because the influence of functionalization and fragmentation is not distinguishable in such models and because chamber experiments generally do not capture later generation atmospherically relevant aging time scales, it is difficult to develop appropriate aging schemes in these models. Fragmentation of SOA precursor VOC and oxidation products can substantially decrease the amount of SOA formed globally [*Shrivastava et al*., 2015]. However, the functionalization-fragmentation branching ratio in most SOA systems is not well constrained and depends on the relative reaction rates involving NO_x, HO_2, and RO_2 radicals [*Loza et al*., 2014; *Xu et al*., 2014]. Better constraints on this branching ratio can be obtained by reformulating SOA parameterizations to include multigenerational aging so that they inherently include both functionalization and fragmentation during fitting of smog-chamber measurements. Examples of such models include the statistical oxidation model or the 2-D-VBS [*Donahue et al*., 2011; *Cappa and Wilson*, 2012; *Donahue et al*., 2012b]. Molecular-level information on radical intermediates and gas- and particle-phase reaction products is critical to provide realistic constraints on multigenerational aging parameterizations.

The atmospheric relevance of mechanistic pathways of SOA formation discovered in the laboratory needs to be assessed by carrying out ambient field measurements. For example, comprehensive radical and SOA precursor measurements, although rare (e.g., measured at the field campaign, Biogenic Aerosols—Effects on Clouds and Climate (BAECC)), can reveal relationships between precursor types, oxidant chemistry, and routes of SOA formation.

7. SOA Interaction With Clouds

The effect of OA on radiative forcing is delineated into two categories: (1) the direct radiative effect of changes in aerosol levels and composition from preindustrial conditions to the present and (2) the effect of changes in aerosol levels and properties on cloud formation from preindustrial conditions to the present [*Seinfeld et al*., 2016]. Quantifying the radiative effect of aerosol changes from preindustrial conditions to the present on Earth's cloudiness is considered as one of the most uncertain aspects of global climate predictions. The connection between aerosol and cloud formation lies in the ability of aerosol to function as CCN and ice nuclei (IN) [*Rosenfeld et al*., 2014], and recent studies have highlighted the importance of understanding how aerosol-cloud-precipitation interactions depend on both natural and anthropogenic aerosol systems [*Z. Li et al*., 2016]. Climate models that include chemistry/aerosol contain a computational module in which a

portion of aerosol is activated to form cloud droplets. The details of each module differ among different climate models, but a fundamental feature of each module is calculation of the activation of particles that depends on particle size and composition as well as specified meteorological conditions [*Ghan et al*., 2011]. Since a considerable fraction of the mass of global aerosol is organic, the activation of organic-containing aerosol represents a key component of CCN [*Mei et al*., 2013b, 2013a; *Levin et al*., 2014].

7.1. SOA Hygroscopicity

Atmospheric aerosol consists of mixtures of inorganic and organic constituents, the proportions and spatial distribution of which have changed from preindustrial time to present. Within the relevant size range for activation, the key aerosol property that impacts cloud microphysics is the propensity of a particle to serve as CCN and IN. Particle hygroscopicity is often characterized through the dimensionless parameter κ [*Petters and Kreidenweis*, 2007; *Petters et al*., 2016]. The κ parameter is calculated as a volume-weighted hygroscopicity of the different chemical components constituting the total particle volume. The CCN activity of particles in the diameter range between 40 and 200 nm is particularly sensitive to particle hygroscopicity (ambient particles outside of this size range either are too small to activate or often contain sufficient soluble species to always activate under ambient supersaturations). Growth of ultrafine particles to CCN-active size is thought to occur in large part due to condensation of organics in many portions of the world [*Riipinen et al*., 2012]. Thus, it is important that variations in particle composition are considered as a function of size if the full influence of SOA on clouds is to be quantitatively understood. Since biogenic emissions would have been proportionately more important to global aerosol composition in preindustrial time, and NO_x levels would have been lower, the proportion of organics represented by HOM could have been larger as compared to the present day.

The hygroscopicity of organics is relatively low as compared to that of sulfate and nitrate. As a result, the influence of organic hygroscopicity (κ_{org}) on CCN activity depends strongly on organic volume fraction. Nonetheless, variations in SOA hygroscopicity may have limited influence on the net CCN activity in environments wherein sulfate and nitrate make up more than ~50% of particle volume [*Wang et al*., 2008]. However, in environments where organics represent 80% or more of the particle volume, the calculated CCN concentration can be very sensitive to the organic fraction [*Mei et al*., 2013b]. Additionally, when the organic fraction is sufficiently large, surface partitioning of organics in growing droplets may lead to a decrease in the surface tension, thereby enhancing the effective hygroscopicity [*Ruehl et al*., 2012, 2016].

With stricter control of sulfur emissions, aerosol organic fraction is likely to increase in the future, and simulated CCN concentration will likely exhibit a stronger dependence on κ_{org} value. Simulated CCN number concentrations are predicted to be significantly more sensitive to κ_{org} during preindustrial times than in the present day due to the much smaller expected sulfate concentrations at that time [*Liu and Wang*, 2010]. As the radiative forcing is the difference in radiative fluxes between the preindustrial era and the present day, this difference in the sensitivity leads to a dependence of simulated aerosol indirect forcing on the assumed value of κ_{org} [*Liu and Wang*, 2010]. This highlights the necessity of better understanding κ_{org} and its variation in the atmosphere.

Laboratory and field studies suggest that organics exhibit a fairly wide distribution of κ values ranging from 0 to 0.3, and κ_{org} can increase substantially during chemical aging in the atmosphere [*Jimenez et al*., 2009]. One approach proposed for representing the variation of κ_{org} is parameterization based on the organic oxidation level (e.g., O:C atomic ratio), which can be measured by AMS [*Aiken et al*., 2008] and other techniques. Whereas increasing κ_{org} with increasing oxidation level has been observed in a number of field and laboratory studies [*Chang et al*., 2010; *Massoli et al*., 2010; *Lambe et al*., 2011; *Mei et al*., 2013b, 2013a; *Pajunoja et al*., 2015], other studies found no significant correlation between κ_{org} and oxidation level [*Frosch et al*., 2011; *Cerully et al*., 2015; *Zhao et al*., 2016]. Further studies of the relationship between κ_{org} and chemical composition are needed for ambient aerosol from representative OA sources before the variation of κ_{org} can be better understood and sufficiently represented in climate models.

7.2. SOA Production in Clouds

On average ~70% of the Earth surface is covered by clouds. About 90% of these clouds dissipate leading to the evaporation of volatile species and to the condensation of lower volatility species [*Herrmann et al*., 2015]. Water-soluble organic gases like glyoxal, methylglyoxal, glycolaldehyde, acetic acid, epoxides, and possibly

hydroperoxides are being oxidized to produce lower volatility SOA precursors, e.g., organic acids [*Sareen et al*., 2016] and their corresponding salts, oligomers [*Zhang et al*., 2004; *Carlton et al*., 2007; *Perri et al*., 2009; *Y. Liu et al*., 2012; *Tan et al*., 2012; *Lim et al*., 2013; *Reed Harris et al*., 2014; *Kurtén et al*., 2015], and organosulfates [*Blando and Turpin*, 2000; *Warneck*, 2003; *Liggio et al*., 2005; *Sorooshian et al*., 2007; *Tan et al*., 2012; *Boone et al*., 2015]. Laboratory studies show that aqueous-phase reactions can produce SOA mainly from carbonyl compounds, such as glyoxal and methylglyoxal, creating carboxylic acids such as oxalic acid as the major oxidation products [*Carlton et al*., 2007; *Altieri et al*., 2008; *Perri et al*., 2009; *Ervens and Volkamer*, 2010; *Ervens et al*., 2011; *Tan et al*., 2012]. Note that those studies were carried out in bulk aqueous solution, which might not accurately reproduce the kinetics or thermodynamics associated with cloud droplets. There are relatively few studies that focus on chemistry within actual droplets. For example, the aqueous-phase oxidation of SO_2 by O_3 (a major source of sulfate aerosol) was recently investigated in dispersed, warm, and supercooled populations of droplets [*Hoyle et al*., 2016]. It was shown that rate constants measured in bulk solutions can accurately represent the chemistry occurring in dispersed aqueous systems. However, actual cloud-induced SOA formation in droplets is more complex. Isoprene/NO_x photooxidation during cloud condensation-evaporation cycles was observed to form metastable SOA composed of organics, nitrate, and ammonium fragments [*Brégonzio-Rozier et al*., 2016]. Quantitative assessments of SOA yields formed in clouds, and model predictions, warrant further study and require careful assessments of gas phase/chamber wall repartitioning after cloud dissipation. In addition, variations in liquid water content of cloud droplets or aqueous aerosol may also affect partitioning of organic oxidation products [*Daumit et al*., 2014]. Furthermore, as a cloud dissipates, the partitioning of soluble gases in cloud droplet residuals is modified strongly due to salting-in/out effects [*Kampf et al*., 2013; *Topping et al*., 2013; *Kurtén et al*., 2015; *Waxman et al*., 2015], and the formation of ammonium salts [*Ortiz-Montalvo et al*., 2014, 2016], with implications for SOA volatility and yield. For example, ammonium and pH strongly decrease the volatility and increase the SOA yield from glyoxal in a single cloud cycle [*Ortiz-Montalvo et al*., 2014], while no similar effect is observed for methyl glyoxal [*Ortiz-Montalvo et al*., 2016]. Further laboratory studies elucidating the molality- and ion-specific impacts of various salts, pH, on the partitioning and chemistry of IEPOX, ISOPOOH, and other soluble product gases are needed to improve model representation of aqueous SOA formation in clouds.

While some field studies showed high aqueous SOA production [*Lin et al*., 2010; *Sorooshian et al*., 2010; *Lee et al*., 2012; *Sareen et al*., 2016; *Sullivan et al*., 2016], other field campaigns showed very little change in OA amounts between cloud droplet residuals and interstitial aerosols (nonactivated) [*Zelenyuk et al*., 2010; *Shrivastava et al*., 2013b]. In contrast, sulfate and nitrate were clearly higher in cloud droplet residuals. Similarly, analysis of vertical profiles in the southeastern United States under fair weather cumulus conditions also indicated a small and statistically insignificant addition of SOA in clouds [*Wagner et al*., 2015]. *Lee et al*. [2012] found enhancements of AMS-measurable organic mass by up to 30% during the initial stage of oxidation of cloud water organics, which was followed by a decline at the later stages of oxidation. These observations are in support of the general hypothesis that cloud water oxidation is a viable route for SOA formation for water-soluble organic compounds of intermediate volatility (IVOC), such as *cis*-pinonic acid, produced via gas-phase oxidation of monoterpenes. Model studies have found mixed results about the ability to simulate water-soluble organic carbon. *Carlton et al*. [2008] showed an improvement to predict water-soluble organic carbon in aerosol from aircraft measurements using a simplified mechanism with a fixed yield of 4% to simulate conversion of glyoxal to aqueous SOA. Global modeling studies that compared the potential SOA formation from several aqueous SOA formation schemes showed consistently significant aqueous SOA formation, but none of the current aqueous SOA formation mechanisms stands out to produce a best fit to observations [*Heald et al*., 2011; *G. Lin et al*., 2012]. Future field campaigns could be planned to focus more directly on assessing the impacts of cloud processing on aqueous-phase SOA and SOA precursors.

7.3. SOA Impacts on Ice Nucleation

SOA may affect IN formation. Changes in IN concentrations can significantly affect the mixed-phase and ice-phase microphysical processes and precipitation [*Connolly et al*., 2006; *Pratt et al*., 2009; *DeMott et al*., 2010; *Yun and Penner*, 2012; *Xie et al*., 2013; *Fan et al*., 2014]. Studies have shown that SOA-coated dust has significantly reduced IN abilities [*Mohler et al*., 2008]. But glassy SOA can serve as effective heterogeneous IN due to kinetic limitations to water diffusion into SOA particles [*Berkemeier et al*., 2014]. Modeling work has yet to consider this pathway relating SOA impacts on clouds through changing IN. Future studies could explore the

SOA impacts on IN through their impacts on coating dust and increased IN effectiveness of semisolid (glassy) SOA. More measurements of IN concentrations together with detailed SOA precursor and SOA composition measurements are needed to improve our understanding of the role of SOA in ice nucleation, both in the laboratory and the field. A large uncertainty in aerosol-cloud interactions may well be associated with the ice nucleation parameterization and its SOA properties.

8. Optical Properties of SOA and Direct Radiative Forcing

SOA interfere with propagation of solar and terrestrial radiation by direct scattering and absorption of light. Inherent to the complexity of SOA chemical composition as driven by variability of VOC precursors, formation mechanisms, and aging processes, the optical properties of SOA are not consistently described by a single set of optical constants [*Moise et al*., 2015]. As a result, assessment of the SOA direct radiative forcing (RF_{SOA}) by different climate models has low confidence, to the point that both sign and magnitude of RF_{SOA} are not well understood. The Fifth Assessment Report of the Intergovernmental Panel on Climate Change estimates values of the annual mean top of the atmosphere radiative forcing in a range of -0.27 to $+0.20$ W m^{-2} [*Boucher et al*., 2013]. Some of this estimated variability is likely due to differences in representation of global SOA life cycle processes in different models [*Tsigaridis et al*., 2014]. As described in this work, the uncertainty in estimates of the radiative forcing from aerosol-radiation interactions may be even larger than such studies suggest due to inadequate representation of SOA processes and properties in current climate models. However, another less explored uncertainty in the estimation of aerosol-radiation interactions is the understanding of the optical properties of SOA, i.e., scattering and absorbing components.

Most global climate models represent OA as nearly "white" particles with a very small absorbing component [*Hoyle et al*., 2009; *Spracklen et al*., 2011; *Myhre et al*., 2013]. Scattering by particles has a cooling effect on climate, whereas light absorption by particles has a warming influence. Results of the AeroCom intercomparison study between 16 global aerosol models report mean value of $RF_{SOA} = -0.08$ W m^{-2}, with the highest cooling estimate of -0.4 W m^{-2} [*Myhre et al*., 2013]. Thus, such estimates suggest that scattering dominates the direct climate effects of SOA. However, certain types of SOA can also be light absorbing. Absorbing SOA is part of the broad class of absorbing OA that is commonly referred to as atmospheric "brown carbon" (BrC). The distinguishing feature of BrC is that its absorption exhibits a much stronger wavelength dependence compared to absorption by black carbon (BC), with the absorptivity increasing sharply with decreasing wavelength [*Andreae and Gelencser*, 2006; *P. F. Liu et al*., 2013; *Laskin et al*., 2015; *Liu et al*., 2015; *Moise et al*., 2015]. Aerosol absorptivity is often characterized by the mass absorption coefficient (MAC), which describes the absorptivity per unity mass. The absorptivity of SOA relative to that of BC varies with wavelength, due to their differing wavelength dependencies. At longer wavelengths the absorptivity of SOA is typically thought to be much weaker than that of BC, but as wavelength decreases the absorptivity of BrC can be comparable to BC [*Bond and Bergstrom*, 2006; *Moise et al*., 2015]. Since the atmospheric burden of SOA is expected to be much larger than that of BC [*Shrivastava et al*., 2015], and because BrC can absorb so strongly at short wavelengths, absorption by SOA is potentially important. For example, radiation closure studies suggest that BrC light absorption can add about 40% to the light absorption of BC in Mexico City [*Barnard et al*., 2008]. The relative importance of SOA as a source of BrC versus primary OA is not fully established yet is important to understand the spatial distribution and variability in BrC absorption.

The wavelength-specific absorptivity of SOA depends on the precursor VOC and the formation pathway and thus varies by geographic location [*X. L. Zhang et al*., 2011]. For example, some SOA, such as that formed from reaction between α-pinene and OH, is largely not absorbing ($MAC_{405nm} < 0.02$ m^2 g^{-1}), while other SOA, such as that formed from toluene +OH/NO_x, is absorbing with MAC_{405nm} ~0.4 m^2 g^{-1}) [*Lin et al*., 2015]. The absorptivity of SOA can be additionally influenced by reactions with species such as ammonia, which tends to increase the MAC [*Updyke et al*., 2012]. Further, the dynamic evolution of SOA during its atmospheric aging may either enhance or inhibit light-absorption properties and therefore brings additional complexity for modeling efforts. For example, sunlight may photobleach and decompose certain types of the light-absorbing components in SOA [*Sareen et al*., 2013; *Lee et al*., 2014; *Forrister et al*., 2015; *Hinks et al*., 2016], while other light absorbers may be formed through oligomerization multiphase chemistry of nonabsorbing components of SOA [*Zhao et al*., 2015; *Hinks et al*., 2016]. The evaporation of water from aerosol and cloud droplets may result in enhanced formation of light-absorbing oligomeric compounds, while water uptake

promotes their hydrolysis and impedes light absorption [*Nguyen et al*., 2012b; *Zarzana et al*., 2012; *Lee et al*., 2013]. Furthermore, specific light-absorbers such as imidazoles act as photosensitizers and promote alternative mechanisms of SOA formation and aging [*Aregahegn et al*., 2013; *Rossignol et al*., 2014] that further alter the optical properties of SOA [*Yu et al*., 2014; *George et al*., 2015]. In addition, certain components of brown carbon aerosol can also be a source of radicals that can modify OA sources and sinks [*González Palacios et al*., 2016]. Given the myriad processes that can influence and transform SOA absorptivity, accurate inclusion of SOA absorption in models is challenging.

Additionally, it is important to consider the SOA absorption in the context of absorption by other OA types. In particular, biomass burning has been reported to be an important source of BrC in the atmosphere [*Lack et al*., 2012; *Feng et al*., 2013; *Washenfelder et al*., 2015]. The absorptivity of primary biomass burning OA (BBOA) is thought to be generally larger than that of SOA, with some estimates of the MAC_{405nm} for fresh BBOA ~0.5–1 $m^2\ g^{-1}$, depending on the source [*Chakrabarty et al*., 2010; *Lack et al*., 2012; *Zhang et al*., 2016]. However, the absorptivity of BBOA may be especially susceptible to degradation in the atmosphere [*Forrister et al*., 2015]. Thus, understanding the relative importance of SOA absorption requires better understanding and appropriate model representation of the processes that transform OA in the atmosphere.

Despite the challenges in understanding the full lifecycle of absorption by OA, in general, and SOA in particular, there have been a few recent climate modeling studies that have examined the potential importance of BrC (SOA + POA) on the radiation balance in certain geographic areas [*Chung et al*., 2012; *Feng et al*., 2013; *G. Lin et al*., 2014; *X. Wang et al*., 2014]. These modeling studies are complemented by studies that utilize regional aerosol optical depth measurements [*Arola et al*., 2011; *Bahadur et al*., 2012; *Wang et al*., 2013, 2016] and satellite-based observations [*Jethva and Torres*, 2011] to estimate BrC contributions to the global absorption. The overall magnitude of BrC contribution to radiative forcing on Earth is estimated at the level of 0.1–0.25 $W\ m^{-2}$, while regional effects are substantially higher [*Feng et al*., 2013]. The warming effect over regions affected by the light-absorbing OA from biomass burning and anthropogenic emissions is comparable to the estimated SOA cooling. However, the cumulative wavelength-specific results of both light-scattering and light-absorbing effects are ambiguous, inherent to complexity and variability of particle composition.

Overall, the complexity of chemistry and aging processes described above suggests that absorptive properties of brown carbon aerosol need to be constrained as a function of atmospheric aging parameters within climate models. Recent measurements, both laboratory and field based, provide guidance, but the understanding of BrC remains generally inadequate. While initial phenomenological knowledge in these areas has been accumulated over the last decade, more studies are needed to quantify and parameterize optical properties of SOA specific to aerosol source, chemical composition, and aging processes.

In addition to the optical properties, several other processes described in this article may impact our understanding of global climate forcing by SOA. The following section qualitatively discusses the implications of processes, described in this article.

9. Implications for Global Climate Forcing

This review selectively emphasizes results from measurements and theory over the past decade that have advanced an understanding of new processes governing the formation and evolution of SOA particles. Due to computational burden, global climate models often use SOA treatments that do not account for recently discovered SOA pathways. However, as our understanding continues to evolve, a comprehensive inclusion of all relevant processes is necessary, since several of these processes may have nonlinear and/or competing effects on SOA formation and its atmospheric lifecycle.

More than a decade ago, *Chung and Seinfeld* [2002] suggested that only hydrocarbons of biogenic origin contributed significantly to SOA formation based on measured aerosol yield parameters, reaction rate constants, and estimated global emissions. Using a top-down approach, *Hallquist et al*. [2009] estimated a global biogenic SOA source of 88 Tg C yr^{-1}. Even today, the dominant SOA type in most global climate models is suggested to be of predominantly biogenic origin [*Chung and Seinfeld*, 2002; *Heald et al*., 2011; *Scott et al*., 2014; *Tsigaridis et al*., 2014; *Lin et al*., 2016]. Annual global source of biogenic SOA in several recent global models ranges 13–40 Tg yr^{-1} [*Heald et al*., 2011; *Spracklen et al*., 2011; *D'Andrea et al*., 2013; *Scott et al*., 2014; *Shrivastava et al*., 2015]. *Hodzic et al*. [2016] recently estimated that global biogenic SOA source

increased from 21.5 to 99.3 Tg yr^{-1} when wall losses of vapors were included during fitting of SOA yields. Consistent with variation in SOA predicted by different global models, estimates of direct and indirect radiative forcing attributed to SOA vary widely in the literature. In AeroCom Phase II model experiments, the estimated direct radiative forcing from SOA calculated as a difference between present-day and preindustrial conditions ranged −0.01 to −0.21 W m^{-2} (median −0.02 and mean −0.06) [*Myhre et al*., 2013]. Recently, Spracklen et al. estimated that anthropogenically controlled SOA results in a direct radiative forcing of −0.26 W m^{-2} and an indirect (cloud albedo) forcing of −0.6 W m^{-2}. Another study estimated that both direct and indirect radiative forcing of SOA can each be as large as −0.77 W m^{-2} [*Scott et al*., 2014].

However, climate forcing due to biogenic SOA could be different from what most models are calculating now because of nonlinear SOA processes that are not currently included in these models. For example, climate forcing estimates could change when the influence of anthropogenic species such as sulfur and nitrogen oxides on biogenic SOA formation pathways is included in models (as described in this study). This study also highlights that the effects of NO_x and SO_2 on biogenic SOA are more complex than their representation in recent atmospheric chemistry models [e.g., *Marais et al*., 2016] and need to be reevaluated as new understanding emerges. In addition, the role of biomass burning SOA is uncertain as described in section 5. Both biogenic and biomass burning SOA affect the background aerosol state in present-day and preindustrial conditions. Background aerosol state strongly affects calculations of climate forcing, since natural aerosol state acts as a baseline on which anthropogenic aerosol forcing is calculated [*Carslaw et al*., 2013]. Therefore, it is essential to accurately represent the processes that affect the background aerosol state in global models.

Fundamental physical properties of SOA such as volatility and viscosity govern their formation, evolution, and lifetime. These properties can evolve in the atmosphere as a function of atmospheric aging and environmental conditions (e.g., effect of relative humidity on particle-phase diffusivity). While several models have included gas-phase chemistry of SOA precursors to varying degrees [*Tsigaridis et al*., 2014], the role of particle-phase processes can be fairly rapid [*Cappa and Wilson*, 2011; *Kolesar et al*., 2015a] and could greatly impact total SOA loadings and lifetimes [*Shrivastava et al*., 2015]. For example, *Shrivastava et al*. [2015] demonstrated that rapid decreases in SOA volatility due to particle-phase oligomerization increased the direct radiative forcing of SOA from −0.26 W m^{-2} to −0.5 W m^{-2}. The viscosity of particles affects kinetic limitations for mass transport of species within the particle bulk and in turn affects growth rate and size evolution of SOA. However, viscosity can affect uptake of gas-phase organic species on particles to varying degrees in the atmosphere as a function of atmospheric aging of SOA, temperature, and relative humidity. The implications of variations in both volatility and viscosity of SOA on global climate forcing need to be investigated.

Formation of highly oxidized compounds (contributing greatly to ELVOC concentrations) in the gas phase has been recently shown to increase nucleation and the growth rates of freshly nucleated particles [*Kirkby et al*., 2016; *Trostl et al*., 2016]. The addition of these ELVOC compounds to global models increase predicted CCN concentrations, but this effect may be minor under present-day conditions or limited to regions rich in BVOC emissions [*Jokinen et al*., 2015]. The minor impact of ELVOC on CCN could be due to compensating effects. Thus, on one hand new particle formation and the growth rate of ultrafine particles increase due to ELVOC; on the other hand, these new particles can coagulate faster and also act as increased condensational sink for ELVOC. These compensating effects are referred to as "microphysical dampening" in the literature and are responsible for a modest (<10 times) increase in CCN, although the nucleation (and early growth) rates increase by orders of magnitude (~1000 times) [*D'Andrea et al*., 2013; *Pierce et al*., 2013; *Westervelt et al*., 2014]. We note that the role of ELVOC on the difference between present-day and preindustrial conditions is yet to be investigated, but this will also depend on better representation of other processes, e.g., role of NO_x within climate models.

In contrast to HOM, which according to experimental evidence are generated rapidly (within seconds to minutes) [*Ehn et al*., 2014; *Jokinen et al*., 2015], gas-phase multigenerational chemistry could be a constant source of low-volatility and semivolatile organic compounds. These compounds formed through multiple reactions with oxidants could represent a constant atmospheric source of SOA at much longer time scales (approximately days) and are responsible for the condensational growth of particles from nucleation clusters to CCN sizes. The magnitude of the microphysical dampening effects may differ between ELVOC (that are quickly generated and condense) and SVOC that are formed in the atmosphere over longer periods

[*Pierce et al*., 2011]. The budgets of SVOC and ELVOC between present-day and preindustrial conditions could also be different due to several aspects such as differing oxidant regimes, role of anthropogenic species such as sulfur and NO_x on SOA formation (e.g., IEPOX-SOA pathway), as discussed in this work. We also note that compared to biogenic SOA, fewer global models include biomass burning and anthropogenic SOA sources [e.g., *Shrivastava et al*., 2015]. Biomass burning SOA sources are not well constrained and can have large variability between individual fires/sources [*Cubison et al*., 2011; *Ortega et al*., 2013; *Jathar et al*., 2014].

Although a limited number of studies have included some representation of SOA processes (e.g., IEPOX-SOA, effect of rapid oligomerization, effects of wall loss on SOA yields, effects of ELVOC on CCN, biomass burning SOA, and aqueous-phase SOA formation), future studies need to investigate the implications of all these processes on climate forcing holistically. Physically and chemically realistic representations of all SOA relevant processes are needed to understand which of these processes are most influential in terms of climate forcing of SOA. In addition, there may be nonlinear interactions among these processes wherein some processes can either be synergistic or act to compensate each other.

10. Conclusions

SOA represent complex aerosol systems. Significant advances in understanding of SOA formation and properties have occurred over the past decade, but substantial gaps remain, presenting challenges for accurate characterization of SOA's role in climate.

A better understanding of SOA formation mechanisms and physical properties is needed to improve estimates of the extent to which anthropogenic emissions and land use changes have modified global OA concentrations and size distributions since preindustrial times. A major unifying goal is to determine the net radiative forcing of SOA from anthropogenic activities more reliably and reduce one of the factors that can complicate estimates of the climate response to changing greenhouse gas concentrations (i.e., the climate sensitivity). Ultimately, climate models need to capture enough important features of the chemical and dynamic evolution of SOA, both in terms of aerosol number and aerosol mass, as a function of atmospheric variables and anthropogenic perturbations to reasonably predict the spatial and temporal distributions of SOA. This study identifies a number of process-level mechanisms related to the interactions between anthropogenic and biogenic SOA precursors, for which the corresponding impacts on the radiative effects of SOA need to be investigated in atmospheric chemistry-climate models.

During the past decade, significant progress has been made in understanding the processes through which anthropogenic emissions affect biogenic SOA formation. Gas-phase oxidation of isoprene, the most prevalent VOC, to produce SOA, and its dependence on sulfate, NO_x level, relative humidity, and temperature is a major area of importance. IEPOX chemistry, particle-phase oligomerization, and potential diffusion limitations in particles are frequently missing in atmospheric models, though a varying degree of understanding of these factors does exist.

Particle-phase processes, such as oligomerization, act to decrease the overall volatility of the aerosol and increase its viscosity. Molecular speciation of gas and particle phases provides bottom-up information on reaction mechanisms and volatility, and the evolution of particle size distributions provides top-down insights on growth mechanisms and particle properties.

The SOA-forming potential of a VOC is determined through chamber studies and represented by the experimentally measured SOA yield. Models of the SOA formation of a particular VOC have traditionally been fit to the experimental data assuming instantaneous equilibrium of semivolatile species between the gas phase and particle phase without explicit consideration of the influence of other processes (e.g., oligomerization) or properties (e.g., viscosity). Recent discovery of the semisolid nature of a number of SOA systems and heterogeneous oligomer formation has caused a reconsideration of how the traditional gas-particle equilibrium model is applied to SOA systems. Recently, transient diffusion-reaction models have been developed that account for finite times for accommodation of vapors into growing particle. These finite mass transfer rates of SOA precursor species are reflected, for example, in the size distribution of the evolving SOA. The atmospheric applicability of these transient diffusion-reaction models awaits a better understanding of how diffusion limitations and/or reactive uptake kinetics vary for a range of

SOA systems under different atmospherically relevant conditions at varying temperature, relative humidity, aerosol acidity, and water content.

While it is known that SOA particle becomes less viscous with increasing RH, most of these high-RH measurements have been made at room temperature. In the atmosphere, higher RH occurs close to the top of the boundary layer, where lower temperature favors increase in particle viscosity and the resulting diffusion limitations. Further studies aimed at measuring the diffusion limitations within SOA particles at low temperature and high-RH conditions are needed for a range of different SOA precursors and regimes. Transient diffusion-reaction models will be valuable to interpret volatility distributions of SOA particles corresponding to laboratory measurements, which are conducted at controlled conditions.

Importantly, since the volatility distributions used in some modeling parameterizations to define the lumped properties of the SOA precursors are operationally determined from chamber experiments and depend on assumptions about other SOA properties—e.g., low viscosity and processes such as wall losses—they are, in fact, "theory-specific volatility distributions." Combining the molecular information of gas- and particle-phase composition with the size distribution dynamics could help constrain both the volatility distribution of SOA precursor organics and the dominant growth mechanisms.

Biomass burning is a globally important source of OA. But different field studies vary in terms of SOA-forming potential in biomass burning plumes. Similarly, global modeling studies on role of SOA from biomass burning vary substantially. Further research is needed to constrain this important source of SOA.

Also, since even a small refractive index for absorption can significantly influence absorption by SOA (as described in section 8), parameterization of brown carbon properties in SOA models will need to be revisited. More field and laboratory studies are needed to provide sufficient observations and fundamental scientific knowledge for development and constraining future models.

In summary, molecular-level interactions between anthropogenic and biogenic SOA precursor species, oligomerization, heterogeneous oxidation, organic salt formation, effects of losses of SOA precursors on chamber walls, mass transfer limitations in particles, and aqueous-phase chemistry in both aerosols and cloud droplets could have large and nonlinear effects on the formation, lifetime, composition, and atmospheric evolution of particles. A frequently asked question is the following: Do we need to represent the great complexity of SOA in climate models that are already computationally expensive? These nonlinear processes imply that currently simplified SOA representations in global climate models most likely do not accurately reflect either the climate forcing of SOA or our ability to project future sensitivity to greenhouse gases. Measurements and modeling studies need to determine the most influential processes and investigate how they impact our understanding of climate forcing including aerosol-radiation and aerosol-cloud interactions. In some cases, model-ready parameterizations exist (e.g., role of IEPOX chemistry on SOA) and could be used to assess the sensitivity of SOA distributions to these parameterizations, while other cases (e.g., diffusion limitations within particles) likely require more refined fundamental process-level understanding. Therefore, it remains important to continue improving the experimental constraints on as many relevant processes as are likely to go into models and that both bottom-up and top-down constraints are applied.

Glossary of Acronyms

AMS	Aerosol Mass Spectrometer
ASR	Atmospheric Systems Research Program
AVOC	Anthropogenic Volatile Organic Compounds
BAECC	Biogenic Aerosols—Effects on Clouds and Climate
BB	Biomass Burning
BBOA	Biomass Burning Organic Aerosol
BrC	Brown Carbon
BVOC	Biogenic Volatile Organic Compounds
CCN	Cloud Condensation Nuclei
CIMS	Chemical Ionization Mass Spectrometer
DOE	U.S. Department of Energy
DOP	Dioctyl Phthalate

DOS	Dioctyl Sebacate
ELVOC	Extremely Low-Volatility organic compounds
ERFaci	Effective Radiative Forcing due to Aerosol-Cloud Interactions
ERFari	Effective Radiative Forcing due to Aerosol-Radiation Interactions
FIGAERO	Filter Inlet for Gases and Aerosols
HOM	Highly Oxygenated Organic Molecules
HPALD	Hydroperoxyaldehyde
HR-ToF-CIMS	High-Resolution, time-of-flight Chemical Ionization Mass Spectrometer
IEPOX	Isoprene Epoxydiols
IN	Ice Nuclei
ISOPOOH	Isoprene Hydroxyl Hydroperoxides
IVOC	Intermediate Volatility Organic Compounds
KM-GAP	A detailed Multilayer Kinetic Flux Model
LVSOA	Low-Volatility Secondary Organic Aerosol
MAC	Mass Absorption Coefficient
MACR	Methacrolein
MOSAIC	Model for Simulating Aerosol Interactions and Chemistry
MPAN	Peroxy Methacryloyl Nitrate
MVK	MethylVinyl ketone
NMOC	Nonmethane Organic Compound
NVSOA	Effectively Nonvolatile Secondary Organic Aerosol
OA	Organic Aerosol
PAHs	Polycyclic Aromatic Hydrocarbons
PMF	Positive Matrix Factorization
PNNL	Pacific Northwest National Laboratory
POA	Primary Organic Aerosol
RH	Relative Humidity
SIVOC	Semivolatile and Intermediate-Volatility Organic Compounds
SOA	Secondary Organic Aerosol
SVOC	Semivolatile Organic Compounds
SVSOA	Semivolatile Secondary Organic Aerosol
SV-TAG	Semivolatile Thermal Desorption Aerosol Gas Chromatograph
TD-AMS	Thermal Denuder-Aerosol Mass Spectrometer
VFR	Volume Fraction Remaining
VBS	Volatility Basis Set
VOC	Volatile Organic Compounds

Acknowledgments

This work was supported by the U.S. Department of Energy (DOE), Office of Science, Biological and Environmental Research's Atmospheric System Research (ASR) program. The manuscript is based on an ASR-supported workshop "New Strategies for Addressing Anthropogenic-Biogenic Interactions of Organic Aerosol in Climate Models," which was held at the Pacific Northwest National Laboratory (PNNL) on 8 and 9 June 2015. The Pacific Northwest National Laboratory is operated for DOE by Battelle Memorial Institute under contract DE-AC05-76RL01830. C.D.C was supported by National Science Foundation (ATM-1151062). P.J.R. was supported by the U.S. DOE, Office of Science, Biological and Environmental Research program as part of the Earth System Modeling Program. The authors thank Jerome Fast, Charlette Geffen, Ashley Williamson, and Shaima Nasiri for their support and encouragement. Sources of figures adapted from previous publications are duly cited and conform to copyright requirements from their respective publications. No other data was utilized in this study.

References

Abramson, E., D. Imre, J. Beranek, J. Wilson, and A. Zelenyuk (2013), Experimental determination of chemical diffusion within secondary organic aerosol particles, *Phys. Chem. Chem. Phys.*, *15*(8), 2983–2991.

Aiken, A. C., et al. (2008), O/C and OM/OC ratios of primary, secondary, and ambient organic aerosols with high-resolution time-of-flight aerosol mass spectrometry, *Environ. Sci. Technol.*, *42*(12), 4478–4485.

Akagi, S. K., R. J. Yokelson, C. Wiedinmyer, M. J. Alvarado, J. S. Reid, T. Karl, J. D. Crounse, and P. O. Wennberg (2011), Emission factors for open and domestic biomass burning for use in atmospheric models, *Atmos. Chem. Phys.*, *11*(9), 4039–4072.

Akagi, S. K., et al. (2012), Evolution of trace gases and particles emitted by a chaparral fire in California, *Atmos. Chem. Phys.*, *12*(3), 1397–1421.

Allan, J. D., W. T. Morgan, E. Darbyshire, M. J. Flynn, P. I. Williams, D. E. Oram, P. Artaxo, J. Brito, J. D. Lee, and H. Coe (2014), Airborne observations of IEPOX-derived isoprene SOA in the Amazon during SAMBBA, *Atmos. Chem. Phys.*, *14*(20), 11,393–11,407.

Almeida, M. B., A. M. Alvarez, E. M. Demiguel, and E. S. Delhoyo (1983), Setchenow coefficients for naphthols by distribution method, *Can. J. Chem.-Revue Canadienne De Chimie*, *61*(2), 244–248.

Altieri, K. E., S. P. Seitzinger, A. G. Carlton, B. J. Turpin, G. C. Klein, and A. G. Marshall (2008), Oligomers formed through in-cloud methylglyoxal reactions: Chemical composition, properties, and mechanisms investigated by ultra-high resolution FT-ICR mass spectrometry, *Atmos. Environ.*, *42*(7), 1476–1490.

Andreae, M. O., and A. Gelencser (2006), Black carbon or brown carbon? The nature of light-absorbing carbonaceous aerosols, *Atmos. Chem. Phys.*, *6*, 3131–3148.

Andreae, M. O., and P. Merlet (2001), Emission of trace gases and aerosols from biomass burning, *Global Biogeochem. Cycles*, *15*(4), 955–966.

Aregahegn, K. Z., B. Noziere, and C. George (2013), Organic aerosol formation photo-enhanced by the formation of secondary photosensitizers in aerosols, *Faraday Discuss.*, *165*, 123–134.

Arola, A., G. Schuster, G. Myhre, S. Kazadzis, S. Dey, and S. N. Tripathi (2011), Inferring absorbing organic carbon content from AERONET data, *Atmos. Chem. Phys.*, *11*(1), 215–225.

Atkinson, R., S. M. Aschmann, E. C. Tuazon, J. Arey, and B. Zielinska (1989), Formation of 3-Methylfuran from the gas-phase reaction of oh radicals with isoprene and the rate constant for its reaction with the OH radical, *Int. J. Chem. Kinet.*, *21*(7), 593–604.

Atkinson, R. (1997), Gas-phase tropospheric chemistry of volatile organic compounds: 1. Alkanes and alkenes, *J. Phys. Chem. Ref. Data*, *26*(2), 215–290.

Axson, J. L., K. Takahashi, D. O. De Haan, and V. Vaida (2010), Gas-phase water-mediated equilibrium between methylglyoxal and its geminal diol, *Proc. Natl. Acad. Sci. U.S.A.*, *107*(15), 6687–6692.

Bahadur, R., P. S. Praveen, Y. Y. Xu, and V. Ramanathan (2012), Solar absorption by elemental and brown carbon determined from spectral observations, *Proc. Natl. Acad. Sci. U.S.A.*, *109*(43), 17,366–17,371.

Bakwin, P. S., S. C. Wofsy, S. M. Fan, M. Keller, S. E. Trumbore, and J. M. Dacosta (1990), Emission of nitric oxide (No) from tropical forest soils and exchange of NO between the forest canopy and atmospheric boundary layers, *J. Geophys. Res.*, *95*(D10), 16,755–16,764.

Barnard, J. C., R. Volkamer, and E. I. Kassianov (2008), Estimation of the mass absorption cross section of the organic carbon component of aerosols in the Mexico City Metropolitan Area, *Atmos. Chem. Phys.*, *8*(22), 6665–6679.

Barsanti, K. C., and J. F. Pankow (2004), Thermodynamics of the formation of atmospheric organic particulate matter by accretion reactions—Part 1: Aldehydes and ketones, *Atmos. Environ.*, *38*(26), 4371–4382.

Barsanti, K. C., and J. F. Pankow (2005), Thermodynamics of the formation of atmospheric organic particulate matter by accretion reactions—2. Dialdehydes, methylglyoxal, and diketones, *Atmos. Environ.*, *39*(35), 6597–6607.

Barsanti, K. C., and J. F. Pankow (2006), Thermodynamics of the formation of atmospheric organic particulate matter by accretion reactions—Part 3: Carboxylic and dicarboxylic acids, *Atmos. Environ.*, *40*(34), 6676–6686.

Barsanti, K. C., P. H. McMurry, and J. N. Smith (2009), The potential contribution of organic salts to new particle growth, *Atmos. Chem. Phys.*, *9*(9), 2949–2957.

Barsanti, K. C., J. N. Smith, and J. F. Pankow (2011), Application of the *n*p+*m*P modeling approach for simulating secondary organic particulate matter formation from alpha-pinene oxidation, *Atmos. Environ.*, *45*(37), 6812–6819.

Bateman, A. P., A. K. Bertram, and S. T. Martin (2015), Hygroscopic influence on the semisolid-to-liquid transition of secondary organic materials, *J. Phys. Chem. A*, *119*(19), 4386–4395.

Bateman, A. P., et al. (2016), Sub-micrometre particulate matter is primarily in liquid form over Amazon rainforest, *Nat. Geosci.*, *9*(1), 34–37.

Bateman, A. P., et al. (2017), Anthropogenic influences on the physical state of submicron particulate matter over a tropical forest, *Atmos. Chem. Phys.*, *17*(3), 1759–1773.

Bates, K. H., J. D. Crounse, J. M. S. Clair, N. B. Bennett, T. B. Nguyen, J. H. Seinfeld, B. M. Stoltz, and P. O. Wennberg (2014), Gas phase production and loss of isoprene epoxydiols, *J. Phys. Chem. A*, *118*(7), 1237–1246.

Bates, K. H., T. B. Nguyen, A. P. Teng, J. D. Crounse, H. G. Kjaergaard, B. M. Stoltz, J. H. Seinfeld, and P. O. Wennberg (2016), Production and fate of C_4 dihydroxycarbonyl compounds from isoprene oxidation, *J. Phys. Chem. A*, *120*(1), 106–117.

Beaver, M. R., et al. (2012), Importance of biogenic precursors to the budget of organic nitrates: Observations of multifunctional organic nitrates by CIMS and TD-LIF during BEARPEX 2009, *Atmos. Chem. Phys.*, *12*(13), 5773–5785.

Bell, D. M., D. Imre, S. T. Martin, and A. Zelenyuk (2017), Properties and behavior of α-pinene secondary organic aerosol particles exposed to ammonia under dry conditions, *Phys. Chem. Chem. Phys.*, *19*, 6497–6507, doi:10.1039/c6cp08839b.

Berkemeier, T., M. Shiraiwa, U. Pöschl, and T. Koop (2014), Competition between water uptake and ice nucleation by glassy organic aerosol particles, *Atmos. Chem. Phys.*, *14*(22), 12,513–12,531.

Berndt, T. (2012), Formation of carbonyls and hydroperoxyenals (HPALDs) from the OH radical reaction of isoprene for low-NO_x conditions: Influence of temperature and water vapour content, *J. Atmos. Chem.*, *69*(4), 253–272.

Berndt, T., S. Richters, R. Kaethner, J. Voigtländer, F. Stratmann, M. Sipilä, M. Kulmala, and H. Herrmann (2015), Gas-phase ozonolysis of cycloalkenes: Formation of highly oxidized RO_2 radicals and their reactions with NO, NO_2, SO_2, and other RO_2 radicals, *Chem. A Eur. J.*, *119*(41), 10,336–10,348.

Blanchard, C. L., G. M. Hidy, S. Shaw, K. Baumann, and E. S. Edgerton (2016), Effects of emission reductions on organic aerosol in the southeastern United States, *Atmos. Chem. Phys.*, *16*(1), 215–238.

Blando, J. D., and B. J. Turpin (2000), Secondary organic aerosol formation in cloud and fog droplets: A literature evaluation of plausibility, *Atmos. Environ.*, *34*(10), 1623–1632.

Bond, T. C., and R. W. Bergstrom (2006), Light absorption by carbonaceous particles: An investigative review, *Aerosol Sci. Technol.*, *40*(1), 27–67.

Bond, T. C., et al. (2013), Bounding the role of black carbon in the climate system: A scientific assessment, *J. Geophys. Res. Atmos.*, *118*, 5380–5552, doi:10.1002/jgrd.50171.

Boone, E. J., A. Laskin, J. Laskin, C. Wirth, P. B. Shepson, B. H. Stirm, and K. A. Pratt (2015), Aqueous processing of atmospheric organic particles in cloud water collected via aircraft sampling, *Environ. Sci. Technol.*, *49*(14), 8523–8530.

Boucher, O., et al. (2013), Clouds and Aerosols, in *Climate Change 2013: The Physical Science Basis. Contribution of Working Group I to the Fifth Assessment Report of the Intergovernmental Panel on Climate Change*, edited by T. F. Stocker et al., Cambridge Univ. Press, Cambridge, U. K., and New York.

Boyd, C. M., J. Sanchez, L. Xu, A. J. Eugene, T. Nah, W. Y. Tuet, M. I. Guzman, and N. L. Ng (2015), Secondary organic aerosol formation from the β-pinene+NO_3 system: Effect of humidity and peroxy radical fate, *Atmos. Chem. Phys.*, *15*(13), 7497–7522.

Bregonzio-Rozier, L., et al. (2015), Gaseous products and secondary organic aerosol formation during long term oxidation of isoprene and methacrolein, *Atmos. Chem. Phys.*, *15*(6), 2953–2968.

Brégonzio-Rozier, L., et al. (2016), Secondary organic aerosol formation from isoprene photooxidation during cloud condensation–evaporation cycles, *Atmos. Chem. Phys.*, *16*(3), 1747–1760.

Brown, S. S., et al. (2009), Nocturnal isoprene oxidation over the Northeast United States in summer and its impact on reactive nitrogen partitioning and secondary organic aerosol, *Atmos. Chem. Phys.*, *9*(9), 3027–3042.

Brown, S. S., et al. (2013), Biogenic VOC oxidation and organic aerosol formation in an urban nocturnal boundary layer: Aircraft vertical profiles in Houston, TX, *Atmos. Chem. Phys.*, *13*(22), 11,317–11,337.

Bruns, E. A., I. El Haddad, J. G. Slowik, D. Kilic, F. Klein, U. Baltensperger, and A. S. H. Prévôt (2016), Identification of significant precursor gases of secondary organic aerosols from residential wood combustion, *Sci. Rep.*, *6*, 27881.

Budisulistiorini, S., et al. (2015), Examining the effects of anthropogenic emissions on isoprene-derived secondary organic aerosol formation during the 2013 Southern Oxidant and Aerosol Study (SOAS) at the Look Rock, Tennessee, ground site, *Atmos. Chem. Phys.*, *15*, 8871–8888.

Budisulistiorini, S. H., K. Baumann, E. S. Edgerton, S. T. Bairai, S. Mueller, S. L. Shaw, E. M. Knipping, A. Gold, and J. D. Surratt (2016), Seasonal characterization of submicron aerosol chemical composition and organic aerosol sources in the southeastern United States: Atlanta, Georgia, and Look Rock, Tennessee, *Atmos. Chem. Phys.*, *16*(8), 5171–5189.

Budisulistiorini, S. H., et al. (2013), Real-time continuous characterization of secondary organic aerosol derived from isoprene epoxydiols in downtown Atlanta, Georgia, using the Aerodyne Aerosol Chemical Speciation Monitor, *Environ. Sci. Technol.*, *47*(11), 5686–5694.

Bzdek, B. R., and M. V. Johnston (2010), New particle formation and growth in the troposphere, *Anal. Chem.*, *82*(19), 7871–7878.

Capes, G., B. Johnson, G. McFiggans, P. I. Williams, J. Haywood, and H. Coe (2008), Aging of biomass burning aerosols over West Africa: Aircraft measurements of chemical composition, microphysical properties, and emission ratios, *J. Geophys. Res.*, *113*, D00C15, doi:10.1029/2008JD009845.

Cappa, C. D., and J. L. Jimenez (2010), Quantitative estimates of the volatility of ambient organic aerosol, *Atmos. Chem. Phys.*, *10*(12), 5409–5424.

Cappa, C. D., and K. R. Wilson (2011), Evolution of organic aerosol mass spectra upon heating: Implications for OA phase and partitioning behavior, *Atmos. Chem. Phys.*, *11*(5), 1895–1911.

Cappa, C. D., and K. R. Wilson (2012), Multi-generation gas-phase oxidation, equilibrium partitioning, and the formation and evolution of secondary organic aerosol, *Atmos. Chem. Phys.*, *12*(20), 9505–9528.

Cappa, C. D., S. H. Jathar, M. J. Kleeman, K. S. Docherty, J. L. Jimenez, J. H. Seinfeld, and A. S. Wexler (2016), Simulating secondary organic aerosol in a regional air quality model using the statistical oxidation model—Part 2: Assessing the influence of vapor wall losses, *Atmos. Chem. Phys.*, *16*(5), 3041–3059.

Carlton, A. G., C. Wiedinmyer, and J. H. Kroll (2009), A review of Secondary Organic Aerosol (SOA) formation from isoprene, *Atmos. Chem. Phys.*, *9*(14), 4987–5005.

Carlton, A. G., R. W. Pinder, P. V. Bhave, and G. A. Pouliot (2010), To what extent can biogenic SOA be controlled?, *Environ. Sci. Technol.*, *44*(9), 3376–3380.

Carlton, A. G., B. J. Turpin, K. E. Altieri, S. Seitzinger, A. Reff, H.-J. Lim, and B. Ervens (2007), Atmospheric oxalic acid and SOA production from glyoxal: Results of aqueous photooxidation experiments, *Atmos. Environ.*, *41*(35), 7588–7602.

Carlton, A. G., B. J. Turpin, K. E. Altieri, S. P. Seitzinger, R. Mathur, S. J. Roselle, and R. J. Weber (2008), CMAQ model performance enhanced when in-cloud secondary organic aerosol is included: Comparisons of organic carbon predictions with measurements, *Environ. Sci. Technol.*, *42*(23), 8798–8802.

Carslaw, K. S., et al. (2013), Large contribution of natural aerosols to uncertainty in indirect forcing, *Nature*, *503*(7474), 67–71.

Cerully, K. M., A. Bougiatioti, J. R. Hite, H. Guo, L. Xu, N. L. Ng, R. Weber, and A. Nenes (2015), On the link between hygroscopicity, volatility, and oxidation state of ambient and water-soluble aerosols in the southeastern United States, *Atmos. Chem. Phys.*, *15*(15), 8679–8694.

Chacon-Madrid, H. J., and N. M. Donahue (2011), Fragmentation vs. functionalization: Chemical aging and organic aerosol formation, *Atmos. Chem. Phys.*, *11*(20), 10,553–10,563.

Chakrabarty, R. K., H. Moosmuller, L. W. A. Chen, K. Lewis, W. P. Arnott, C. Mazzoleni, M. K. Dubey, C. E. Wold, W. M. Hao, and S. M. Kreidenweis (2010), Brown carbon in tar balls from smoldering biomass combustion, *Atmos. Chem. Phys.*, *10*(13), 6363–6370.

Chan, A., M. N. Chan, J. D. Surratt, P. S. Chhabra, C. L. Loza, J. D. Crounse, L. D. Yee, R. C. Flagan, P. O. Wennberg, and J. H. Seinfeld (2010), Role of aldehyde chemistry and NO_x concentrations in secondary organic aerosol formation, *Atmos. Chem. Phys.*, *10*(15), 7169–7188.

Chan, M. N., et al. (2010), Characterization and quantification of isoprene-derived epoxydiols in ambient aerosol in the southeastern United States, *Environ. Sci. Technol.*, *44*(12), 4590–4596.

Chang, R. Y. W., J. G. Slowik, N. C. Shantz, A. Vlasenko, J. Liggio, S. J. Sjostedt, W. R. Leaitch, and J. P. D. Abbatt (2010), The hygroscopicity parameter (κ) of ambient organic aerosol at a field site subject to biogenic and anthropogenic influences: Relationship to degree of aerosol oxidation, *Atmos. Chem. Phys.*, *10*(11), 5047–5064.

Chen, Q., Y. J. Liu, N. M. Donahue, J. E. Shilling, and S. T. Martin (2011), Particle-phase chemistry of secondary organic material: Modeled compared to measured O:C and H:C elemental ratios provide constraints, *Environ. Sci. Technol.*, *45*(11), 4763–4770.

Chen, Q., et al. (2015), Submicron particle mass concentrations and sources in the Amazonian wet season (AMAZE-08), *Atmos. Chem. Phys.*, *15*(7), 3687–3701.

Chhabra, P. S., N. L. Ng, M. R. Canagaratna, A. L. Corrigan, L. M. Russell, D. R. Worsnop, R. C. Flagan, and J. H. Seinfeld (2011), Elemental composition and oxidation of chamber organic aerosol, *Atmos. Chem. Phys.*, *11*(17), 8827–8845.

Chung, C. E., V. Ramanathan, and D. Decremer (2012), Observationally constrained estimates of carbonaceous aerosol radiative forcing, *Proc. Natl. Acad. Sci. U.S.A.*, *109*(29), 11,624–11,629.

Chung, S. H., and J. H. Seinfeld (2002), Global distribution and climate forcing of carbonaceous aerosols, *J. Geophys. Res.*, *107*(D19), AAC 14-1–AAC 14-33, doi:10.1029/2001JD001397.

Claeys, M., et al. (2004), Formation of secondary organic aerosols through photooxidation of isoprene, *Science*, *303*(5661), 1173–1176.

Claeys, M., et al. (2009), Terpenylic acid and related compounds from the oxidation of alpha-pinene: Implications for New particle formation and growth above forests, *Environ. Sci. Technol.*, *43*(18), 6976–6982.

Cocker, D. R., R. C. Flagan, and J. H. Seinfeld (2001), State-of-the-art chamber facility for studying atmospheric aerosol chemistry, *Environ. Sci. Technol.*, *35*(12), 2594–2601.

Collier, S., et al. (2016), Regional influence of aerosol emissions from wildfires driven by combustion efficiency: Insights from the BBOP campaign, *Environ. Sci. Technol.*, *50*(16), 8613–8622.

Connolly, P. J., T. W. Choularton, M. W. Gallagher, K. N. Bower, M. J. Flynn, and J. A. Whiteway (2006), Cloud-resolving simulations of intense tropical Hector thunderstorms: Implications for aerosol-cloud interactions, *Q. J. R. Meteorol. Soc.*, *132*(621), 3079–3106.

Crounse, J. D., F. Paulot, H. G. Kjaergaard, and P. O. Wennberg (2011), Peroxy radical isomerization in the oxidation of isoprene, *Phys. Chem. Chem. Phys.*, *13*(30), 13,607–13,613.

Crounse, J. D., H. C. Knap, K. B. Ornso, S. Jorgensen, F. Paulot, H. G. Kjaergaard, and P. O. Wennberg (2012), Atmospheric fate of methacrolein: 1. Peroxy radical isomerization following addition of OH and O_2, *J. Phys. Chem. A*, *116*(24), 5756–5762.

Crounse, J. D., L. B. Nielsen, S. Jorgensen, H. G. Kjaergaard, and P. O. Wennberg (2013), Autoxidation of organic compounds in the atmosphere, *J. Phys. Chem. Lett.*, *4*(20), 3513–3520.

Crump, J. G., and J. H. Seinfeld (1981), Turbulent deposition and gravitational sedimentation of an aerosol in a vessel of arbitrary shape, *J. Aerosol Sci.*, *12*(5), 405–415.

Cubison, M. J., et al. (2011), Effects of aging on organic aerosol from open biomass burning smoke in aircraft and laboratory studies, *Atmos. Chem. Phys.*, *11*(23), 12,049–12,064.

D'Ambro, E. L., et al. (2016), Molecular composition and volatility of isoprene photochemical oxidation secondary organic aerosol under low and high NO_x conditions, *Atmos. Chem. Phys. Discuss.*, *2016*, 1–45.

D'Andrea, S. D., S. A. K. Hakkinen, D. M. Westervelt, C. Kuang, E. J. T. Levin, V. P. Kanawade, W. R. Leaitch, D. V. Spracklen, I. Riipinen, and J. R. Pierce (2013), Understanding global secondary organic aerosol amount and size-resolved condensational behavior, *Atmos. Chem. Phys.*, *13*(22), 11,519–11,534.

Da Silva, G., C. Graham, and Z. F. Wang (2010), Unimolecular β-hydroxyperoxy radical decomposition with OH recycling in the photochemical oxidation of isoprene, *Environ. Sci. Technol.*, *44*(1), 250–256.

Darer, A. I., N. C. Cole-Filipiak, A. E. O'Connor, and M. J. Elrod (2011), Formation and stability of atmospherically relevant isoprene-derived organosulfates and organonitrates, *Environ. Sci. Technol.*, *45*(5), 1895–1902.

Daumit, K. E., A. J. Carrasquillo, J. F. Hunter, and J. H. Kroll (2014), Laboratory studies of the aqueous-phase oxidation of polyols: Submicron particles vs. bulk aqueous solution, *Atmos. Chem. Phys.*, *14*(19), 10,773–10,784.

Day, D. A., S. Liu, L. M. Russell, and P. J. Ziemann (2010), Organonitrate group concentrations in submicron particles with high nitrate and organic fractions in coastal southern California, *Atmos. Environ.*, *44*(16), 1970–1979.

De Gouw, J., and J. L. Jimenez (2009), Organic aerosols in the Earth's atmosphere, *Environ. Sci. Technol.*, *43*(20), 7614–7618.

de Gouw, J. A., et al. (2005), Budget of organic carbon in a polluted atmosphere: Results from the New England Air Quality Study in 2002, *J. Geophys. Res.*, *110*, D16305, doi:10.1029/2004JD005623.

DeMott, P. J., A. J. Prenni, X. Liu, S. M. Kreidenweis, M. D. Petters, C. H. Twohy, M. S. Richardson, T. Eidhammer, and D. C. Rogers (2010), Predicting global atmospheric ice nuclei distributions and their impacts on climate, *Proc. Natl. Acad. Sci. U.S.A.*, *107*(25), 11,217–11,222.

Deng, W., et al. (2017), Secondary organic aerosol formation from photo-oxidation of toluene with NO_x and SO_2: Chamber simulation with purified air versus urban ambient air as matrix, *Atmos. Environ.*, *150*, 67–76.

Docherty, K. S., and P. J. Ziemann (2003), Effects of stabilized Criegee intermediate and OH radical scavengers on aerosol formation from reactions of β-Pinene with O_3, *Aerosol Sci. Technol.*, *37*(11), 877–891.

Dommen, J., A. Metzger, J. Duplissy, M. Kalberer, M. R. Alfarra, A. Gascho, E. Weingartner, A. S. H. Prevot, B. Verheggen, and U. Baltensperger (2006), Laboratory observation of oligomers in the aerosol from isoprene/NO_x photooxidation, *Geophys. Res. Lett.*, *33*, L13805, doi:10.1029/2006GL026523.

Donahue, N. M., A. L. Robinson, C. O. Stanier, and S. N. Pandis (2006), Coupled partitioning, dilution, and chemical aging of semivolatile organics, *Environ. Sci. Technol.*, *40*(8), 02,635–02,643.

Donahue, N. M., S. A. Epstein, S. N. Pandis, and A. L. Robinson (2011), A two-dimensional volatility basis set: 1. Organic-aerosol mixing thermodynamics, *Atmos. Chem. Phys.*, *11*(7), 3303–3318.

Donahue, N. M., J. H. Kroll, S. N. Pandis, and A. L. Robinson (2012a), A two-dimensional volatility basis set—Part 2: Diagnostics of organic-aerosol evolution, *Atmos. Chem. Phys.*, *12*(2), 615–634.

Donahue, N. M., et al. (2012b), Aging of biogenic secondary organic aerosol via gas-phase OH radical reactions, *Proc. Natl. Acad. Sci. U.S.A.*, *109*(34), 13,503–13,508.

Eddingsaas, N. C., D. G. VanderVelde, and P. O. Wennberg (2010), Kinetics and products of the acid-catalyzed ring-opening of atmospherically relevant butyl epoxy alcohols, *J. Phys. Chem. A*, *114*(31), 8106–8113.

Ehn, M., T. Petaja, W. Birmili, H. Junninen, P. Aalto, and M. Kulmala (2007), Non-volatile residuals of newly formed atmospheric particles in the boreal forest, *Atmos. Chem. Phys.*, *7*, 677–684.

Ehn, M., et al. (2012), Gas phase formation of extremely oxidized pinene reaction products in chamber and ambient air, *Atmos. Chem. Phys.*, *12*(11), 5113–5127.

Ehn, M., et al. (2014), A large source of low-volatility secondary organic aerosol, *Nature*, *506*(7489), 476–479.

Ervens, B., and R. Volkamer (2010), Glyoxal processing by aerosol multiphase chemistry: Towards a kinetic modeling framework of secondary organic aerosol formation in aqueous particles, *Atmos. Chem. Phys.*, *10*(17), 8219–8244.

Ervens, B., B. J. Turpin, and R. J. Weber (2011), Secondary organic aerosol formation in cloud droplets and aqueous particles (aqSOA): A review of laboratory, field and model studies, *Atmos. Chem. Phys.*, *11*(21), 11,069–11,102.

Fan, J., et al. (2014), Aerosol impacts on California winter clouds and precipitation during CalWater 2011: Local pollution versus long-range transported dust, *Atmos. Chem. Phys.*, *14*(1), 81–101.

Fan, J. W., L. R. Leung, D. Rosenfeld, Q. Chen, Z. Q. Li, J. Q. Zhang, and H. R. Yan (2013), Microphysical effects determine macrophysical response for aerosol impacts on deep convective clouds, *Proc. Natl. Acad. Sci. U.S.A.*, *110*(48), E4581–E4590.

Feng, Y., V. Ramanathan, and V. R. Kotamarthi (2013), Brown carbon: A significant atmospheric absorber of solar radiation?, *Atmos. Chem. Phys.*, *13*(17), 8607–8621.

Fischer, H., D. Wagenbach, and J. Kipfstuhl (1998), Sulfate and nitrate firn concentrations on the Greenland ice sheet—2. Temporal anthropogenic deposition changes, *J. Geophys. Res.*, *103*(D17), 21,935–21,942.

Forrister, H., et al. (2015), Evolution of brown carbon in wildfire plumes, *Geophys. Res. Lett.*, *42*, 4623–4630, doi:10.1002/2015GL063897.

Frosch, M., M. Bilde, P. F. DeCarlo, Z. Juranyi, T. Tritscher, J. Dommen, N. M. Donahue, M. Gysel, E. Weingartner, and U. Baltensperger (2011), Relating cloud condensation nuclei activity and oxidation level of α-pinene secondary organic aerosols, *J. Geophys. Res.*, *116*, D22212, doi:10.1029/2011JD016401.

Froyd, K. D., S. M. Murphy, D. M. Murphy, J. A. de Gouw, N. C. Eddingsaas, and P. O. Wennberg (2010), Contribution of isoprene-derived organosulfates to free tropospheric aerosol mass, *Proc. Natl. Acad. Sci. U.S.A.*, *107*(50), 21,360–21,365.

Fry, J. L., et al. (2013), Observations of gas- and aerosol-phase organic nitrates at BEACHON-RoMBAS 2011, *Atmos. Chem. Phys.*, *13*(17), 8585–8605.

Fry, J. L., et al. (2014), Secondary organic aerosol formation and organic nitrate yield from NO_3 oxidation of biogenic hydrocarbons, *Environ. Sci. Technol.*, *48*(20), 11,944–11,953.

Fuchs, H., et al. (2013), Experimental evidence for efficient hydroxyl radical regeneration in isoprene oxidation, *Nat. Geosci.*, *6*(12), 1023–1026.

Galloway, M. M., C. L. Loza, P. S. Chhabra, A. W. H. Chan, L. D. Yee, J. H. Seinfeld, and F. N. Keutsch (2011), Analysis of photochemical and dark glyoxal uptake: Implications for SOA formation, *Geophys. Res. Lett.*, *38*, L17811, doi:10.1029/2011GL048514.

Gao, S., et al. (2004), Particle phase acidity and oligomer formation in secondary organic aerosol, *Environ. Sci. Technol.*, *38*(24), 6582–6589.

Garcia-Montiel, D. C., P. A. Steudler, M. C. Piccolo, J. M. Melillo, C. Neill, and C. C. Cerri (2001), Controls on soil nitrogen oxide emissions from forest and pastures in the Brazilian Amazon, *Global Biogeochem. Cycles*, *15*(4), 1021–1030.

Gaston, C. J., T. P. Riedel, Z. Zhang, A. Gold, J. D. Surratt, and J. A. Thornton (2014), Reactive uptake of an isoprene-derived epoxydiol to submicron aerosol particles, *Environ. Sci. Technol.*, *48*(19), 11,178–11,186.

Gentner, D. R., et al. (2017), Review of urban secondary organic aerosol formation from gasoline and diesel motor vehicle emissions, *Environ. Sci. Technol.*, *51*(3), 1074–1093.

George, C., M. Ammann, B. D'Anna, D. J. Donaldson, and S. A. Nizkorodov (2015), Heterogeneous photochemistry in the atmosphere, *Chem. Rev.*, *115*(10), 4218–4258.

Ghan, S. J., H. Abdul-Razzak, A. Nenes, Y. Ming, X. H. Liu, M. Ovchinnikov, B. Shipway, N. Meskhidze, J. Xu, and X. J. Shi (2011), Droplet nucleation: Physically-based parameterizations and comparative evaluation, *J. Adv. Model. Earth Syst.*, *3*.

Glasius, M., and A. H. Goldstein (2016), Recent discoveries and future challenges in atmospheric organic chemistry, *Environ. Sci. Technol.*, *50*(6), 2754–2764.

Goldstein, A. H., and I. E. Galbally (2007), Known and unexplored organic constituents in the Earth's atmosphere, *Environ. Sci. Technol.*, *41*(5), 1514–1521.

Goldstein, A. H., C. D. Koven, C. L. Heald, and I. Y. Fung (2009), Biogenic carbon and anthropogenic pollutants combine to form a cooling haze over the southeastern United States, *Proc. Natl. Acad. Sci. U.S.A.*, *106*(22), 8835–8840.

González Palacios, L., P. Corral Arroyo, K. Z. Aregahegn, S. S. Steimer, T. Bartels-Rausch, B. Nozière, M. Ammann, C. George, and R. Volkamer (2016), Heterogeneous photochemistry of imidazole-2-carboxaldehyde: HO_2 radical formation and aerosol growth, *Atmos. Chem. Phys. Discuss.*, *2016*, 1–32.

Grayson, J. W., Y. Zhang, A. Mutzel, L. Renbaum-Wolff, O. Böge, S. Kamal, H. Herrmann, S. T. Martin, and A. K. Bertram (2016), Effect of varying experimental conditions on the viscosity of α-pinene derived secondary organic material, *Atmos. Chem. Phys.*, *16*(10), 6027–6040.

Grieshop, A. P., J. M. Logue, N. M. Donahue, and A. L. Robinson (2009), Laboratory investigation of photochemical oxidation of organic aerosol from wood fires 1: Measurement and simulation of organic aerosol evolution, *Atmos. Chem. Phys.*, *9*(4), 1263–1277.

Griffin, R. J., D. R. Cocker, R. C. Flagan, and J. H. Seinfeld (1999), Organic aerosol formation from the oxidation of biogenic hydrocarbons, *J. Geophys. Res.*, *104*(D3), 3555–3567.

Grosjean, D., K. Van Cauwenberghe, J. P. Schmid, P. E. Kelley, and J. N. Pitts (1978), Identification of C3-C10 aliphatic dicarboxylic acids in airborne particulate matter, *Environ. Sci. Technol.*, *12*(3), 313–317.

Guenther, A., T. Karl, P. Harley, C. Wiedinmyer, P. I. Palmer, and C. Geron (2006), Estimates of global terrestrial isoprene emissions using MEGAN (Model of Emissions of Gases and Aerosols from Nature), *Atmos. Chem. Phys.*, *6*, 3181–3210.

Guenther, A. B., X. Jiang, C. L. Heald, T. Sakulyanontvittaya, T. Duhl, L. K. Emmons, and X. Wang (2012), The Model of Emissions of Gases and Aerosols from Nature version 2.1 (MEGAN2.1): An extended and updated framework for modeling biogenic emissions, *Geosci. Model Dev.*, *5*(6), 1471–1492.

Guo, H., et al. (2015), Fine-particle water and pH in the southeastern United States, *Atmos. Chem. Phys.*, *15*(9), 5211–5228.

Hakkinen, S. A. K., et al. (2012), Long-term volatility measurements of submicron atmospheric aerosol in Hyytiala, Finland, *Atmos. Chem. Phys.*, *12*(22), 10,771–10,786.

Hall, W. A., and M. V. Johnston (2011), Oligomer content of α-pinene secondary organic aerosol, *Aerosol Sci. Technol.*, *45*(1), 37–45.

Hall, W. A., and M. V. Johnston (2012), Oligomer formation pathways in secondary organic aerosol from MS and MS/MS measurements with high mass accuracy and resolving power, *J. Am. Soc. Mass Spectrom.*, *23*(6), 1097–1108.

Hallquist, M., et al. (2009), The formation, properties and impact of secondary organic aerosol: Current and emerging issues, *Atmos. Chem. Phys.*, *9*(14), 5155–5236.

Hastings, W. P., C. A. Koehler, E. L. Bailey, and D. O. De Haan (2005), Secondary organic aerosol formation by glyoxal hydration and oligomer formation: Humidity effects and equilibrium shifts during analysis, *Environ. Sci. Technol.*, *39*(22), 8728–8735.

Hayes, P. L., et al. (2013), Organic aerosol composition and sources in Pasadena, California, during the 2010 CalNex campaign, *J. Geophys. Res. Atmos.*, *118*, 9233–9257, doi:10.1002/jgrd.50530.

Hayes, P. L., et al. (2015), Modeling the formation and aging of secondary organic aerosols in Los Angeles during CalNex 2010, *Atmos. Chem. Phys.*, *15*(10), 5773–5801.

Heald, C. L., D. J. Jacob, R. J. Park, L. M. Russell, B. J. Huebert, J. H. Seinfeld, H. Liao, and R. J. Weber (2005), A large organic aerosol source in the free troposphere missing from current models, *Geophys. Res. Lett.*, *32*, L18809, doi:10.1029/2005GL023831.

Heald, C. L., et al. (2011), Exploring the vertical profile of atmospheric organic aerosol: Comparing 17 aircraft field campaigns with a global model, *Atmos. Chem. Phys.*, *11*(24), 12,673–12,696.

Hennigan, C. J., et al. (2011), Chemical and physical transformations of organic aerosol from the photo-oxidation of open biomass burning emissions in an environmental chamber, *Atmos. Chem. Phys.*, *11*(15), 7669–7686.

Henze, D. K., J. H. Seinfeld, N. L. Ng, J. H. Kroll, T. M. Fu, D. J. Jacob, and C. L. Heald (2008), Global modeling of secondary organic aerosol formation from aromatic hydrocarbons: High- vs. low-yield pathways, *Atmos. Chem. Phys.*, *8*(9), 2405–2420.

Herrmann, H., T. Schaefer, A. Tilgner, S. A. Styler, C. Weller, M. Teich, and T. Otto (2015), Tropospheric aqueous-phase chemistry: Kinetics, mechanisms, and its coupling to a changing gas phase, *Chem. Rev.*, *115*(10), 4259–4334.

Hewitt, C. N., et al. (2009), Nitrogen management is essential to prevent tropical oil palm plantations from causing ground-level ozone pollution, *Proc. Natl. Acad. Sci. U.S.A.*, *106*(44), 18,447–18,451.

Hildebrandt, L., N. M. Donahue, and S. N. Pandis (2009), High formation of secondary organic aerosol from the photo-oxidation of toluene, *Atmos. Chem. Phys.*, *9*(9), 2973–2986.

Hildemann, L. M., M. A. Mazurek, G. R. Cass, and B. R. T. Simoneit (1991), Quantitative characterization of urban sources of organic aerosol by high-resolution gas chromatography, *Environ. Sci. Technol.*, *25*(7), 1311–1325.

Hinks, M. L., M. V. Brady, H. Lignell, M. J. Song, J. W. Grayson, A. K. Bertram, P. Lin, A. Laskin, J. Laskin, and S. A. Nizkorodov (2016), Effect of viscosity on photodegradation rates in complex secondary organic aerosol materials, *Phys. Chem. Chem. Phys.*, *18*(13), 8785–8793.

Hobbs, P. V., P. Sinha, R. J. Yokelson, T. J. Christian, D. R. Blake, S. Gao, T. W. Kirchstetter, T. Novakov, and P. Pilewskie (2003), Evolution of gases and particles from a savanna fire in South Africa, *J. Geophys. Res.*, *108*(D13), 8485, doi:10.1029/2002JD002352.

Hodzic, A., S. Madronich, B. Aumont, J. Lee-Taylor, T. Karl, M. Camredon, and C. Mouchel-Vallon (2013), Limited influence of dry deposition of semivolatile organic vapors on secondary organic aerosol formation in the urban plume, *Geophys. Res. Lett.*, *40*, 3302–3307, doi:10.1002/grl.50611.

Hodzic, A., P. S. Kasibhatla, D. S. Jo, C. D. Cappa, J. L. Jimenez, S. Madronich, and R. J. Park (2016), Rethinking the global secondary organic aerosol (SOA) budget: Stronger production, faster removal, shorter lifetime, *Atmos. Chem. Phys.*, *16*(12), 7917–7941.

Hoyle, C. R., G. Myhre, T. K. Berntsen, and I. S. A. Isaksen (2009), Anthropogenic influence on SOA and the resulting radiative forcing, *Atmos. Chem. Phys.*, *9*(8), 2715–2728.

Hoyle, C. R., et al. (2016), Aqueous phase oxidation of sulphur dioxide by ozone in cloud droplets, *Atmos. Chem. Phys.*, *16*(3), 1693–1712.

Hu, K. S., A. I. Darer, and M. J. Elrod (2011), Thermodynamics and kinetics of the hydrolysis of atmospherically relevant organonitrates and organosulfates, *Atmos. Chem. Phys.*, *11*(16), 8307–8320.

Hu, W., et al. (2016), Volatility and lifetime against OH heterogeneous reaction of ambient isoprene-epoxydiols-derived secondary organic aerosol (IEPOX-SOA), *Atmos. Chem. Phys.*, *16*(18), 11,563–11,580.

Hu, W. W., et al. (2015), Characterization of a real-time tracer for isoprene epoxydiols-derived secondary organic aerosol (IEPOX-SOA) from aerosol mass spectrometer measurements, *Atmos. Chem. Phys.*, *15*(20), 11,807–11,833.

Inomata, S., K. Sato, J. Hirokawa, Y. Sakamoto, H. Tanimoto, M. Okumura, S. Tohno, and T. Imamura (2014), Analysis of secondary organic aerosols from ozonolysis of isoprene by proton transfer reaction mass spectrometry, *Atmos. Environ.*, *97*, 397–405.
Isaacman-VanWertz, G., et al. (2016), Ambient gas-particle partitioning of tracers for biogenic oxidation, *Environ. Sci. Technol.*, *50*, 9952–9962, doi:10.1021/acs.est.6b01674.
Isaacman, G., N. M. Kreisberg, L. D. Yee, D. R. Worton, A. W. H. Chan, J. A. Moss, S. V. Hering, and A. H. Goldstein (2014), Online derivatization for hourly measurements of gas- and particle-phase semi-volatile oxygenated organic compounds by thermal desorption aerosol gas chromatography (SV-TAG), *Atmos. Meas. Tech.*, *7*(12), 4417–4429.
Jang, M. S., and R. M. Kamens (2001), Atmospheric secondary aerosol formation by heterogeneous reactions of aldehydes in the presence of a sulfuric acid aerosol catalyst, *Environ. Sci. Technol.*, *35*(24), 4758–4766.
Jang, M. S., N. M. Czoschke, S. Lee, and R. M. Kamens (2002), Heterogeneous atmospheric aerosol production by acid-catalyzed particle-phase reactions, *Science*, *298*(5594), 814–817.
Järvinen, E., et al. (2016), Observation of viscosity transition in α-pinene secondary organic aerosol, *Atmos. Chem. Phys.*, *16*(7), 4423–4438.
Jathar, S. H., T. D. Gordon, C. J. Hennigan, H. O. T. Pye, G. Pouliot, P. J. Adams, N. M. Donahue, and A. L. Robinson (2014), Unspeciated organic emissions from combustion sources and their influence on the secondary organic aerosol budget in the United States, *Proc. Natl. Acad. Sci. U.S.A.*, *111*(29), 10,473–10,478.
Jethva, H., and O. Torres (2011), Satellite-based evidence of wavelength-dependent aerosol absorption in biomass burning smoke inferred from Ozone Monitoring Instrument, *Atmos. Chem. Phys.*, *11*(20), 10,541–10,551.
Jimenez, J. L., et al. (2009), Evolution of organic aerosols in the atmosphere, *Science*, *326*(5959), 1525–1529.
Jokinen, T., et al. (2015), Production of extremely low volatile organic compounds from biogenic emissions: Measured yields and atmospheric implications, *Proc. Natl. Acad. Sci. U.S.A.*, *112*(23), 7123–7128.
Jolleys, M. D., et al. (2012), Characterizing the aging of biomass burning organic aerosol by use of mixing ratios: A meta-analysis of four regions, *Environ. Sci. Technol.*, *46*(24), 13,093–13,102.
Jolleys, M. D., et al. (2015), Properties and evolution of biomass burning organic aerosol from Canadian boreal forest fires, *Atmos. Chem. Phys.*, *15*(6), 3077–3095.
Kalberer, M., et al. (2004), Identification of polymers as major components of atmospheric organic aerosols, *Science*, *303*(5664), 1659–1662.
Kamens, R. M., M. W. Gery, H. E. Jeffries, M. Jackson, and E. I. Cole (1982), Ozone–isoprene reactions: Product formation and aerosol potential, *Int. J. Chem. Kinet.*, *14*(9), 955–975.
Kammermann, L., M. Gysel, E. Weingartner, H. Herich, D. J. Cziczo, T. Holst, B. Svenningsson, A. Arneth, and U. Baltensperger (2010), Subarctic atmospheric aerosol composition: 3. Measured and modeled properties of cloud condensation nuclei, *J. Geophys. Res.*, *115*, D04202, doi:10.1029/2009JD012447.
Kampf, C. J., E. M. Waxman, J. G. Slowik, J. Dommen, L. Pfaffenberger, A. P. Praplan, A. S. H. Prevot, U. Baltensperger, T. Hoffmann, and R. Volkamer (2013), Effective Henry's law partitioning and the salting constant of glyoxal in aerosols containing sulfate, *Environ. Sci. Technol.*, *47*(9), 4236–4244.
Kangasluoma, J., C. Kuang, D. Wimmer, M. P. Rissanen, K. Lehtipalo, M. Ehn, D. R. Worsnop, J. Wang, M. Kulmala, and T. Petaja (2014), Sub-3 nm particle size and composition dependent response of a nano-CPC battery, *Atmos. Meas. Tech.*, *7*(3), 689–700.
Karl, T., P. K. Misztal, H. H. Jonsson, S. Shertz, A. H. Goldstein, and A. B. Guenther (2013), Airborne flux measurements of BVOCs above Californian oak forests: Experimental investigation of surface and entrainment fluxes, OH densities, and Damkohler numbers, *J. Atmos. Sci.*, *70*(10), 3277–3287.
Kaser, L., et al. (2015), Chemistry-turbulence interactions and mesoscale variability influence the cleansing efficiency of the atmosphere, *Geophys. Res. Lett.*, *42*, 10,894–10,903, doi:10.1002/2015GL066641.
Keskinen, H., et al. (2013), Evolution of nanoparticle composition in CLOUD in presence of sulphuric acid, ammonia and organics, in *Nucleation and Atmospheric Aerosols*, edited by P. J. DeMott and C. D. Odowd, pp. 291–294, Amer Inst Physics, Melville.
King, S. M., T. Rosenoern, J. E. Shilling, Q. Chen, Z. Wang, G. Biskos, K. A. McKinney, U. Poschl, and S. T. Martin (2010), Cloud droplet activation of mixed organic-sulfate particles produced by the photooxidation of isoprene, *Atmos. Chem. Phys.*, *10*(8), 3953–3964.
Kirkby, J., et al. (2016), Ion-induced nucleation of pure biogenic particles, *Nature*, *533*(7604), 521–526.
Knote, C., A. Hodzic, and J. L. Jimenez (2014a), The effect of dry and wet deposition of condensable vapors on secondary organic aerosols concentrations over the continental US, *Atmos. Chem. Phys. Discuss.*, *14*, 13,731–13,767.
Knote, C., et al. (2014b), Simulation of semi-explicit mechanisms of SOA formation from glyoxal in aerosol in a 3-D model, *Atmos. Chem. Phys.*, *14*(12), 6213–6239.
Kokkola, H., et al. (2014), The role of low volatile organics on secondary organic aerosol formation, *Atmos. Chem. Phys.*, *14*(3), 1689–1700.
Kolesar, K. R., Z. Li, K. R. Wilson, and C. D. Cappa (2015a), Heating-induced evaporation of nine different secondary organic aerosol types, *Environ. Sci. Technol.*, *49*(20), 12,242–12,252.
Kolesar, K. R., C. Chen, D. Johnson, and C. D. Cappa (2015b), The influences of mass loading and rapid dilution of secondary organic aerosol on particle volatility, *Atmos. Chem. Phys.*, *15*(16), 9327–9343.
Koop, T., J. Bookhold, M. Shiraiwa, and U. Poschl (2011), Glass transition and phase state of organic compounds: Dependency on molecular properties and implications for secondary organic aerosols in the atmosphere, *Phys. Chem. Chem. Phys.*, *13*(43), 19,238–19,255.
Krechmer, J. E., et al. (2015), Formation of low volatility organic compounds and secondary organic aerosol from isoprene hydroxyhydroperoxide low-NO oxidation, *Environ. Sci. Technol.*, *49*(17), 10,330–10,339.
Krechmer, J. E., D. Pagonis, P. J. Ziemann, and J. L. Jimenez (2016a), Quantification of gas-wall partitioning in Teflon environmental chambers using rapid bursts of low-volatility oxidized species generated in situ, *Environ. Sci. Technol.*, *50*(11), 5757–5765.
Krechmer, J. E., et al. (2016b), Ion mobility spectrometry–mass spectrometry (IMS–MS) for on- and offline analysis of atmospheric gas and aerosol species, *Atmos. Meas. Tech.*, *9*(7), 3245–3262.
Kristensen, K., T. Cui, H. Zhang, A. Gold, M. Glasius, and J. D. Surratt (2014), Dimers in alpha-pinene secondary organic aerosol: Effect of hydroxyl radical, ozone, relative humidity and aerosol acidity, *Atmos. Chem. Phys.*, *14*(8), 4201–4218.
Kristensen, K., Å. K. Watne, J. Hammes, A. Lutz, T. Petäjä, M. Hallquist, M. Bilde, and M. Glasius (2016), High-molecular weight dimer esters are major products in aerosols from α-pinene ozonolysis and the boreal forest, *Environ. Sci. Technol. Lett.*, *3*(8), 280–285.
Kroll, J. H., and J. H. Seinfeld (2008), Chemistry of secondary organic aerosol: Formation and evolution of low-volatility organics in the atmosphere, *Atmos. Environ.*, *42*(16), 3593–3624.
Kroll, J. H., N. L. Ng, S. M. Murphy, R. C. Flagan, and J. H. Seinfeld (2005a), Secondary organic aerosol formation from isoprene photooxidation under high-NO_x conditions, *Geophys. Res. Lett.*, *32*, L18808, doi:10.1029/2005GL023637.
Kroll, J. H., N. L. Ng, S. M. Murphy, V. Varutbangkul, R. C. Flagan, and J. H. Seinfeld (2005b), Chamber studies of secondary organic aerosol growth by reactive uptake of simple carbonyl compounds, *J. Geophys. Res.*, *110*, D23207, doi:10.1029/2005JD006004.

Kroll, J. H., N. L. Ng, S. M. Murphy, R. C. Flagan, and J. H. Seinfeld (2006), Secondary organic aerosol formation from isoprene photooxidation, *Environ. Sci. Technol.*, *40*(6), 1869–1877.
Kroll, J. H., A. W. H. Chan, N. L. Ng, R. C. Flagan, and J. H. Seinfeld (2007), Reactions of semivolatile organics and their effects on secondary organic aerosol formation, *Environ. Sci. Technol.*, *41*(10), 3545–3550.
Kroll, J. H., et al. (2011), Carbon oxidation state as a metric for describing the chemistry of atmospheric organic aerosol, *Nat. Chem.*, *3*, 133–139, doi:10.1038/NCHEM.948.
Kuang, C., P. H. McMurry, and A. V. McCormick (2009), Determination of cloud condensation nuclei production from measured new particle formation events, *Geophys. Res. Lett.*, *36*, L09822, doi:10.1029/2009GL037584.
Kuang, C., I. Riipinen, S. L. Sihto, M. Kulmala, A. V. McCormick, and P. H. McMurry (2010), An improved criterion for new particle formation in diverse atmospheric environments, *Atmos. Chem. Phys.*, *10*(17), 8469–8480.
Kulmala, M., A. Toivonen, J. M. Makela, and A. Laaksonen (1998), Analysis of the growth of nucleation mode particles observed in Boreal forest, *Tellus B Chem. Phys. Meteorol.*, *50*(5), 449–462.
Kulmala, M., et al. (2007), Toward direct measurement of atmospheric nucleation, *Science*, *318*(5847), 89–92.
Kulmala, M., et al. (2013), Direct observations of atmospheric aerosol nucleation, *Science*, *339*(6122), 943–946.
Kurten, T., M. P. Rissanen, K. Mackeprang, J. A. Thornton, N. Hyttinen, S. Jorgensen, M. Ehn, and H. G. Kjaergaard (2015), Computational study of hydrogen shifts and ring-opening mechanisms in α-pinene ozonolysis products, *J. Phys. Chem. A*, *119*(46), 11,366–11,375.
Kurtén, T., J. Elm, N. L. Prisle, K. V. Mikkelsen, C. J. Kampf, E. M. Waxman, and R. Volkamer (2015), Computational study of the effect of glyoxal–sulfate clustering on the Henry's law coefficient of glyoxal, *Chem. A Eur. J.*, *119*(19), 4509–4514.
Kurtén, T., K. Tiusanen, P. Roldin, M. Rissanen, J.-N. Luy, M. Boy, M. Ehn, and N. Donahue (2016), α-pinene autoxidation products may not have extremely low saturation vapor pressures despite high O:C ratios, *Chem. A Eur. J.*, *120*(16), 2569–2582.
Kuwata, M., and S. T. Martin (2012), Phase of atmospheric secondary organic material affects its reactivity, *Proc. Natl. Acad. Sci. U.S.A.*, *109*(43), 17,354–17,359.
Kuwata, M., Y. J. Liu, K. McKinney, and S. T. Martin (2015), Physical state and acidity of inorganic sulfate can regulate the production of secondary organic material from isoprene photooxidation products, *Phys. Chem. Chem. Phys.*, *17*(8), 5670–5678.
Kwok, E. S. C., R. Atkinson, and J. Arey (1995), Observation of hydroxycarbonyls from the OH radical-initiated reaction of isoprene, *Environ. Sci. Technol.*, *29*(9), 2467–2469.
La, Y. S., M. Camredon, P. J. Ziemann, R. Valorso, A. Matsunaga, V. Lannuque, J. Lee-Taylor, A. Hodzic, S. Madronich, and B. Aumont (2016), Impact of chamber wall loss of gaseous organic compounds on secondary organic aerosol formation: Explicit modeling of SOA formation from alkane and alkene oxidation, *Atmos. Chem. Phys.*, *16*(3), 1417–1431.
Lack, D. A., J. M. Langridge, R. Bahreini, C. D. Cappa, A. M. Middlebrook, and J. P. Schwarz (2012), Brown carbon and internal mixing in biomass burning particles, *Proc. Natl. Acad. Sci. U.S.A.*, *109*(37), 14,802–14,807.
Lambe, A. T., T. B. Onasch, P. Massoli, D. R. Croasdale, J. P. Wright, A. T. Ahern, L. R. Williams, D. R. Worsnop, W. H. Brune, and P. Davidovits (2011), Laboratory studies of the chemical composition and cloud condensation nuclei (CCN) activity of secondary organic aerosol (SOA) and oxidized primary organic aerosol (OPOA), *Atmos. Chem. Phys.*, *11*(17), 8913–8928.
Lambe, A. T., et al. (2012), Transitions from functionalization to fragmentation reactions of laboratory secondary organic aerosol (SOA) generated from the OH oxidation of alkane precursors, *Environ. Sci. Technol.*, *46*(10), 5430–5437.
Lambe, A. T., et al. (2015), Effect of oxidant concentration, exposure time, and seed particles on secondary organic aerosol chemical composition and yield, *Atmos. Chem. Phys.*, *15*(6), 3063–3075.
Lane, T. E., N. M. Donahue, and S. N. Pandis (2008), Effect of NO_x on secondary organic aerosol concentrations, *Environ. Sci. Technol.*, *42*(16), 6022–6027.
Laskin, A., J. Laskin, and S. A. Nizkorodov (2012), Mass spectrometric approaches for chemical characterisation of atmospheric aerosols: Critical review of the most recent advances, *Environ. Chem.*, *9*(3), 163–189.
Laskin, A., J. Laskin, and S. A. Nizkorodov (2015), Chemistry of atmospheric brown carbon, *Chem. Rev.*, *115*(10), 4335–4382.
Laskin, J., A. Laskin, and S. A. Nizkorodov (2013), New mass spectrometry techniques for studying physical chemistry of atmospheric heterogeneous processes, *Int. Rev. Phys. Chem.*, *32*(1), 128–170.
Lee, A. K. Y., K. L. Hayden, P. Herckes, W. R. Leaitch, J. Liggio, A. M. Macdonald, and J. P. D. Abbatt (2012), Characterization of aerosol and cloud water at a mountain site during WACS 2010: Secondary organic aerosol formation through oxidative cloud processing, *Atmos. Chem. Phys.*, *12*(15), 7103–7116.
Lee, A. K. Y., R. Zhao, R. Li, J. Liggio, S.-M. Li, and J. P. D. Abbatt (2013), Formation of light absorbing organo-nitrogen species from evaporation of droplets containing glyoxal and ammonium sulfate, *Environ. Sci. Technol.*, *47*(22), 12,819–12,826.
Lee, B. H., et al. (2016), Highly functionalized organic nitrates in the southeast United States: Contribution to secondary organic aerosol and reactive nitrogen budgets, *Proc. Natl. Acad. Sci. U.S.A.*, *113*(6), 1516–1521.
Lee, H. J., P. K. Aiona, A. Laskin, J. Laskin, and S. A. Nizkorodov (2014), Effect of solar radiation on the optical properties and molecular composition of laboratory proxies of atmospheric brown carbon, *Environ. Sci. Technol.*, *48*, 10,217–10,226.
Lee, S., et al. (2008), Diagnosis of aged prescribed burning plumes impacting an urban area, *Environ. Sci. Technol.*, *42*(5), 1438–1444.
Levin, E. J. T., A. J. Prenni, B. B. Palm, D. A. Day, P. Campuzano-Jost, P. M. Winkler, S. M. Kreidenweis, P. J. DeMott, J. L. Jimenez, and J. N. Smith (2014), Size-resolved aerosol composition and its link to hygroscopicity at a forested site in Colorado, *Atmos. Chem. Phys.*, *14*(5), 2657–2667.
Li, L. J., P. Tang, and D. R. Cocker (2015), Instantaneous nitric oxide effect on secondary organic aerosol formation from m-xylene photooxidation, *Atmos. Environ.*, *119*, 144–155.
Li, Y., U. Poeschl, and M. Shiraiwa (2016), Molecular corridors and parameterizations of volatility in the chemical evolution of organic aerosols, *Atmos. Chem. Phys.*, *16*(5), 3327–3344.
Li, Y. J., P. Liu, Z. Gong, Y. Wang, A. P. Bateman, C. Bergoend, A. K. Bertram, and S. T. Martin (2015), Chemical reactivity and liquid/nonliquid states of secondary organic material, *Environ. Sci. Technol.*, *49*(22), 13,264–13,274.
Li, Z., et al. (2016), Aerosol and monsoon climate interactions over Asia, *Rev. Geophys.*, *54*, 866–929, doi:10.1002/2015RG000500.
Liao, J., et al. (2015), Airborne measurements of organosulfates over the continental US, *J. Geophys. Res. Atmos.*, *120*, 2990–3005, doi:10.1002/2014JD022378.
Liggio, J., and S. M. Li (2006), Organosulfate formation during the uptake of pinonaldehyde on acidic sulfate aerosols, *Geophys. Res. Lett.*, *33*, L13808, doi:10.1029/2006GL026079.
Liggio, J., S. M. Li, and R. McLaren (2005), Heterogeneous reactions of glyoxal on particulate matter: Identification of acetals and sulfate esters, *Environ. Sci. Technol.*, *39*(6), 1532–1541.

Lim, Y. B., Y. Tan, and B. J. Turpin (2013), Chemical insights, explicit chemistry, and yields of secondary organic aerosol from OH radical oxidation of methylglyoxal and glyoxal in the aqueous phase, *Atmos. Chem. Phys.*, *13*(17), 8651–8667.
Lin, G., J. E. Penner, S. Sillman, D. Taraborrelli, and J. Lelieveld (2012), Global modeling of SOA formation from dicarbonyls, epoxides, organic nitrates and peroxides, *Atmos. Chem. Phys.*, *12*(10), 4743–4774.
Lin, G., J. E. Penner, M. G. Flanner, S. Sillman, L. Xu, and C. Zhou (2014), Radiative forcing of organic aerosol in the atmosphere and on snow: Effects of SOA and brown carbon, *J. Geophys. Res. Atmos.*, *119*, 7453–7476, doi:10.1002/2013JD021186.
Lin, G., J. E. Penner, and C. Zhou (2016), How will SOA change in the future?, *Geophys. Res. Lett.*, *43*, 1718–1726, doi:10.1002/2015GL067137.
Lin, P., X. F. Huang, L. Y. He, and J. Z. Yu (2010), Abundance and size distribution of HULIS in ambient aerosols at a rural site in South China, *J. Aerosol Sci.*, *41*(1), 74–87.
Lin, P., J. Liu, J. E. Shilling, S. M. Kathmann, J. Laskin, and A. Laskin (2015), Molecular characterization of brown carbon (BrC) chromophores in secondary organic aerosol generated from photo-oxidation of toluene, *Phys. Chem. Chem. Phys.*, *17*(36), 23,312–23,325.
Lin, Y. H., et al. (2012), Isoprene epoxydiols as precursors to secondary organic aerosol formation: Acid-catalyzed reactive uptake studies with authentic compounds, *Environ. Sci. Technol.*, *46*(1), 250–258.
Lin, Y. H., E. M. Knipping, E. S. Edgerton, S. L. Shaw, and J. D. Surratt (2013a), Investigating the influences of SO_2 and NH_3 levels on isoprene-derived secondary organic aerosol formation using conditional sampling approaches, *Atmos. Chem. Phys.*, *13*(16), 8457–8470.
Lin, Y. H., et al. (2013b), Epoxide as a precursor to secondary organic aerosol formation from isoprene photooxidation in the presence of nitrogen oxides, *Proc. Natl. Acad. Sci. U.S.A.*, *110*(17), 6718–6723.
Lin, Y. H., H. Budisulistiorini, K. Chu, R. A. Siejack, H. F. Zhang, M. Riva, Z. F. Zhang, A. Gold, K. E. Kautzman, and J. D. Surratt (2014), Light-absorbing oligomer formation in secondary organic aerosol from reactive uptake of isoprene epoxydiols, *Environ. Sci. Technol.*, *48*(20), 12,012–12,021.
Liu, J., et al. (2016), Efficient isoprene secondary organic aerosol formation from a non-IEPOX pathway, *Environ. Sci. Technol.*, *50*(18), 9872–9880.
Liu, P. F., Y. Zhang, and S. T. Martin (2013), Complex refractive indices of thin films of secondary organic materials by spectroscopic ellipsometry from 220 to 1200 nm, *Environ. Sci. Technol.*, *47*(23), 13,594–13,601.
Liu, P. F., N. Abdelmalki, H. M. Hung, Y. Wang, W. H. Brune, and S. T. Martin (2015), Ultraviolet and visible complex refractive indices of secondary organic material produced by photooxidation of the aromatic compounds toluene and m-xylene, *Atmos. Chem. Phys.*, *15*(3), 1435–1446.
Liu, P. F., Y. J. Li, Y. Wang, M. K. Gilles, R. A. Zaveri, A. K. Bertram, and S. T. Martin (2016), Lability of secondary organic particulate matter, *Proc. Natl. Acad. Sci. U.S.A.*, *113*(45), 12,643–12,648.
Liu, T., et al. (2016), Formation of secondary aerosols from gasoline vehicle exhaust when mixing with SO_2, *Atmos. Chem. Phys.*, *16*(2), 675–689.
Liu, X., et al. (2012), Toward a minimal representation of aerosols in climate models: Description and evaluation in the Community Atmosphere Model CAM5, *Geosci. Model Dev.*, *5*(3), 709–739.
Liu, X., et al. (2016), Agricultural fires in the southeastern U.S. during SEAC4RS: Emissions of trace gases and particles and evolution of ozone, reactive nitrogen, and organic aerosol, *J. Geophys. Res. Atmos.*, *121*, 7383–7414, doi:10.1002/2016JD025040.
Liu, X. H., and J. A. Wang (2010), How important is organic aerosol hygroscopicity to aerosol indirect forcing?, *Environ. Res. Lett.*, *5*, 044010, doi:10.1088/1748-9326/5/4/044010.
Liu, Y., F. Siekmann, P. Renard, A. El Zein, G. Salque, I. El Haddad, B. Temime-Roussel, D. Voisin, R. Thissen, and A. Monod (2012), Oligomer and SOA formation through aqueous phase photooxidation of methacrolein and methyl vinyl ketone, *Atmos. Environ.*, *49*, 123–129.
Liu, Y. J., I. Herdlinger-Blatt, K. A. McKinney, and S. T. Martin (2013), Production of methyl vinyl ketone and methacrolein via the hydroperoxyl pathway of isoprene oxidation, *Atmos. Chem. Phys.*, *13*(11), 5715–5730.
Liu, Y. J., M. Kuwata, K. A. McKinney, and S. T. Martin (2016), Uptake and release of gaseous species accompanying the reactions of isoprene photo-oxidation products with sulfate particles, *Phys. Chem. Chem. Phys.*, *18*(3), 1595–1600.
Lockwood, A. L., P. B. Shepson, M. N. Fiddler, and M. Alaghmand (2010), Isoprene nitrates: preparation, separation, identification, yields, and atmospheric chemistry, *Atmos. Chem. Phys.*, *10*(13), 6169–6178.
Loeffler, K. W., C. A. Koehler, N. M. Paul, and D. O. De Haan (2006), Oligomer formation in evaporating aqueous glyoxal and methyl glyoxal solutions, *Environ. Sci. Technol.*, *40*(20), 6318–6323.
Lopez-Hilfiker, F. D., et al. (2014), A novel method for online analysis of gas and particle composition: Description and evaluation of a Filter Inlet for Gases and AEROsols (FIGAERO), *Atmos. Meas. Tech.*, *7*(4), 983–1001.
Lopez-Hilfiker, F. D., et al. (2015), Phase partitioning and volatility of secondary organic aerosol components formed from α-pinene ozonolysis and OH oxidation: The importance of accretion products and other low volatility compounds, *Atmos. Chem. Phys.*, *15*, 7765–7776, doi:10.5194/acp-15-7765-2015, 2015.
Lopez-Hilfiker, F. D., et al. (2016), Molecular composition and volatility of organic aerosol in the southeastern U.S.: Implications for IEPOX derived SOA, *Environ. Sci. Technol.*, *50*(5), 2200–2209.
Loza, C. L., A. W. H. Chan, M. M. Galloway, F. N. Keutsch, R. C. Flagan, and J. H. Seinfeld (2010), Characterization of vapor wall loss in laboratory chambers, *Environ. Sci. Technol.*, *44*(13), 5074–5078.
Loza, C. L., P. S. Chhabra, L. D. Yee, J. S. Craven, R. C. Flagan, and J. H. Seinfeld (2012), Chemical aging of m-xylene secondary organic aerosol: Laboratory chamber study, *Atmos. Chem. Phys.*, *12*(1), 151–167.
Loza, C. L., M. M. Coggon, T. B. Nguyen, A. Zuend, R. C. Flagan, and J. H. Seinfeld (2013), On the mixing and evaporation of secondary organic aerosol components, *Environ. Sci. Technol.*, *47*(12), 6173–6180.
Loza, C. L., et al. (2014), Secondary organic aerosol yields of 12-carbon alkanes, *Atmos. Chem. Phys.*, *14*(3), 1423–1439.
Mai, H. J., M. Shiraiwa, R. C. Flagan, and J. H. Seinfeld (2015), Under what conditions can equilibrium gas-particle partitioning be expected to hold in the atmosphere?, *Environ. Sci. Technol.*, *49*(19), 11,485–11,491.
Marais, E. A., et al. (2016), Aqueous-phase mechanism for secondary organic aerosol formation from isoprene: application to the southeast United States and co-benefit of SO_2 emission controls, *Atmos. Chem. Phys.*, *16*(3), 1603–1618.
Martin, S. T., et al. (2010), Sources and properties of Amazonian aerosol particles, *Rev. Geophys.*, *48*, RG2002, doi:10.1029/2008RG000280.
Martin, S. T., et al. (2016), Introduction: Observations and modeling of the Green Ocean Amazon (GoAmazon2014/5), *Atmos. Chem. Phys.*, *16*(8), 4785–4797.
Massoli, P., et al. (2010), Relationship between aerosol oxidation level and hygroscopic properties of laboratory generated secondary organic aerosol (SOA) particles, *Geophys. Res. Lett.*, *37*, L24801, doi:10.1029/2010GL045258.
Matsunaga, A., and P. J. Ziemann (2010), Gas-wall partitioning of organic compounds in a Teflon film chamber and potential effects on reaction product and aerosol yield measurements, *Aerosol Sci. Technol.*, *44*(10), 881–892.

May, A. A., T. Lee, G. R. McMeeking, S. Akagi, A. P. Sullivan, S. Urbanski, R. J. Yokelson, and S. M. Kreidenweis (2015), Observations and analysis of organic aerosol evolution in some prescribed fire smoke plumes, *Atmos. Chem. Phys.*, *15*(11), 6323–6335.
McFiggans, G., et al. (2006), The effect of physical and chemical aerosol properties on warm cloud droplet activation, *Atmos. Chem. Phys.*, *6*, 2593–2649.
McMurry, P. H., and D. J. Rader (1985), Aerosol wall losses in electrically charged chambers, *Aerosol Sci. Technol.*, *4*(3), 249–268.
McMurry, P. H., and D. Grosjean (1985), Gas and aerosol wall losses in Teflon film SMOG chambers, *Environ. Sci. Technol.*, *19*(12), 1176–1182.
McVay, R. C., C. D. Cappa, and J. H. Seinfeld (2014), Vapor-wall deposition in chambers: Theoretical considerations, *Environ. Sci. Technol.*, *48*(17), 10,251–10,258.
Mei, F., A. Setyan, Q. Zhang, and J. Wang (2013a), CCN activity of organic aerosols observed downwind of urban emissions during CARES, *Atmos. Chem. Phys.*, *13*(24), 12,155–12,169.
Mei, F., P. L. Hayes, A. Ortega, J. W. Taylor, J. D. Allan, J. Gilman, W. Kuster, J. de Gouw, J. L. Jimenez, and J. Wang (2013b), Droplet activation properties of organic aerosols observed at an urban site during CalNex-LA, *J. Geophys. Res. Atmos.*, *118*, 2903–2917, doi:10.1002/jgrd.50285.
Merikanto, J., D. V. Spracklen, G. W. Mann, S. J. Pickering, and K. S. Carslaw (2009), Impact of nucleation on global CCN, *Atmos. Chem. Phys.*, *9*(21), 8601–8616.
Misztal, P. K., J. C. Avise, T. Karl, K. Scott, H. H. Jonsson, A. B. Guenther, and A. H. Goldstein (2016), Evaluation of regional isoprene emission factors and modeled fluxes in California, *Atmos. Chem. Phys. Discuss.*, *2016*, 1–28.
Miyoshi, A., S. Hatakeyama, and N. Washida (1994), OM radical-initiated photooxidation of isoprene: An estimate of global CO production, *J. Geophys. Res.*, *99*(D9), 18,779–18,787.
Mohler, O., S. Benz, H. Saathoff, M. Schnaiter, R. Wagner, J. Schneider, S. Walter, V. Ebert, and S. Wagner (2008), The effect of organic coating on the heterogeneous ice nucleation efficiency of mineral dust aerosols, *Environ. Res. Lett.*, *3*(2).
Moise, T., J. M. Flores, and Y. Rudich (2015), Optical properties of secondary organic aerosols and their changes by chemical processes, *Chem. Rev.*, *115*(10), 4400–4439.
Murphy, D. M., D. J. Cziczo, K. D. Froyd, P. K. Hudson, B. M. Matthew, A. M. Middlebrook, R. E. Peltier, A. Sullivan, D. S. Thomson, and R. J. Weber (2006), Single-particle mass spectrometry of tropospheric aerosol particles, *J. Geophys. Res.*, *111*, D23S32, doi:10.1029/2006JD007340.
Myhre, G., et al. (2013), Radiative forcing of the direct aerosol effect from AeroCom Phase II simulations, *Atmos. Chem. Phys.*, *13*(4), 1853–1877.
Nah, T., J. Sanchez, C. M. Boyd, and N. L. Ng (2016a), Photochemical Aging of alpha-pinene and beta-pinene Secondary Organic Aerosol formed from Nitrate Radical Oxidation, *Environ. Sci. Technol.*, *50*(1), 222–231.
Nah, T., R. C. McVay, J. R. Pierce, J. H. Seinfeld, and N. L. Ng (2016b), Constraining uncertainties in particle wall-deposition correction during SOA formation in chamber experiments, *Atmos. Chem. Phys. Discuss.*, *2016*, 1–35.
Nah, T., R. C. McVay, X. Zhang, C. M. Boyd, J. H. Seinfeld, and N. L. Ng (2016c), Influence of seed aerosol surface area and oxidation rate on vapor wall deposition and SOA mass yields: A case study with α-pinene ozonolysis, *Atmos. Chem. Phys.*, *16*(14), 9361–9379.
Nakao, S., Y. Liu, P. Tang, C. L. Chen, J. Zhang, and D. R. Cocker (2012), Chamber studies of SOA formation from aromatic hydrocarbons: observation of limited glyoxal uptake, *Atmos. Chem. Phys.*, *12*(9), 3927–3937.
National Academies of Sciences, Engineering, and Medicine (2016), *The Future of Atmospheric Chemistry Research: Remembering Yesterday, Understanding Today, Anticipating Tomorrow*, pp. 1–207, The Natl. Acad. Press, Washington, D. C., doi:10.17226/23573.
Ng, N. L., J. H. Kroll, M. D. Keywood, R. Bahreini, V. Varutbangkul, R. C. Flagan, J. H. Seinfeld, A. Lee, and A. H. Goldstein (2006), Contribution of first- versus second-generation products to secondary organic aerosols formed in the oxidation of biogenic hydrocarbons, *Environ. Sci. Technol.*, *40*(7), 2283–2297.
Ng, N. L., J. H. Kroll, A. W. H. Chan, P. S. Chhabra, R. C. Flagan, and J. H. Seinfeld (2007a), Secondary organic aerosol formation from *m*-xylene, toluene, and benzene, *Atmos. Chem. Phys.*, *7*, 3909–3922.
Ng, N. L., et al. (2007b), Effect of NO_x level on secondary organic aerosol (SOA) formation from the photooxidation of terpenes, *Atmos. Chem. Phys.*, *7*(19), 5159–5174.
Ng, N. L., et al. (2008), Secondary organic aerosol (SOA) formation from reaction of isoprene with nitrate radicals (NO_3), *Atmos. Chem. Phys.*, *8*(14), 4117–4140.
Ng, N. L., et al. (2016), Nitrate radicals and biogenic volatile organic compounds: Oxidation, mechanisms and organic aerosol, *Atmos. Chem. Phys. Discuss.*, *2016*, 1–111.
Ng, N. L., et al. (2017), Nitrate radicals and biogenic volatile organic compounds: Oxidation, mechanisms, and organic aerosol, *Atmos. Chem. Phys.*, *17*(3), 2103–2162.
Nguyen, T. B., A. P. Bateman, D. L. Bones, S. A. Nizkorodov, J. Laskin, and A. Laskin (2010), High-resolution mass spectrometry analysis of secondary organic aerosol generated by ozonolysis of isoprene, *Atmos. Environ.*, *44*(8), 1032–1042.
Nguyen, T. B., J. Laskin, A. Laskin, and S. A. Nizkorodov (2011a), Nitrogen-containing organic compounds and oligomers in secondary organic aerosol formed by photooxidation of isoprene, *Environ. Sci. Technol.*, *45*(16), 6908–6918.
Nguyen, T. B., P. J. Roach, J. Laskin, A. Laskin, and S. A. Nizkorodov (2011b), Effect of humidity on the composition of isoprene photooxidation secondary organic aerosol, *Atmos. Chem. Phys.*, *11*(14), 6931–6944.
Nguyen, T. B., A. Laskin, J. Laskin, and S. A. Nizkorodov (2012a), Direct aqueous photochemistry of isoprene high-NO_x secondary organic aerosol, *Phys. Chem. Chem. Phys.*, *14*(27), 9702–9714.
Nguyen, T. B., P. B. Lee, K. M. Updyke, D. L. Bones, J. Laskin, A. Laskin, and S. A. Nizkorodov (2012b), Formation of nitrogen- and sulfur-containing light-absorbing compounds accelerated by evaporation of water from secondary organic aerosols, *J. Geophys. Res.*, *117*, D01207, doi:10.01029/02011JD016944.
Nguyen, T. B., M. M. Coggon, K. H. Bates, X. Zhang, R. H. Schwantes, K. A. Schilling, C. L. Loza, R. C. Flagan, P. O. Wennberg, and J. H. Seinfeld (2014a), Organic aerosol formation from the reactive uptake of isoprene epoxydiols (IEPOX) onto non-acidified inorganic seeds, *Atmos. Chem. Phys.*, *14*(7), 3497–3510.
Nguyen, T. B., et al. (2014b), Overview of the Focused Isoprene eXperiment at the California Institute of Technology (FIXCIT): Mechanistic chamber studies on the oxidation of biogenic compounds, *Atmos. Chem. Phys.*, *14*(24), 13,531–13,549.
Nguyen, T. B., et al. (2015), Mechanism of the hydroxyl radical oxidation of methacryloyl peroxynitrate (MPAN) and its pathway toward secondary organic aerosol formation in the atmosphere, *Phys. Chem. Chem. Phys.*, *17*(27), 17,914–17,926.
Nizkorodov, S. A., J. Laskin, and A. Laskin (2011), Molecular chemistry of organic aerosols through the application of high resolution mass spectrometry, *Phys. Chem. Chem. Phys.*, *13*(9), 3612–3629.
O'Brien, R. E., A. Neu, S. A. Epstein, A. C. MacMillan, B. Wang, S. T. Kelly, S. A. Nizkorodov, A. Laskin, R. C. Moffet, and M. K. Gilles (2014), Physical properties of ambient and laboratory-generated secondary organic aerosol, *Geophys. Res. Lett.*, *41*, 4347–4353, doi:10.1002/2014GL060219.

O'Meara, S., A. M. Booth, M. H. Barley, D. Topping, and G. McFiggans (2014), An assessment of vapour pressure estimation methods, *Phys. Chem. Chem. Phys.*, *16*(36), 19,453–19,469.
O'Meara, S., D. O. Topping, and G. McFiggans (2016), The rate of equilibration of viscous aerosol particles, *Atmos. Chem. Phys.*, *16*(8), 5299–5313.
Odum, J. R., T. Hoffmann, F. Bowman, D. Collins, R. C. Flagan, and J. H. Seinfeld (1996), Gas/particle partitioning and secondary organic aerosol yields, *Environ. Sci. Technol.*, *30*(8), 2580–2585.
Odum, J. R., T. P. W. Jungkamp, R. J. Griffin, R. C. Flagan, and J. H. Seinfeld (1997a), The atmospheric aerosol-forming potential of whole gasoline vapor, *Science*, *276*(5309), 96–99.
Odum, J. R., T. P. W. Jungkamp, R. J. Griffin, H. J. L. Forstner, R. C. Flagan, and J. H. Seinfeld (1997b), Aromatics, reformulated gasoline, and atmospheric organic aerosol formation, *Environ. Sci. Technol.*, *31*(7), 1890–1897.
Orlando, J. J., and G. S. Tyndall (2012), Laboratory studies of organic peroxy radical chemistry: An overview with emphasis on recent issues of atmospheric significance, *Chem. Soc. Rev.*, *41*(19), 6294–6317.
Ortega, A. M., D. A. Day, M. J. Cubison, W. H. Brune, D. Bon, J. A. de Gouw, and J. L. Jimenez (2013), Secondary organic aerosol formation and primary organic aerosol oxidation from biomass-burning smoke in a flow reactor during FLAME-3, *Atmos. Chem. Phys.*, *13*(22), 11,551–11,571.
Ortiz-Montalvo, D. L., S. A. K. Hakkinen, A. N. Schwier, Y. B. Lim, V. F. McNeill, and B. J. Turpin (2014), Ammonium addition (and aerosol pH) has a dramatic impact on the volatility and yield of glyoxal secondary organic aerosol, *Environ. Sci. Technol.*, *48*(1), 255–262.
Ortiz-Montalvo, D. L., A. N. Schwier, Y. B. Lim, V. F. McNeill, and B. J. Turpin (2016), Volatility of methylglyoxal cloud SOA formed through OH radical oxidation and droplet evaporation, *Atmos. Environ.*, *130*, 145–152.
Pajunoja, A., et al. (2015), Adsorptive uptake of water by semisolid secondary organic aerosols, *Geophys. Res. Lett.*, *42*, 3063–3068, doi:10.1002/2015GL063142.
Pandis, S. N., S. E. Paulson, J. H. Seinfeld, and R. C. Flagan (1991), Aerosol formation in the photooxidation of isoprene and beta-pinene, *Atmos. Environ., Part A*, *25*(5-6), 997–1008.
Pankow, J. F. (1994), An absorption model of the gas aerosol partitioning involved in the formation of secondary organic aerosol, *Atmos. Environ.*, *28*(2), 189–193.
Patchen, A. K., M. J. Pennino, A. C. Kiep, and M. J. Elrod (2007), Direct kinetics study of the product-forming channels of the reaction of isoprene-derived hydroxyperoxy radicals with NO, *Int. J. Chem. Kinet.*, *39*(6), 353–361.
Pathak, R. K., A. A. Presto, T. E. Lane, C. O. Stanier, N. M. Donahue, and S. N. Pandis (2007), Ozonolysis of alpha-pinene: Parameterization of secondary organic aerosol mass fraction, *Atmos. Chem. Phys.*, *7*(14), 3811–3821.
Paulot, F., J. D. Crounse, H. G. Kjaergaard, J. H. Kroll, J. H. Seinfeld, and P. O. Wennberg (2009a), Isoprene photooxidation: New insights into the production of acids and organic nitrates, *Atmos. Chem. Phys.*, *9*(4), 1479–1501.
Paulot, F., J. D. Crounse, H. G. Kjaergaard, A. Kurten, J. M. S. Clair, J. H. Seinfeld, and P. O. Wennberg (2009b), Unexpected epoxide formation in the gas-phase photooxidation of isoprene, *Science*, *325*(5941), 730–733.
Paulson, S. E., and J. H. Seinfeld (1992), Development and evaluation of a photooxidation mechanism for isoprene, *J. Geophys. Res.*, *97*(D18), 20,703–20,715.
Peeters, J., and T. L. Nguyen (2012), Unusually fast 1,6-H shifts of enolic hydrogens in peroxy radicals: Formation of the first-generation C-2 and C-3 carbonyls in the oxidation of isoprene, *J. Phys. Chem. A*, *116*(24), 6134–6141.
Peeters, J., T. L. Nguyen, and L. Vereecken (2009), HO_x radical regeneration in the oxidation of isoprene, *Phys. Chem. Chem. Phys.*, *11*(28), 5935–5939.
Peeters, J., J. F. Muller, T. Stavrakou, and V. S. Nguyen (2014), Hydroxyl radical recycling in isoprene oxidation driven by hydrogen bonding and hydrogen tunneling: The upgraded LIM1 mechanism, *J. Phys. Chem. A*, *118*(38), 8625–8643.
Peng, Z., D. A. Day, H. Stark, R. Li, J. Lee-Taylor, B. B. Palm, W. H. Brune, and J. L. Jimenez (2015), HO_x radical chemistry in oxidation flow reactors with low-pressure mercury lamps systematically examined by modeling, *Atmos. Meas. Tech.*, *8*(11), 4863–4890.
Perraud, V., et al. (2012), Nonequilibrium atmospheric secondary organic aerosol formation and growth, *Proc. Natl. Acad. Sci. U.S.A.*, *109*(8), 2836–2841.
Perri, M. J., S. Seitzinger, and B. J. Turpin (2009), Secondary organic aerosol production from aqueous photooxidation of glycolaldehyde: Laboratory experiments, *Atmos. Environ.*, *43*(8), 1487–1497.
Petaja, T., M. Sipila, P. Paasonen, T. Nieminen, T. Kurten, I. K. Ortega, F. Stratmann, H. Vehkamaki, T. Berndt, and M. Kulmala (2011), Experimental observation of strongly bound dimers of sulfuric acid: Application to nucleation in the atmosphere, *Phys. Rev. Lett.*, *106*(22), doi:10.1103/PhysRevLett.106.228302.
Petters, M. D., and S. M. Kreidenweis (2007), A single parameter representation of hygroscopic growth and cloud condensation nucleus activity, *Atmos. Chem. Phys.*, *7*(8), 1961–1971.
Petters, M. D., S. M. Kreidenweis, and P. J. Ziemann (2016), Prediction of cloud condensation nuclei activity for organic compounds using functional group contribution methods, *Geosci. Model Dev.*, *9*(1), 111–124.
Pfrang, C., M. Shiraiwa, and U. Poschl (2011), Chemical ageing and transformation of diffusivity in semi-solid multi-component organic aerosol particles, *Atmos. Chem. Phys.*, *11*, 7343–7354.
Pierce, J. R., and P. J. Adams (2009), Uncertainty in global CCN concentrations from uncertain aerosol nucleation and primary emission rates, *Atmos. Chem. Phys.*, *9*(4), 1339–1356.
Pierce, J. R., G. J. Engelhart, L. Hildebrandt, E. A. Weitkamp, R. K. Pathak, N. M. Donahue, A. L. Robinson, P. J. Adams, and S. N. Pandis (2008), Constraining particle evolution from wall losses, coagulation, and condensation-evaporation in smog-chamber experiments: Optimal estimation based on size distribution measurements, *Aerosol Sci. Technol.*, *42*(12), 1001–1015.
Pierce, J. R., I. Riipinen, M. Kulmala, M. Ehn, T. Petaja, H. Junninen, D. R. Worsnop, and N. M. Donahue (2011), Quantification of the volatility of secondary organic compounds in ultrafine particles during nucleation events, *Atmos. Chem. Phys.*, *11*, 9019–9036.
Pierce, J. R., M. J. Evans, C. E. Scott, S. D. D'Andrea, D. K. Farmer, E. Swietlicki, and D. V. Spracklen (2013), Weak global sensitivity of cloud condensation nuclei and the aerosol indirect effect to Criegee + SO_2 chemistry, *Atmos. Chem. Phys.*, *13*(6), 3163–3176.
Poschl, U., Y. Rudich, and M. Ammann (2007), Kinetic model framework for aerosol and cloud surface chemistry and gas-particle interactions —Part 1: General equations, parameters, and terminology, *Atmos. Chem. Phys.*, *7*(23), 5989–6023.
Poschl, U., et al. (2010), rainforest aerosols as biogenic nuclei of clouds and precipitation in the Amazon, *Science*, *329*(5998), 1513–1516.
Pratt, K. A., P. J. DeMott, J. R. French, Z. Wang, D. L. Westphal, A. J. Heymsfield, C. H. Twohy, A. J. Prenni, and K. A. Prather (2009), In situ detection of biological particles in cloud ice-crystals, *Nat. Geosci.*, *2*(6), 397–400.
Presto, A. A., K. E. H. Hartz, and N. M. Donahue (2005a), Secondary organic aerosol production from terpene ozonolysis: 2. Effect of NO_x concentration, *Environ. Sci. Technol.*, *39*(18), 7046–7054.

Presto, A. A., K. E. H. Hartz, and N. M. Donahue (2005b), Secondary organic aerosol production from terpene ozonolysis: 2. Effect of NO_x concentration, *Environ. Sci. Technol.*, *39*(18), 7046–7054.
Price, H. C., et al. (2015), Water diffusion in atmospherically relevant alpha-pinene secondary organic material, *Chem. Sci.*, *6*(8), 4876–4883.
Pye, H. O. T., A. W. H. Chan, M. P. Barkley, and J. H. Seinfeld (2010), Global modeling of organic aerosol: The importance of reactive nitrogen (NO_x and NO_3), *Atmos. Chem. Phys.*, *10*(22), 11,261–11,276.
Pye, H. O. T., et al. (2013), Epoxide pathways improve model predictions of isoprene markers and reveal key role of acidity in aerosol formation, *Environ. Sci. Technol.*, *47*(19), 11,056–11,064.
Quaas, J., et al. (2009), Aerosol indirect effects—General circulation model intercomparison and evaluation with satellite data, *Atmos. Chem. Phys.*, *9*(22), 8697–8717.
Rattanavaraha, W., et al. (2016), Assessing the impact of anthropogenic pollution on isoprene-derived secondary organic aerosol formation in $PM_{2.5}$ collected from the Birmingham, Alabama, ground site during the 2013 Southern Oxidant and Aerosol Study, *Atmos. Chem. Phys.*, *16*(8), 4897–4914.
Reed Harris, A. E., B. Ervens, R. K. Shoemaker, J. A. Kroll, R. J. Rapf, E. C. Griffith, A. Monod, and V. Vaida (2014), Photochemical kinetics of pyruvic acid in aqueous solution, *J. Phys. Chem. A*, *118*(37), 8505–8516.
Renbaum-Wolff, L., J. W. Grayson, A. P. Bateman, M. Kuwata, M. Sellier, B. J. Murray, J. E. Shilling, S. T. Martin, and A. K. Bertram (2013), Viscosity of alpha-pinene secondary organic material and implications for particle growth and reactivity, *Proc. Natl. Acad. Sci. U.S.A.*, *110*(20), 8014–8019.
Riccobono, F., et al. (2014), Oxidation products of biogenic emissions contribute to nucleation of atmospheric particles, *Science*, *344*(6185), 717–721.
Riedel, T. P., Y.-H. Lin, H. Budisulistiorini, C. J. Gaston, J. A. Thornton, Z. Zhang, W. Vizuete, A. Gold, and J. D. Surrattt (2015), Heterogeneous reactions of isoprene-derived epoxides: Reaction probabilities and molar secondary organic aerosol yield estimates, *Environ. Sci. Technol. Lett.*, *2*(2), 38–42.
Riipinen, I., et al. (2011), Organic condensation: A vital link connecting aerosol formation to cloud condensation nuclei (CCN) concentrations, *Atmos. Chem. Phys.*, *11*(8), 3865–3878.
Riipinen, I., T. Yli-Juuti, J. R. Pierce, T. Petaja, D. R. Worsnop, M. Kulmala, and N. M. Donahue (2012), The contribution of organics to atmospheric nanoparticle growth, *Nat. Geosci.*, *5*(7), 453–458.
Rindelaub, J. D., K. M. McAvey, and P. B. Shepson (2015), The photochemical production of organic nitrates from alpha-pinene and loss via acid-dependent particle phase hydrolysis, *Atmos. Environ.*, *100*, 193–201.
Rissanen, M. P., et al. (2014), The formation of highly oxidized multifunctional products in the ozonolysis of cyclohexene, *J. Am. Chem. Soc.*, *136*(44), 15,596–15,606.
Rissanen, M. P., et al. (2015), Effects of chemical complexity on the autoxidation mechanisms of endocyclic alkene ozonolysis products: From methylcyclohexenes toward understanding alpha-pinene, *J. Phys. Chem. A*, *119*(19), 4633–4650.
Riva, M., S. H. Budisulistiorini, Z. Zhang, A. Gold, and J. D. Surratt (2016a), Chemical characterization of secondary organic aerosol constituents from isoprene ozonolysis in the presence of acidic aerosol, *Atmos. Environ.*, *130*, 5–13.
Riva, M., D. M. Bell, A.-M. K. Hansen, G. T. Drozd, Z. Zhang, A. Gold, D. Imre, J. D. Surratt, M. Glasius, and A. Zelenyuk (2016b), Effect of organic coatings, humidity and aerosol acidity on multiphase chemistry of isoprene epoxydiols, *Environ. Sci. Technol.*, *50*(11), 5580–5588.
Riva, M., et al. (2016c), Chemical characterization of secondary organic aerosol from oxidation of isoprene hydroxyhydroperoxides, *Environ. Sci. Technol.*, *50*(18), 9889–9899.
Riva, M., S. H. Budisulistiorini, Z. Zhang, A. Gold, J. A. Thornton, B. J. Turpin, and J. D. Surratt (2017), Multiphase reactivity of gaseous hydroperoxide oligomers produced from isoprene ozonolysis in the presence of acidified aerosols, *Atmos. Environ.*, *152*, 314–322.
Robinson, A. L., N. M. Donahue, M. Shrivastava, E. A. Weitkamp, A. M. Sage, A. P. Grieshop, T. E. Lane, J. R. Pierce, and S. N. Pandis (2007), Rethinking organic aerosols: Semivolatile emissions and photochemical aging, *Science*, *315*(5816), 1259–1262.
Robinson, E. S., R. Saleh, and N. M. Donahue (2013), Organic aerosol mixing observed by single-particle mass spectrometry, *Chem. A Eur. J.*, *117*(51), 13,935–13,945.
Robinson, N. H., et al. (2011), Evidence for a significant proportion of Secondary Organic Aerosol from isoprene above a maritime tropical forest, *Atmos. Chem. Phys.*, *11*(3), 1039–1050.
Roldin, P., et al. (2014), Modelling non-equilibrium secondary organic aerosol formation and evaporation with the aerosol dynamics, gas- and particle-phase chemistry kinetic multilayer model ADCHAM, *Atmos. Chem. Phys.*, *14*(15), 7953–7993.
Roldin, P., et al. (2015), Modelling the contribution of biogenic volatile organic compounds to new particle formation in the Jülich plant atmosphere chamber, *Atmos. Chem. Phys.*, *15*(18), 10,777–10,798.
Rollins, A. W., et al. (2012), Evidence for NO_x control over nighttime SOA formation, *Science*, *337*(6099), 1210–1212.
Romonosky, D. E., A. Laskin, J. Laskin, and S. A. Nizkorodov (2015), High-resolution mass spectrometry and molecular characterization of aqueous photochemistry products of common types of secondary organic aerosols, *Chem. A Eur. J.*, *119*(11), 2594–2606.
Rosenfeld, D., et al. (2014), Global observations of aerosol-cloud-precipitation-climate interactions, *Rev. Geophys.*, *52*, 750–808, doi:10.1002/2013RG000441.
Rossignol, S., K. Z. Aregahegn, L. Tinel, L. Fine, B. Noziere, and C. George (2014), Glyoxal induced atmospheric photosensitized chemistry leading to organic aerosol growth, *Environ. Sci. Technol.*, *48*(6), 3218–3227.
Ruehl, C. R., P. Y. Chuang, A. Nenes, C. D. Cappa, K. R. Kolesar, and A. H. Goldstein (2012), Strong evidence of surface tension reduction in microscopic aqueous droplets, *Geophys. Res. Lett.*, *39*, L23801, doi:10.1029/2012GL053706.
Ruehl, C. R., J. F. Davies, and K. R. Wilson (2016), An interfacial mechanism for cloud droplet formation on organic aerosols, *Science*, *351*(6280), 1447–1450.
Ruppert, L., and K. H. Becker (2000), A product study of the OH radical-initiated oxidation of isoprene: Formation of C_5-unsaturated diols, *Atmos. Environ.*, *34*(10), 1529–1542.
Sagebiel, J. C., and J. N. Seiber (1993), Studies on the occurrence and distribution of wood smoke marker compounds in foggy atmospheres, *Environ. Toxicol. Chem.*, *12*(5), 813–822.
Saide, P. E., et al. (2015), Revealing important nocturnal and day-to-day variations in fire smoke emissions through a multiplatform inversion, *Geophys. Res. Lett.*, *42*, 3609–3618, doi:10.1002/2015GL063737.
Sanchez, J., D. J. Tanner, D. Chen, L. G. Huey, and N. L. Ng (2016), A new technique for the direct detection of HO_2 radicals using bromide chemical ionization mass spectrometry (Br-CIMS): Initial characterization, *Atmos. Meas. Tech.*, *9*(8), 3851–3861.
Sander, R. (1999), Modeling atmospheric chemistry: Interactions between gas-phase species and liquid cloud/aerosol particles, *Surv. Geophys.*, *20*(1), 1–31.

Sareen, N., S. G. Moussa, and V. F. McNeill (2013), Photochemical aging of light-absorbing secondary organic aerosol material, *J. Phys. Chem. A*, *117*(14), 2987–2996.
Sareen, N., et al. (2016), Identifying precursors and aqueous organic aerosol formation pathways during the SOAS campaign, *Atmos. Chem. Phys.*, *16*(22), 14,409–14,420.
Schauer, J. J., M. J. Kleeman, G. R. Cass, and B. R. T. Simoneit (2001), Measurement of emissions from air pollution sources: 3. C_1–C_{29} organic compounds from fireplace combustion of wood, *Environ. Sci. Technol.*, *35*(9), 1716–1728.
Schichtel, B. A., W. C. Malm, G. Bench, S. Fallon, C. E. McDade, J. C. Chow, and J. G. Watson (2008), Fossil and contemporary fine particulate carbon fractions at 12 rural and urban sites in the United States, *J. Geophys. Res.*, *113*, D02311, doi:10.1029/2007JD008605.
Scott, C. E., et al. (2014), The direct and indirect radiative effects of biogenic secondary organic aerosol, *Atmos. Chem. Phys.*, *14*(1), 447–470.
Seinfeld, J. H., and S. N. Pandis (1998), *Atmospheric Chemistry and Physics: From Air Pollution to Climate Change*, vol. 809, pp. 656–690, John Wiley, New York.
Seinfeld, J. H., et al. (2016), Improving our fundamental understanding of the role of aerosol-cloud interactions in the climate system, *Proc. Natl. Acad. Sci. U.S.A.*, *113*(21), 5781–5790.
Setschenow, J. (1889), Concerning the constitution of salt solutions on the basis of their behavior to carbonic acid, *Z. Phys. Chem.*, *4*, 117–125.
Shilling, J. E., et al. (2013), Enhanced SOA formation from mixed anthropogenic and biogenic emissions during the CARES campaign, *Atmos. Chem. Phys.*, *13*(4), 2091–2113.
Shiraiwa, M., and J. H. Seinfeld (2012), Equilibration timescale of atmospheric secondary organic aerosol partitioning, *Geophys. Res. Lett.*, *39*, L24801, doi:10.1029/2012GL054008.
Shiraiwa, M., C. Pfrang, and U. Poschl (2010), Kinetic multi-layer model of aerosol surface and bulk chemistry (KM-SUB): The influence of interfacial transport and bulk diffusion on the oxidation of oleic acid by ozone, *Atmos. Chem. Phys.*, *10*(8), 3673–3691.
Shiraiwa, M., C. Pfrang, T. Koop, and U. Pöschl (2012), Kinetic multi-layer model of gas-particle interactions in aerosols and clouds (KM-GAP): Linking condensation, evaporation and chemical reactions of organics, oxidants and water, *Atmos. Chem. Phys.*, *12*(5), 2777–2794.
Shiraiwa, M., A. Zuend, A. K. Bertram, and J. H. Seinfeld (2013a), Gas-particle partitioning of atmospheric aerosols: Interplay of physical state, non-ideal mixing and morphology, *Phys. Chem. Chem. Phys.*, *15*(27), 11,441–11,453.
Shiraiwa, M., L. D. Yee, K. A. Schilling, C. L. Loza, J. S. Craven, A. Zuend, P. J. Ziemann, and J. H. Seinfeld (2013b), Size distribution dynamics reveal particle-phase chemistry in organic aerosol formation, *Proc. Natl. Acad. Sci. U.S.A.*, *110*(29), 11,746–11,750.
Shrivastava, M., A. Zelenyuk, D. Imre, R. Easter, J. Beranek, R. A. Zaveri, and J. Fast (2013a), Implications of low volatility SOA and gas-phase fragmentation reactions on SOA loadings and their spatial and temporal evolution in the atmosphere, *J. Geophys. Res. Atmos.*, *118*, 3328–3342, doi:10.1002/jgrd.50160.
Shrivastava, M., L. K. Berg, J. D. Fast, R. C. Easter, A. Laskin, E. G. Chapman, W. I. Gustafson, Y. Liu, and C. M. Berkowitz (2013b), Modeling aerosols and their interactions with shallow cumuli during the 2007 CHAPS field study, *J. Geophys. Res. Atmos.*, *118*, 1343–1360, doi:10.1029/2012JD018218.
Shrivastava, M., et al. (2015), Global transformation and fate of SOA: Implications of low-volatility SOA and gas-phase fragmentation reactions, *J. Geophys. Res. Atmos.*, *120*, 4169–4195, doi:10.1002/2014JD022563.
Shrivastava, M., C. Zhao, R. C. Easter, Y. Qian, A. Zelenyuk, J. Fast, Y. Liu, Q. Zhang, and A. Guenther (2016), Sensitivity analysis of simulated SOA loadings using a variance-based statistical approach, *J. Adv. Model. Earth Syst.*, *8*, 499–519, doi:10.1002/2015MS000554.
Shrivastava, M., et al. (2017), Global long-range transport and lung cancer risk from polycyclic aromatic hydrocarbons shielded by coatings of organic aerosol, *Proc. Natl. Acad. Sci. U.S.A.*, *114*(6), 1246–1251.
Sipila, M., et al. (2010), The role of sulfuric acid in atmospheric nucleation, *Science*, *327*(5970), 1243–1246.
Slowik, J. G., et al. (2011), Photochemical processing of organic aerosol at nearby continental sites: Contrast between urban plumes and regional aerosol, *Atmos. Chem. Phys.*, *11*(6), 2991–3006.
Smith, J. D., V. Sio, L. Yu, Q. Zhang, and C. Anastasio (2014), Secondary organic aerosol production from aqueous reactions of atmospheric phenols with an organic triplet excited state, *Environ. Sci. Technol.*, *48*(2), 1049–1057.
Smith, J. D., H. Kinney, and C. Anastasio (2015), Aqueous benzene-diols react with an organic triplet excited state and hydroxyl radical to form secondary organic aerosol, *Phys. Chem. Chem. Phys.*, *17*(15), 10,227–10,237.
Smith, J. D., H. Kinney, and C. Anastasio (2016), Phenolic carbonyls undergo rapid aqueous photodegradation to form low-volatility, light-absorbing products, *Atmos. Environ.*, *126*, 36–44.
Smith, J. N., M. J. Dunn, T. M. VanReken, K. Iida, M. R. Stolzenburg, P. H. McMurry, and L. G. Huey (2008), Chemical composition of atmospheric nanoparticles formed from nucleation in Tecamac, Mexico: Evidence for an important role for organic species in nanoparticle growth, *Geophys. Res. Lett.*, *35*, L04808, doi:10.1029/2007GL032523.
Smith, J. N., K. C. Barsanti, H. R. Friedli, M. Ehn, M. Kulmala, D. R. Collins, J. H. Scheckman, B. J. Williams, and P. H. McMurry (2010), Observations of aminium salts in atmospheric nanoparticles and possible climatic implications, *Proc. Natl. Acad. Sci. U.S.A.*, *107*(15), 6634–6639.
Song, C., K. S. Na, and D. R. Cocker (2005), Impact of the hydrocarbon to NO_x ratio on secondary organic aerosol formation, *Environ. Sci. Technol.*, *39*(9), 3143–3149.
Song, M., P. F. Liu, S. J. Hanna, Y. J. Li, S. T. Martin, and A. K. Bertram (2015), Relative humidity-dependent viscosities of isoprene-derived secondary organic material and atmospheric implications for isoprene-dominant forests, *Atmos. Chem. Phys.*, *15*(9), 5145–5159.
Song, M., P. F. Liu, S. J. Hanna, R. A. Zaveri, K. Potter, Y. You, S. T. Martin, and A. K. Bertram (2016), Relative humidity-dependent viscosity of secondary organic material from toluene photo-oxidation and possible implications for organic particulate matter over megacities, *Atmos. Chem. Phys.*, *16*(14), 8817–8830.
Sorooshian, A., M. L. Lu, F. J. Brechtel, H. Jonsson, G. Feingold, R. C. Flagan, and J. H. Seinfeld (2007), On the source of organic acid aerosol layers above clouds, *Environ. Sci. Technol.*, *41*(13), 4647–4654.
Sorooshian, A., S. M. Murphy, S. Hersey, R. Bahreini, H. Jonsson, R. C. Flagan, and J. H. Seinfeld (2010), Constraining the contribution of organic acids and AMS m/z 44 to the organic aerosol budget: On the importance of meteorology, aerosol hygroscopicity, and region, *Geophys. Res. Lett.*, *37*, L21807, doi:10.1029/2010GL044951.
Spracklen, D. V., et al. (2010), Explaining global surface aerosol number concentrations in terms of primary emissions and particle formation, *Atmos. Chem. Phys.*, *10*(10), 4775–4793.
Spracklen, D. V., et al. (2011), Aerosol mass spectrometer constraint on the global secondary organic aerosol budget, *Atmos. Chem. Phys.*, *11*(23), 12,109–12,136.
St. Clair, J. M., J. C. Rivera-Rios, J. D. Crounse, H. C. Knap, K. H. Bates, A. P. Teng, S. Jørgensen, H. G. Kjaergaard, F. N. Keutsch, and P. O. Wennberg (2016), Kinetics and products of the reaction of the first-generation Isoprene Hydroxy Hydroperoxide (ISOPOOH) with OH, *Chem. A Eur. J.*, *120*(9), 1441–1451.

Stavrakou, T., J. Peeters, and J. F. Muller (2010), Improved global modelling of HO_x recycling in isoprene oxidation: Evaluation against the GABRIEL and INTEX-A aircraft campaign measurements, *Atmos. Chem. Phys.*, *10*(20), 9863–9878.
Stevens, B., and G. Feingold (2009), Untangling aerosol effects on clouds and precipitation in a buffered system, *Nature*, *461*(7264), 607–613.
Stocker, T. F., D. Qin, G.-K. Plattner, M. Tignor, S. K. Allen, J. Boschung, A. Nauels, Y. Xia, V. Bex, and P. M. Midgley (2013), IPCC, 2013: Climate Change 2013—The Physical Sciences Basis, Contribution of Working Group I to the Fifth Assessment Report of the Intergovernmental Panel on Climate Change, Cambridge Univ. Press, Cambridge, U. K., and New York.
Stockwell, C. E., P. R. Veres, J. Williams, and R. J. Yokelson (2015), Characterization of biomass burning emissions from cooking fires, peat, crop residue, and other fuels with high-resolution proton-transfer-reaction time-of-flight mass spectrometry, *Atmos. Chem. Phys.*, *15*(2), 845–865.
Stroeve, P. (1975), On the diffusion of gases in protein solutions, *Ind. Eng. Chem. Fundam.*, *14*, 140–141.
Sullivan, A. P., et al. (2016), Evidence for ambient dark aqueous SOA formation in the Po Valley, Italy, *Atmos. Chem. Phys.*, *16*(13), 8095–8108.
Sun, Y. L., Q. Zhang, C. Anastasio, and J. Sun (2010), Insights into secondary organic aerosol formed via aqueous-phase reactions of phenolic compounds based on high resolution mass spectrometry, *Atmos. Chem. Phys.*, *10*(10), 4809–4822.
Surratt, J. D., et al. (2006), Chemical composition of secondary organic aerosol formed from the photooxidation of isoprene, *J. Phys. Chem. A*, *110*(31), 9665–9690.
Surratt, J. D., M. Lewandowski, J. H. Offenberg, M. Jaoui, T. E. Kleindienst, E. O. Edney, and J. H. Seinfeld (2007a), Effect of acidity on secondary organic aerosol formation from isoprene, *Environ. Sci. Technol.*, *41*(15), 5363–5369.
Surratt, J. D., et al. (2007b), Evidence for organosulfates in secondary organic aerosol, *Environ. Sci. Technol.*, *41*(2), 517–527.
Surratt, J. D., et al. (2008), Organosulfate formation in biogenic secondary organic aerosol, *J. Phys. Chem. A*, *112*(36), 8345–8378.
Surratt, J. D., A. W. H. Chan, N. C. Eddingsaas, M. N. Chan, C. L. Loza, A. J. Kwan, S. P. Hersey, R. C. Flagan, P. O. Wennberg, and J. H. Seinfeld (2010), Reactive intermediates revealed in secondary organic aerosol formation from isoprene, *Proc. Natl. Acad. Sci. U.S.A.*, *107*(15), 6640–6645.
Szmigielski, R., J. D. Surratt, R. Vermeylen, K. Szmigielska, J. H. Kroll, N. L. Ng, S. M. Murphy, A. Sorooshian, J. H. Seinfeld, and M. Claeys (2007), Characterization of 2-methylglyceric acid oligomers in secondary organic aerosol formed from the photooxidation of isoprene using trimethylsilylation and gas chromatography/ion trap mass spectrometry, *J. Mass Spectrom.*, *42*(1), 101–116.
Tan, Y., Y. B. Lim, K. E. Altieri, S. P. Seitzinger, and B. J. Turpin (2012), Mechanisms leading to oligomers and SOA through aqueous photooxidation: Insights from OH radical oxidation of acetic acid and methylglyoxal, *Atmos. Chem. Phys.*, *12*(2), 801–813.
Tobias, H. J., and P. J. Ziemann (2000), Thermal desorption mass spectrometric analysis of organic aerosol formed from reactions of 1-tetradecene and O_3 in the presence of alcohols and carboxylic acids, *Environ. Sci. Technol.*, *34*(11), 2105–2115.
Tolocka, M. P., M. Jang, J. M. Ginter, F. J. Cox, R. M. Kamens, and M. V. Johnston (2004), Formation of oligomers in secondary organic aerosol, *Environ. Sci. Technol.*, *38*(5), 1428–1434.
Topping, D., M. Barley, and G. McFiggans (2013), Including phase separation in a unified model to calculate partitioning of vapours to mixed inorganic-organic aerosol particles, *Faraday Discuss.*, *165*, 273–288.
Trainic, M., A. A. Riziq, A. Lavi, and Y. Rudich (2012), Role of interfacial water in the heterogeneous uptake of glyoxal by mixed glycine and ammonium sulfate aerosols, *J. Phys. Chem. A*, *116*(24), 5948–5957.
Trostl, J., et al. (2016), The role of low-volatility organic compounds in initial particle growth in the atmosphere, *Nature*, *533*(7604), 527–531.
Trump, E. R., and N. M. Donahue (2014), Oligomer formation within secondary organic aerosols: Equilibrium and dynamic considerations, *Atmos. Chem. Phys.*, *14*(7), 3691–3701.
Tsigaridis, K., and M. Kanakidou (2003), Global modelling of secondary organic aerosol in the troposphere: A sensitivity analysis, *Atmos. Chem. Phys.*, *3*, 1849–1869.
Tsigaridis, K., et al. (2014), The AeroCom evaluation and intercomparison of organic aerosol in global models, *Atmos. Chem. Phys.*, *14*(19), 10,845–10,895.
Tuazon, E. C., and R. Atkinson (1990), A product study of the gas-phase reaction of isoprene with the oh radical in the presence of NO_x, *Int. J. Chem. Kinet.*, *22*(12), 1221–1236.
Updyke, K. M., T. B. Nguyen, and S. A. Nizkorodov (2012), Formation of brown carbon via reactions of ammonia with secondary organic aerosols from biogenic and anthropogenic precursors, *Atmos. Environ.*, *63*, 22–31.
Vaden, T. D., C. Song, R. A. Zaveri, D. Imre, and A. Zelenyuk (2010), Morphology of mixed primary and secondary organic particles and the adsorption of spectator organic gases during aerosol formation, *Proc. Natl. Acad. Sci. U.S.A.*, *107*(15), 6658–6663.
Vaden, T. D., D. Imre, J. Beranek, M. Shrivastava, and A. Zelenyuk (2011), Evaporation kinetics and phase of laboratory and ambient secondary organic aerosol, *Proc. Natl. Acad. Sci. U.S.A.*, *108*, 2190–2195.
Vakkari, V., et al. (2014), Rapid changes in biomass burning aerosols by atmospheric oxidation, *Geophys. Res. Lett.*, *41*, 2644–2651, doi:10.1002/2014GL059396.
Valorso, R., B. Aumont, M. Camredon, T. Raventos-Duran, C. Mouchel-Vallon, N. L. Ng, J. H. Seinfeld, J. Lee-Taylor, and S. Madronich (2011), Explicit modelling of SOA formation from alpha-pinene photooxidation: Sensitivity to vapour pressure estimation, *Atmos. Chem. Phys.*, *11*(14), 6895–6910.
van der Werf, G. R., J. T. Randerson, L. Giglio, G. J. Collatz, M. Mu, P. S. Kasibhatla, D. C. Morton, R. S. DeFries, Y. Jin, and T. T. van Leeuwen (2010), Global fire emissions and the contribution of deforestation, savanna, forest, agricultural, and peat fires (1997–2009), *Atmos. Chem. Phys.*, *10*(23), 11,707–11,735.
Virtanen, A., et al. (2010), An amorphous solid state of biogenic secondary organic aerosol particles, *Nature*, *467*(7317), 824–827.
Volkamer, R., J. L. Jimenez, F. San Martini, K. Dzepina, Q. Zhang, D. Salcedo, L. T. Molina, D. R. Worsnop, and M. J. Molina (2006), Secondary organic aerosol formation from anthropogenic air pollution: Rapid and higher than expected, *Geophys. Res. Lett.*, *33*, L17811, doi:10.1029/2006GL026899.
Volkamer, R., P. J. Ziemann, and M. J. Molina (2009), Secondary organic aerosol formation from acetylene (C_2H_2): Seed effect on SOA yields due to organic photochemistry in the aerosol aqueous phase, *Atmos. Chem. Phys.*, *9*(6), 1907–1928.
Wagner, N. L., et al. (2015), In situ vertical profiles of aerosol extinction, mass, and composition over the southeast United States during SENEX and SEAC^{4}RS: Observations of a modest aerosol enhancement aloft, *Atmos. Chem. Phys.*, *15*(12), 7085–7102.
Wang, C., Y. D. Lei, S. Endo, and F. Wania (2014), Measuring and modeling the salting-out effect in ammonium sulfate solutions, *Environ. Sci. Technol.*, *48*(22), 13,238–13,245.
Wang, J., Y. N. Lee, P. H. Daum, J. Jayne, and M. L. Alexander (2008), Effects of aerosol organics on cloud condensation nucleus (CCN) concentration and first indirect aerosol effect, *Atmos. Chem. Phys.*, *8*(21), 6325–6339.
Wang, L., A. F. Khalizov, J. Zheng, W. Xu, Y. Ma, V. Lal, and R. Y. Zhang (2010), Atmospheric nanoparticles formed from heterogeneous reactions of organics, *Nat. Geosci.*, *3*(4), 238–242.

Wang, L., Z. Li, Q. Tian, Y. Ma, F. Zhang, Y. Zhang, D. Li, K. Li, and L. Li (2013), Estimate of aerosol absorbing components of black carbon, brown carbon, and dust from ground-based remote sensing data of Sun-sky radiometers, *J. Geophys. Res. Atmos.*, *118*, 6534–6543, doi:10.1002/jgrd.50356.

Wang, W., I. Kourtchev, B. Graham, J. Cafmeyer, W. Maenhaut, and M. Claeys (2005), Characterization of oxygenated derivatives of isoprene related to 2-methyltetrols in Amazonian aerosols using trimethylsilylation and gas chromatography/ion trap mass spectrometry, *Rapid Commun. Mass Spectrom.*, *19*(10), 1343–1351.

Wang, X., C. L. Heald, D. A. Ridley, J. P. Schwarz, J. R. Spackman, A. E. Perring, H. Coe, D. Liu, and A. D. Clarke (2014), Exploiting simultaneous observational constraints on mass and absorption to estimate the global direct radiative forcing of black carbon and brown carbon, *Atmos. Chem. Phys.*, *14*(20), 10,989–11,010.

Wang, X., C. L. Heald, A. J. Sedlacek, S. S. de Sá, S. T. Martin, M. L. Alexander, T. B. Watson, A. C. Aiken, S. R. Springston, and P. Artaxo (2016), Deriving brown carbon from multiwavelength absorption measurements: Method and application to AERONET and Aethalometer observations, *Atmos. Chem. Phys.*, *16*(19), 12,733–12,752.

Wania, F., Y. D. Lei, C. Wang, J. P. D. Abbatt, and K. U. Goss (2014), Novel methods for predicting gas-particle partitioning during the formation of secondary organic aerosol, *Atmos. Chem. Phys.*, *14*(23), 13189–13204.

Ward, D. S., T. Eidhammer, W. R. Cotton, and S. M. Kreidenweis (2010), The role of the particle size distribution in assessing aerosol composition effects on simulated droplet activation, *Atmos. Chem. Phys.*, *10*(12), 5435–5447.

Warneck, P. (2003), In-cloud chemistry opens pathway to the formation of oxalic acid in the marine atmosphere, *Atmos. Environ.*, *37*(17), 2423–2427.

Warneke, C., et al. (2010), Biogenic emission measurement and inventories determination of biogenic emissions in the eastern United States and Texas and comparison with biogenic emission inventories, *J. Geophys. Res.*, *115*, D00F18, doi:10.1029/2009JD012445.

Washenfelder, R. A., et al. (2015), Biomass burning dominates brown carbon absorption in the rural southeastern United States, *Geophys. Res. Lett.*, *42*, 653–664, doi:10.1002/2014GL062444.

Waxman, E. M., J. Elm, T. Kurten, K. V. Mikkelsen, P. J. Ziemann, and R. Vokamer (2015), Glyoxal and methylglyoxal setschenow salting constants in sulfate, nitrate, and chloride solutions: Measurements and Gibbs energies, *Environ. Sci. Technol.*, *49*(19), 11,500–11,508.

Weber, R. J., et al. (2007), A study of secondary organic aerosol formation in the anthropogenic-influenced southeastern United States, *J. Geophys. Res.*, *112*, D13302, doi:10.1029/2007JD008408.

Wehner, B., T. Petaja, M. Boy, C. Engler, W. Birmili, T. Tuch, A. Wiedensohler, and M. Kulmala (2005), The contribution of sulfuric acid and non-volatile compounds on the growth of freshly formed atmospheric aerosols, *Geophys. Res. Lett.*, *32*, L17810, doi:10.1029/2005GL023827.

Weitkamp, E. A., A. M. Sage, J. R. Pierce, N. M. Donahue, and A. L. Robinson (2007), Organic aerosol formation from photochemical oxidation of diesel exhaust in a smog chamber, *Environ. Sci. Technol.*, *41*(20), 6969–6975.

Wennberg, P. (2013), Let's abandon the "high NO_X" and "low NO_X" terminology, IGAC News(50), 3-4.

Westervelt, D. M., J. R. Pierce, and P. J. Adams (2014), Analysis of feedbacks between nucleation rate, survival probability and cloud condensation nuclei formation, *Atmos. Chem. Phys.*, *14*(11), 5577–5597.

Williams, B. J., A. H. Goldstein, N. M. Kreisberg, and S. V. Hering (2006), An in-situ instrument for speciated organic composition of atmospheric aerosols: Thermal desorption aerosol GC/MS-FID (TAG), *Aerosol Sci. Technol.*, *40*(8), 627–638.

Wilson, J., D. Imre, J. Beranek, M. Shrivastava, and A. Zelenyuk (2015), Evaporation kinetics of laboratory-generated secondary organic aerosols at elevated relative humidity, *Environ. Sci. Technol.*, *49*(1), 243–249.

Winkler, P. M., J. Ortega, T. Karl, L. Cappellin, H. R. Friedli, K. Barsanti, P. H. McMurry, and J. N. Smith (2012), Identification of the biogenic compounds responsible for size-dependent nanoparticle growth, *Geophys. Res. Lett.*, *39*, L20815, doi:10.1029/2012GL053253.

Wolfe, G. M., J. D. Crounse, J. D. Parrish, J. M. S. Clair, M. R. Beaver, F. Paulot, T. P. Yoon, P. O. Wennberg, and F. N. Keutsch (2012), Photolysis, OH reactivity and ozone reactivity of a proxy for isoprene-derived hydroperoxyenals (HPALDs), *Phys. Chem. Chem. Phys.*, *14*(20), 7276–7286.

Xie, S. C., X. H. Liu, C. F. Zhao, and Y. Y. Zhang (2013), Sensitivity of CAM5-simulated Arctic clouds and radiation to ice nucleation parameterization, *J. Clim.*, *26*(16), 5981–5999.

Xu, L., M. S. Kollman, C. Song, J. E. Shilling, and N. L. Ng (2014), Effects of NO_x on the volatility of secondary organic aerosol from isoprene photooxidation, *Environ. Sci. Technol.*, *48*(4), 2253–2262.

Xu, L., S. Suresh, H. Guo, R. J. Weber, and N. L. Ng (2015a), Aerosol characterization over the southeastern United States using high-resolution aerosol mass spectrometry: Spatial and seasonal variation of aerosol composition and sources with a focus on organic nitrates, *Atmos. Chem. Phys.*, *15*(13), 7307–7336.

Xu, L., et al. (2015b), Effects of anthropogenic emissions on aerosol formation from isoprene and monoterpenes in the southeastern United States, *Proc. Natl. Acad. Sci. U.S.A.*, *112*(1), 37–42.

Xu, L., et al. (2016), Enhanced formation of isoprene-derived organic aerosol in sulfur-rich power plant plumes during Southeast Nexus (SENEX), *J. Geophys. Res. Atmos.*, *121*, 11,137–11,153, doi:10.1002/2016JD025156.

Ye, P., X. Ding, J. Hakala, V. Hofbauer, E. S. Robinson, and N. M. Donahue (2016), Vapor wall loss of semi-volatile organic compounds in a Teflon chamber, *Aerosol Sci. Technol.*, *50*(8), 822–834.

Ye, Q., E. S. Robinson, X. Ding, P. Ye, R. C. Sullivan, and N. M. Donahue (2016), Mixing of secondary organic aerosols versus relative humidity, *Proc. Natl. Acad. Sci. U.S.A.*, *113*(45), 12,649–12,654.

Yee, L. D., et al. (2013), Secondary organic aerosol formation from biomass burning intermediates: phenol and methoxyphenols, *Atmos. Chem. Phys.*, *13*(16), 8019–8043.

Yeh, G. K., and P. J. Ziemann (2014), Alkyl nitrate formation from the reactions of C_8–C_{14} *n*-alkanes with OH radicals in the presence of NO_x: Measured yields with essential corrections for gas-wall partitioning, *J. Phys. Chem. A*, *118*(37), 8147–8157.

Yeh, G. K., and P. J. Ziemann (2015), Gas-wall partitioning of oxygenated organic compounds: Measurements, structure-activity relationships, and correlation with gas chromatographic retention factor, *Aerosol Sci. Technol.*, *49*(9), 726–737.

Yli-Juuti, T., K. Barsanti, L. H. Ruiz, A. J. Kieloaho, U. Makkonen, T. Petaja, T. Ruuskanen, M. Kulmala, and I. Riipinen (2013), Model for acid-base chemistry in nanoparticle growth (MABNAG), *Atmos. Chem. Phys.*, *13*(24), 12,507–12,524.

Yokelson, R. J., T. J. Christian, T. G. Karl, and A. Guenther (2008), The tropical forest and fire emissions experiment: Laboratory fire measurements and synthesis of campaign data, *Atmos. Chem. Phys.*, *8*(13), 3509–3527.

Yokelson, R. J., et al. (2013), Coupling field and laboratory measurements to estimate the emission factors of identified and unidentified trace gases for prescribed fires, *Atmos. Chem. Phys.*, *13*(1), 89–116.

Yu, L., J. Smith, A. Laskin, C. Anastasio, J. Laskin, and Q. Zhang (2014), Chemical characterization of SOA formed from aqueous-phase reactions of phenols with the triplet excited state of carbonyl and hydroxyl radical, *Atmos. Chem. Phys.*, *14*, 13,801–13,816.

Yu, L., J. Smith, A. Laskin, K. M. George, C. Anastasio, J. Laskin, A. M. Dillner, and Q. Zhang (2016), Molecular transformations of phenolic SOA during photochemical aging in the aqueous phase: Competition among oligomerization, functionalization, and fragmentation, *Atmos. Chem. Phys.*, *16*(7), 4511–4527.

Yun, Y. X., and J. E. Penner (2012), Global model comparison of heterogeneous ice nucleation parameterizations in mixed phase clouds, *J. Geophys. Res.*, *117*, D07203, doi:10.1029/2011JD016506.

Zarzana, K. J., D. O. De Haan, M. A. Freedman, C. A. Hasenkopf, and M. A. Tolbert (2012), Optical properties of the products of alpha-dicarbonyl and amine reactions in simulated cloud droplets, *Environ. Sci. Technol.*, *46*(9), 4845–4851.

Zaveri, R. A., R. C. Easter, J. D. Fast, and L. K. Peters (2008), Model for Simulating Aerosol Interactions and Chemistry (MOSAIC), *J. Geophys. Res.*, *113*, D13204, doi:10.1029/2007JD008782.

Zaveri, R. A., et al. (2010), Nighttime chemical evolution of aerosol and trace gases in a power plant plume: Implications for secondary organic nitrate and organosulfate aerosol formation, NO_3 radical chemistry, and N_2O_5 heterogeneous hydrolysis, *J. Geophys. Res.*, *115*, D12304, doi:10.1029/2009JD013250.

Zaveri, R. A., R. C. Easter, J. E. Shilling, and J. H. Seinfeld (2014), Modeling kinetic partitioning of secondary organic aerosol and size distribution dynamics: Representing effects of volatility, phase state, and particle-phase reaction, *Atmos. Chem. Phys.*, *14*(10), 5153–5181.

Zelenyuk, A., D. Imre, M. Earle, R. Easter, A. Korolev, R. Leaitch, P. Liu, A. M. Macdonald, M. Ovchinnikov, and W. Strapp (2010), In situ characterization of cloud condensation nuclei, interstitial, and background particles using the Single Particle Mass Spectrometer, SPLAT II, *Anal. Chem.*, *82*(19), 7943–7951.

Zelenyuk, A., D. Imre, J. Beranek, E. Abramson, J. Wilson, and M. Shrivastava (2012), Synergy between secondary organic aerosols and long-range transport of polycyclic aromatic hydrocarbons, *Environ. Sci. Technol.*, *46*(22), 12,459–12,466.

Zelenyuk, A., D. Imre, J. Wilson, D. M. Bell, K. J. Suski, M. Shrivastava, J. Beranek, A. Kramer, and S. L. Simonich (2017), The effect of gas-phase hydrophobic organics on formation and properties of biogenic secondary organic aerosol particles, *Faraday Discuss.*, doi:10.1039/C7FD00032D.

Zhang, H., J. D. Surratt, Y. H. Lin, J. Bapat, and R. M. Kamens (2011), Effect of relative humidity on SOA formation from isoprene/NO photo-oxidation: Enhancement of 2-methylglyceric acid and its corresponding oligoesters under dry conditions, *Atmos. Chem. Phys.*, *11*(13), 6411–6424.

Zhang, Q., et al. (2007), Ubiquity and dominance of oxygenated species in organic aerosols in anthropogenically-influenced Northern Hemisphere midlatitudes, *Geophys. Res. Lett.*, *34*, L13801, doi:10.1029/2007GL029979.

Zhang, R., A. Khalizov, L. Wang, M. Hu, and W. Xu (2012), Nucleation and growth of nanoparticles in the atmosphere, *Chem. Rev.*, *112*(3), 1957–2011.

Zhang, R. Y., I. Suh, J. Zhao, D. Zhang, E. C. Fortner, X. X. Tie, L. T. Molina, and M. J. Molina (2004), Atmospheric new particle formation enhanced by organic acids, *Science*, *304*(5676), 1487–1490.

Zhang, X., C. D. Cappa, S. H. Jathar, R. C. McVay, J. J. Ensberg, M. J. Kleeman, and J. H. Seinfeld (2014), Influence of vapor wall loss in laboratory chambers on yields of secondary organic aerosol, *Proc. Natl. Acad. Sci. U.S.A.*, *111*(16), 5802–5807.

Zhang, X., R. H. Schwantes, R. C. McVay, H. Lignell, M. M. Coggon, R. C. Flagan, and J. H. Seinfeld (2015), Vapor wall deposition in Teflon chambers, *Atmos. Chem. Phys.*, *15*(8), 4197–4214.

Zhang, X., H. Kim, C. L. Parworth, D. E. Young, Q. Zhang, A. R. Metcalf, and C. D. Cappa (2016), Optical properties of wintertime aerosols from residential wood burning in Fresno, CA: Results from DISCOVER-AQ 2013, *Environ. Sci. Technol.*, *50*(4), 1681–1690.

Zhang, X. L., Y. H. Lin, J. D. Surratt, P. Zotter, A. S. H. Prevot, and R. J. Weber (2011), Light-absorbing soluble organic aerosol in Los Angeles and Atlanta: A contrast in secondary organic aerosol, *Geophys. Res. Lett.*, *38*, L21810, doi:10.1029/2011GL049385.

Zhang, Y., et al. (2015), Changing shapes and implied viscosities of suspended submicron particles, *Atmos. Chem. Phys.*, *15*(14), 7819–7829.

Zhao, D. F., et al. (2016), Cloud condensation nuclei activity, droplet growth kinetics, and hygroscopicity of biogenic and anthropogenic secondary organic aerosol (SOA), *Atmos. Chem. Phys.*, *16*(2), 1105–1121.

Zhao, R., A. K. Y. Lee, L. Huang, X. Li, F. Yang, and J. P. D. Abbatt (2015), Photochemical processing of aqueous atmospheric brown carbon, *Atmos. Chem. Phys.*, *15*(11), 6087–6100.

Zhou, S., M. Shiraiwa, R. D. McWhinney, U. Poeschl, and J. P. D. Abbatt (2013), Kinetic limitations in gas-particle reactions arising from slow diffusion in secondary organic aerosol, *Faraday Discuss.*, *165*, 391–406.

Zhou, S., S. Collier, D. A. Jaffe, N. L. Briggs, J. Hee, A. J. Sedlacek Iii, L. Kleinman, T. B. Onasch, and Q. Zhang (2017), Regional influence of wildfires on aerosol chemistry in the western US and insights into atmospheric aging of biomass burning organic aerosol, *Atmos. Chem. Phys.*, *17*(3), 2477–2493.

Ziemann, P. J. (2011), Effects of molecular structure on the chemistry of aerosol formation from the OH-radical-initiated oxidation of alkanes and alkenes, *Int. Rev. Phys. Chem.*, *30*(2), 161–195.

Ziemann, P. J., and R. Atkinson (2012), Kinetics, products, and mechanisms of secondary organic aerosol formation, *Chem. Soc. Rev.*, *41*(19), 6582–6605.

Zobrist, B., V. Soonsin, B. P. Luo, U. K. Krieger, C. Marcolli, T. Peter, and T. Koop (2011), Ultra-slow water diffusion in aqueous sucrose glasses, *Phys. Chem. Chem. Phys.*, *13*(8), 3514–3526.

Zotter, P., et al. (2014), Diurnal cycle of fossil and nonfossil carbon using radiocarbon analyses during CalNex, *J. Geophys. Res. Atmos.*, *119*, 6818–6835, doi:10.1002/2013JD021114.